

2018

Assessing Groundwater Quantity and Quality Variations in Arid Regions Due to Climate Changes and Anthropogenic Factors: Case Study Saudi Arabia

Othman Abdulrahman Fallatah
University of Rhode Island, ofallatah@kau.edu.sa

Follow this and additional works at: https://digitalcommons.uri.edu/oa_diss

Terms of Use

All rights reserved under copyright.

Recommended Citation

Fallatah, Othman Abdulrahman, "Assessing Groundwater Quantity and Quality Variations in Arid Regions Due to Climate Changes and Anthropogenic Factors: Case Study Saudi Arabia" (2018). *Open Access Dissertations*. Paper 738.

https://digitalcommons.uri.edu/oa_diss/738

This Dissertation is brought to you by the University of Rhode Island. It has been accepted for inclusion in Open Access Dissertations by an authorized administrator of DigitalCommons@URI. For more information, please contact digitalcommons-group@uri.edu. For permission to reuse copyrighted content, contact the author directly.

ASSESSING GROUNDWATER QUANTITY AND QUALITY
VARIATIONS IN ARID REGIONS DUE TO CLIMATE CHANGE
AND ANTHROPOGENIC FACTORS: CASE STUDY SAUDI
ARABIA

BY

OTHMAN ABDULRAHMAN FALLATAH

A DISSERTATION SUBMITTED IN PARTIAL
FULFILLMENT OF THE REQUIREMENTS FOR
THE DEGREE OF DOCTOR OF PHILOSOPHY IN
CIVIL AND ENVIRONMENTAL ENGINEERING

UNIVERSITY OF RHODE ISLAND

2018

DOCTOR OF PHILOSOPHY DISSERTATION

OF

OTHMAN ABDULRAHMAN FALLATAH

APPROVED:

Dissertation Committee

Major Professor

Ali S Akanda

Thomas Boving

Dawn Cardace

Todd Guilfoos

Nasser H. Zawia

DEAN OF THE GRADUATE SCHOOL

UNIVERSITY OF RHODE ISLAND

2018

ABSTRACT

In the Kingdom of Saudi Arabia (KSA), water resources are limited in hyper-arid regions, which are dependent on groundwater (88 percent), desalination water (8 percent) and wastewater treatment (4 percent). The management and development of these resources are essential to sustain population growth and grow the agricultural, industrial, and tourism sectors. Since the groundwater is the most valued water resource in the country, the majority of researchers are focused on the water quantity and water quality in this region in order to find the best solution to face this issue. In 1953 the Ministry of Agriculture and Water was established and assigned the mission of identifying and managing the water resources, aiming to ensure their maximum efficient development and use. The economic future of the Kingdom and the survival of the its people depend alike on the availability of water, its prudent use, and its rational development through long-term program that aim to help fulfill the overriding goal of the government, which is to establish and maintain a better life for the people of the Kingdom.

Previous researchers have focused on the groundwater resources in the Saq aquifer region in northern KSA, where the depletion is the highest, during the past 10-20 years. However, most studies focused on groundwater quality, and not quantity, which is very important in the monitoring and management of water resources, but one the other side monitoring these

resources are significant to sustain and develop our resources. Since the Kingdom does not have a robust database for continuous monitoring groundwater, it is critical to find appropriate scientific methods to monitor the groundwater permanently that can be used to give us a big picture in the present time and in the future to deal with this issue.

Therefore, the overall objective of this dissertation was to design suitable methods for an integrated monitoring mechanism of the groundwater quantity and quality using geophysical and geochemical information of the aquifers and their water resources, hydrologic modeling, satellite Remote Sensing data, and Geographic Information systems (GIS). In order to achieve this, I combined laboratory analysis of water quality variables with modeling of the water resources patterns, and validated the findings with field-level water use and withdrawal data, to develop a suitable scenario to monitor groundwater in this region continuously. The work has been described in the following three manuscripts, as per the Graduate School Manual guidelines:

MANUSCRIPT I (published in Hydrological Processes 2017).

The objective of this work was to utilize month-to-month (April 2002 to April 2015) GRACE (Gravity Recovery and Climate Experiment) data as well as applicable geologic, hydrologic, and remote sensing datasets to inspect the spatial and temporal variations in GRACE-derived terrestrial water and groundwater storage over the Saq aquifer system and to research the components (i.e., natural and anthropogenic) controlling these varieties.

This study extends the investigation of the individuals who have already utilized GRACE data to monitor the Saq aquifer region (e.g., Sultan et al., 2013) by (1) using enhanced state of the art GRACE global mass concentration solutions (mascons), (2) using yields from an improved global land surface model, Global Land Data Assimilation System (GLDAS), to isolate the groundwater storage, (3) developing the area of the study zone to incorporate the Saq aquifer in the KSA and Jordan, and (4) Broadening the time traverse utilized by Sultan et al., (2013) by three years.

MANUSCRIPT II (Submitted to Journal of Hydrology).

In this manuscript, we developed and applied an integrated approach to quantify the recharge rates of the Saq aquifer system. Given the areal distribution of the Saq transboundary aquifer system, the interaction between the Saq aquifer and the overlying aquifers was also assessed. Specifically, we set out to accomplish the following: (1) examine the areal extent of the Saq aquifer recharge domains using geologic, climatic, and remote sensing data; (2) investigate the origin of, and modern contributions to, the groundwater in the Saq aquifer system by examining the isotopic compositions of groundwater samples collected from, and outside of, the Saq aquifer; and (3) estimate, to first order, the magnitude of modern recharge to the Saq aquifer utilizing data from the Gravity Recovery and Climate Experiment (GRACE) and applying the continuous rainfall- runoff model, the Soil and Water Assessment Tool (SWAT).

MANUSCRIPT III (being prepared for Groundwater journal).

The objective of this Chapter is to quantify the groundwater quality of the studying area by measuring the ionic compositions, the characterization of the water quality and radioactive materials by collecting samples and comparing the results with the Water Health Organization of drinking water. Since the Kingdom of Saudi Arabia does not have a continuous water quality control system, it is essential to check the groundwater quality in the study area and make sure it is suitable for drinking and domestic uses. In addition, comparing the previous data in the same studying area with the present data to identify the differences in the groundwater quality data in between the two periods, and understanding the factors controlling the groundwater salinity and total dissolved solids distribution in order to minimize the overexploitation of freshwater resources and to maintain the livelihood of the population and public health.

In conclusion, groundwater monitoring includes both groundwater quantity (e.g., groundwater level and recharge rates) and quality monitoring (analysis of selected physical and chemical variables). The purposes of groundwater monitoring are to manage and develop the policy of the groundwater resources and to predict the groundwater quality and quantity due to natural processes and human impacts in time and space. Therefore, in this situation we need to have a useful database for assessment of the current state, anticipating changes and forecasting trends in the future. My

results in this dissertation will contribute to the effective and efficient utilization of the Saq aquifer water resources and will be used to promote the sustainable development of the Arabian Peninsula and Middle East's natural resources in general. The findings have been and will be shared with stakeholders and decision makers in relevant governmental agencies to develop viable management scenarios for the water resources of the Saq aquifer.

ACKNOWLEDGMENT

First, I would like to thank, ALLAH Almighty for his Blessing, guidance, and bounty to complete this work during four years. Thanks are also regarded to my guide Ali S Akanda, Ph.D. for his excellent supervision, monitoring and constant encouragement throughout my dissertation. His help and advice given by him time to time will carry me a long way in the journey of life on which I am about to embark.

I appreciate the time and efforts of Professors Tom Boving and Dawn Cardace for the invaluable help and feedback they provided me, as my course teachers and committee members, and of Professor Todd Guilfoos for serving as the committee chair for both my comprehensive and the dissertation defense examinations.

I also take this opportunity to express a broad sense of gratitude to University of Rhode Island, Graduate School for their cordial support, valuable information and guidance, which helped me in completing my dissertation in various stages.

I would like to thank my wife, Amjad, for her love, support and patience during the past years it has taken me to graduate and my sweet children as well, Taif, Tariq, and Ayah. I would also like to thank Eng. Yasser Hausawi for his help and for his cordial support. Lastly, I thank my parents, brother, sisters, and friends for their constant encouragement without which this assignment would not be possible.

PREFACE

This dissertation is a final work as a partial fulfillment for the degree of Ph.D. of Environmental Engineering. Rhode Island University of United States of America titled “Assessing Ground Water Quality and Quantity due Climate Change and Anthropogenic Controlling Factors: case study Saudi Arabia.” The format of this dissertation formatted as Manuscript format, publication style. The idea is to combine all three papers as a plan to achieve my objectives in this dissertation.

MANUSCRIPT I: Quantifying temporal variations in water resources of a vulnerable Middle Eastern transboundary aquifer system

This manuscript was published in “Hydrological Processes, 2017.”

MANUSCRIPT II: Assessment of Critical Modern Recharge to Arid Region Aquifer Systems Using an Integrated Geophysical, Geochemical, and Remote Sensing Approach

This manuscript was submitted to “Journal of Hydrology, 2018.”

MANUSCRIPT III. Investigation Groundwater Quality of the depletion region in Arabian Shield and Arabian Shelf

This manuscript is in process. (Being prepared for “Groundwater”)

TABLE OF CONTENTS

ABSTRACT ii

ACKNOWLEDGMENT vii

PREFACE viii

TABLE OF CONTENTS ix

LIST OF FIGURES x

LIST OF TABLES xiii

LIST OF ABBREVIATIONS xiv

Manuscript I 1

Manuscript II 49

Manuscript III 93

APPENDIX A 125

APPENDIX B 154

LIST OF FIGURES

MANUSCRIPT I

Figure 1: (a) Location map showing the spatial distribution of major aquifer outcrops in the KSA and Jordan, spatial domain of the Saq aquifer system (red dashed polygon), and distribution of groundwater wells (black circles) within the KSA's borders.....40

Figure 2: A flowchart showing the main processing steps applied to Gravity Recovery and Climate Experiment (GRACE) and other relevant datasets used in this study. JPL = Jet Propulsion Laboratory; NDVI = normalized difference vegetation index; TWS = terrestrial water storage; UT-CSR = University of Texas Center for Space Research.....41

Figure 3: Secular trend images of TWS_{grace} estimates generated from (a) UT-CSR mascons, (b) JPL mascons, and (c) UT-CSR spherical harmonics over the Arabian Peninsula from April 2002 to April 2015.....42

Figure 4: (A) Temporal variation in TWS_{grace} estimates, along with the associated uncertainties, extracted from the UT-CSR mascons (blue line), JPL mascons (green line), UT-CSR spherical harmonics (red line), and average (black line) solutions over the Saq aquifer system. (b) Temporal variation in the GWS_{grace} estimates over the Saq aquifer system. All of the reported TWS_{grace} and GWS_{grace} trends are significant at > 0.001% significance level.....43

Figure 5: Secular trend in GWS_{grace} estimates generated over the Arabian Peninsula from April 2002 to April 2015.....44

Figure 6: Difference in Average Annual Precipitation (AAP, mm) between 2002-2015 period and 1979-2001 period over the Arabian Peninsula.....45

Figure 7: Validation of the Gravity Recovery and Climate Experiment-derived groundwater storage (GWS_{grace}) storage anomalies (black solid thick line) against the available monthly well observations (individual well: colored circles; average: blue thick line) over the Saq aquifer system.....46

Figure 8: (a) Spatial distribution of areas equipped for irrigation with groundwater expressed as a percentage of the cell area (Siebert et al., 2017). Also shown is the distribution the irrigation wells (blue cross). (b) Secular trends in normalized difference vegetation index (NDVI) estimates over the irrigated area.....47

Figure 9: Temporal variations in the normalized difference vegetation index (NDVI) estimates (red line) along with their linear trend line (black line) over the Saq aquifer system.....48

MANUSCRIPT II

Figure 1: Location map showing the aerial distribution of major aquifer outcrops in Saudi Arabia. Also shown are the spatial domain of the Saq aquifer system (red polygon) and the locations of the groundwater samples (black crosses) examined in this stud.....84

Figure 2: AAR (mm) extracted from TRMM over Saudi. Also shown are the spatial domain of the administrative regions (black dashed lines), Saq aquifer system (black polygon), Saq outcrop (black area), and the recharge domains of the Saq aquifer system (hatched area).....85

Figure 3: $\delta^{2}\text{H}$ versus $\delta^{18}\text{O}$ plot for the groundwater samples collected from Saq aquifer system. Also shown are the isotopic composition of modern rainfall and the Global Meteoric Water Line.....86

Figure 4: Temporal variations in (a) GRACE-derived TWS estimates, (b) GLDAS-derived soil moisture estimates, and (c) GRACE-derived GWS estimates averaged over the Saq aquifer system in Saudi Arabia. Also shown are the error bars in each time series.....87

Figure 5: Comparison between average monthly rainfall estimates reported from rain gauges and GWD-derived estimates. The degree of fitness, R2, is also shown for each plot.....88

Figure 6: The spatial distribution of the four watersheds examined by the SWAT model overlying the SRTM-derived DEM. Also shown are the GWD network and the spatial distribution of the six rain gauges shown in Fig. 5.....89

MANUSCRIPT III

Fig. 1 Geological map for Arabian Shield and Arabian Shelf and samples location.....119

Fig.2 Correlation between measured conductivity and calculated TDS..... 120

Fig. 3 the differences in TDS between 2006 and 2016, showed clearly the change in TDS of the samples those located in the Arabian shield.....121

Fig.4 Piper diagram: Arabian Shelf.....122

Fig.5 Piper diagram: Arabian Shield.....123

LIST OF TABLES

MANUSCRIPT II

Table 1: Well information and O and H isotopic compositions for groundwater samples collected from the Saq aquifer system in Saudi Arabia.....90

Table 2: Trends in water budget components averaged over the Saq aquifer system during the investigated period (April 2002 to December 2016). Trends that are significant at $\geq 65\%$ level of confidence are underlined and at $\geq 95\%$ level of confidence are normal.....91

Table 3: SWAT model results for the four investigated watersheds during the period from 1998 to 2014.....92

MANUSCRIPT III

Table. 1 Preservation conditions of water samples.....123

Table.2 Analytical methods.....124

Tabl.3 Summaries results of water quality data in Arabian Shelf and Arabian Shield.....125

LIST OF ABBREVIATIONS

MOWE, Ministry of Water and Electricity

WHO, World Health Organization

SAQ, Saq Aquifer

GRACE, Gravity Recovery, and Climate Experiment

TWS, Terrestrial Water Storage

GWS, Ground Water Storage

NASA, National Space and Aeronautics Administration

GLDAS, Global Land Data Assimilation System

UT-CSR, University of Texas- Center for Space Research

JPL, Jet Propulsion Laboratory

SM, Soil Moisture

CMAP, Center Merged Analysis of Precipitation

AAP, Average Annual Precipitation

NDVI, Normalized Difference Vegetation Index

SWAT, Soil, and Water Assessment Tool

TRMM, Tropical Rainfall Measuring Mission

NASDA, National Space Development Agency

V- SMOW, Vienna's standard mean ocean water

SCS, Soil Conservation Service

GWD, Global Weather Data

TDS, Total Dissolved Solids

EC, Electrical conductivity

Manuscript I

Published in Hydrological Processes, 2017

Quantifying Temporal Variations in Water Resources of a Vulnerable Middle Eastern Transboundary Aquifer System

Othman Abdurrahman Fallatah^{1,2}, Mohamed Ahmed^{3,4}, Himanshu Save⁵, Ali S. Akanda^{1*}

- 1) Department of Civil and Environmental Engineering, University of Rhode Island, Kingston, Rhode Island 02881
- 2) Faculty of Engineering, Radiation Protection & Training Centre, King Abdulaziz University, P.O. Box 80204, Jeddah 21589, Saudi Arabia
- 3) Department of Geosciences, Western Michigan University, Kalamazoo, Michigan 49008
- 4) Department of Geology, Faculty of Science, Suez Canal University, Ismailia 41522, Egypt
- 5) Center for Space Research, University of Texas at Austin, Austin, Texas 78759

Key Points

1. Transboundary aquifers in Arabian Peninsula show a drastic decline in groundwater storage.
2. The observed declines are associated with increasing groundwater withdrawal for irrigation and decreasing regional rainfall.
3. GRACE data can provide informative and cost-effective ways to monitor vulnerable aquifers.

Abstract

Freshwater resources in the arid Arabian Peninsula, especially transboundary aquifers shared by Saudi Arabia, Jordan, and Iraq, are of critical environmental and geopolitical significance. Monthly Gravity Recovery and Climate Experiment (GRACE) satellite-derived gravity field solutions acquired over the expansive Saq transboundary aquifer system were analyzed and spatiotemporally correlated with relevant land surface model outputs, remote sensing observations, and field data to quantify temporal variations in regional water resources and to identify the controlling factors affecting these resources. Our results show substantial GRACE-derived Terrestrial Water Storage (TWS) and Groundwater Storage (GWS) depletion rates of -9.05 ± 0.25 mm/year (-4.84 ± 0.13 km³/year) and -6.52 ± 0.29 mm/year (-3.49 ± 0.15 km³/year), respectively. The rapid decline is attributed to both climatic and anthropogenic factors; observed TWS depletion is partially related to a decline in regional rainfall, while GWS depletions are highly correlated with increasing groundwater extraction for irrigation and observed water level declines in regional supply wells.

1- Introduction

The scarcity of freshwater is an issue of critical importance in arid and semi-arid countries (Sultan *et al.*, 2011; 2014). Natural freshwater resources in the arid Arabian Peninsula, especially the transboundary aquifers of inland desert regions bordering Saudi Arabia, Syria, Jordan, and Iraq, carry critical environmental and geopolitical significance, due to the extreme water scarcity in this region throughout the year and the sensitive nature of the regional geopolitics, respectively (e.g., Pedraza and Heinrich, 2016). The Kingdom of Saudi Arabia (KSA; Figure 1) is one of the largest countries in this region that faces chronic water scarcity due to a burgeoning population and rapid growth in previously uninhabited areas. Like its neighboring countries, freshwater resources in the KSA are extremely limited and vulnerable to both climate changes and human interventions (Ahmed *et al.*, 2014; Sultan *et al.*, 2014). The average annual rainfall over the entire KSA decreased from 75 mm in 1930 to 65 mm, 52 mm, and 60 mm in 1990, 2000, and 2015, respectively (Sultan *et al.*, 2014). The population of the KSA is on the rise (population in 1960: 4.0×10^6 ; 2010: 27.3×10^6 ; 2050 estimate: 59.5×10^6) (GASTAT, 2016) and as a result, consumption of freshwater resources is increasing as well (2010: 17.9×10^9 m³; 2050 estimate: 19.5×10^9 m³) (MEWA, 2016). In the KSA, groundwater is the most important freshwater resource, with precipitation acting as the recharging source (Kinzelbach *et al.*, 2002; e.g., Scanlon *et al.*, 2002;

Sultan *et al.*, 2008). However, the major recharge process occurred only during the past wet climatic periods and only minimal amounts during the dry periods, like the current day situation (Bayumi, 2008; Sultan *et al.*, 2008, 2011; Wagner, 2011; Abouelmagd *et al.*, 2012, 2014; Zaidi *et al.*, 2015). The management and development of these resources are thus important to sustain KSA's population growth and grow the agricultural, industrial, and tourism sectors. In order to minimize the overexploitation of freshwater resources and to maintain the livelihood of the population and development, understanding the natural phenomena (e.g., rainfall/temperature patterns, duration, and magnitude) together with human-related factors (e.g., population growth, over-exploitation, and pollution) that affect these resources is highly recommended.

Globally, groundwater depletion is a major concern in aquifer systems across the United States, Australia, Northern Africa, South Asia, and South America (e.g., Famiglietti and Rodell, 2013; Famiglietti, 2014; Richey *et al.*, 2015). The KSA-Jordan transboundary aquifer system, also known as the Saq aquifer (Figure 1), is chosen for this study given its expansive nature and significance in the inland regions of the northern Arabian Peninsula. It also provides an opportunity to look at the effects of climatic and anthropogenic forcing on a land-locked hydrological system in the KSA-Jordan region and in similar hyper-arid areas worldwide. The Saq aquifer system covers approximately a total area of 560×10^3 km², of which 15% (82×10^3 km²) is situated in Jordan and 85% (478×10^3 km²) in KSA (MEWA, 2016). In addition, the system is close to the border

regions of southwestern Iraq and the Sinai Peninsula of Egypt, of critical geopolitical and strategic importance in present times (e.g., Pedraza and Heinrich, 2016).

The total population currently living in the Saq aquifer spatial domain (Figure 1) is approximately 750,000, two thirds (66%) of which are located in the Tabuk Province of KSA, whereas, one third (33%) is located in Jordan (GASTAT, 2016; MEWA, 2016). The dependence on the Saq water resources, however, is expected to sharply increase; 3.5 million people living in the Jordanian capital city of Amman will depend on the Saq waters with the completion of the water conveyance system (GASTAT, 2016; MEWA, 2016). Despite its significance to supply freshwater to this water-scarce region, critical difficulties are threatening the sustainable use of Saq waters. For instance, the unsustainable over-exploitation and potential deterioration in water quality may represent significant problems of the Saq aquifer system. In addition, the alarming security situation and ongoing conflicts in the regions of southwestern Iraq, Jordan, and Syria also contribute to the overall threats of this critical freshwater resource.

A comprehensive understanding of the hydrologic and geologic settings, recharge and depletion rates, and the effect of natural and man-made practices on the Saq aquifer system is essential for the proper management of this significant aquifer system in particular and also for the management of the KSA's water resources in general. Extensive field, geophysical, and geochemical explorations are required to comprehend the geologic and

hydrogeological settings of this expansive aquifer system. Additionally, the development, validation, and calibration of groundwater flow models are essential for the exploration of the effect of natural and man-made consequences for this aquifer system. However, the development of such models, for the most part, requires gathering deep subsurface and field information, including, but not limited to, temporal water levels, pressure-driven parameters, and lithological well records. Such data are hard to acquire for the Saq given its broad spatial distribution, inaccessibility, and the general absence of local funding to support the required research-related activities.

The use of recent Earth-observing satellites has greatly facilitated our ability to observe changes in water resources at large scales (e.g., Famiglietti and Rodell, 2013; Famiglietti, 2014). The deployment of the Gravity Recovery and Climate Experiment (GRACE) mission and the acquisition of temporal gravity fields provide significant practical strategies for exploring the temporal mass variations over the Saq and other expansive aquifer systems across the globe. The joint National Space and Aeronautics Administration (NASA)/German Aerospace Center (DLR) GRACE mission was launched on March 2002 to map the Earth's static and temporal gravity fields (Tapley et al., 2004a, 2004b). GRACE measures the spatiotemporal variations in the vertically integrated Terrestrial Water Storage (TWS).

Variations in the GRACE-derived TWS (TWS_{grace}) represent differences in one or more of the following reservoirs: snow/ice, surface water, soil

moisture, groundwater, and wet biomass (e.g., Wahr et al., 1998). GRACE data have been extensively used to quantify aquifers recharge and depletion rates (Ellett et al., 2006; Rodell et al., 2009; Tiwari et al., 2009; Ahmed et al., 2011, 2014, 2016; Feng et al., 2013; Gonçalves et al., 2013; Lenk, 2013; Voss et al., 2013; Joodaki et al., 2014; Wouters et al., 2014; Castle et al., 2014; Döll et al., 2014; Huang et al., 2015, 2016; Li and Rodell, 2015; Al-Zyoud et al., 2015; Chinnasamy and Agoramoorthy, 2015; Chinnasamy et al., 2015; Huo et al., 2016; Jiang et al., 2016; Lakshmi, 2016; Long et al., 2016; Mohamed et al., 2016; Veit and Conrad, 2016; Wada et al., 2016; Yosri et al., 2016; Castellazzi et al., 2016; Chinnasamy and Sunde, 2016)

In this study, 14 years of monthly (April 2002 to April 2015) GRACE were utilized and land surface model (LSM) outputs along with the available geologic, hydrologic, and remote sensing datasets to inspect the spatial and temporal variations in TWS_{grace} and GRACE-derived groundwater storage (GWS_{grace}) over the Saq aquifer system (Figure 1) to explore the natural and anthropogenic drivers of these variations. The calculated GWS_{grace} estimates were then correlated and validated against field measurements from 15 groundwater wells distributed across the Saq aquifer system (Figure 1). Recently, Sultan et al., (2014) used monthly (January 2003–September 2012) GRACE data to quantify the TWS_{grace} depletion over the Saq aquifer. They concluded that excessive groundwater extraction, not climatic changes, is responsible for the observed TWS_{grace} depletion ($6.11 \pm 1.83 \text{ km}^3$) over the Saq aquifer. Our study extends the

investigations of Sultan et al., (2014) by (1) utilizing enhanced state-of-the-art TWSgrace solutions; the global mass concentration solutions (mascons), (2) utilizing outputs from several LSMs; four versions of the Global Land Data Assimilation System (GLDAS), to isolate the GWSgrace, (3) expanding the study area to incorporate the Saq aquifer in the KSA and Jordan border region, (4) broadening the time interval by three years, and (5) validating GRACE observations of groundwater variations with field water level data from regional supply wells.

Study Area

2.1 Geology, Hydrogeology, and Geomorphology

The Arabian Peninsula contains several aquifer systems sitting, in an arc shape, directly over the Precambrian Arabian Shield (Figure 1). These aquifer systems could be grouped into (1) Paleozoic (sandstone: Saq, Al-Wajid, Tabuk; limestone: Khuff) aquifers; (2) Mesozoic (sandstone: Dhurma, Al-Biyadh and Al-Wasia; limestone/dolomite: Umm-Radmah, and Al-Dammam) aquifers; and (3) Cenozoic (alluvial deposits) aquifers (e.g., Al Alawi, J., Abdulrazzak, 1994; Alsharhan and Nairn, 1997).

The Saq aquifer system is characterized by a thick sedimentary succession of Cambrian sandstone that overly the crystalline basement rocks of the Red Sea hills. The Saq formation dips and thickens transitionally towards the east. The foothills of the Red Sea hill represent the recharge domains of the Saq aquifer (e.g., Alsharhan and Nairn, 1997; Alsharhan, 2001, 2003; Sultan et al., 2008). Groundwater in the Saq aquifer system flows from the

west, where the Red Sea Hills are located, towards the east and drains naturally in and close to the Arabian Gulf. The Saq aquifer is unconfined in recharge domains in the west and becomes confined towards the discharge domains in the east (Alsharhan and Nairn, 1997; Alsharhan, 2001, e.g., 2003; Sultan et al., 2008). The water-bearing layer of the Saq aquifer exhibits a large thickness (400-1200 meters), and high storage capacity (storage: 258 km³) (BRGM, 2008). The Saq aquifer waters are believed to have originated, largely, from paleo-precipitation during the previous wet climatic periods, which recharged the aquifers through outcrop locations at the foothills of the Red Sea hills. However, recent studies have also demonstrated that locally, the Saq aquifer is receiving present- day recharge in regions with moderately high precipitation in northwestern Red Sea Hills (Beaumont, 1977; Bayumi, 2008; Sultan et al., 2008, 2011; Wagner, 2011; Abouelmagd et al., 2012, 2014; Zaidi et al., 2015).

2.2 Shared Water Resources of the Arabian Peninsula

In 1970, the KSA started to use the water of the Saq aquifer for human consumption; however, the amount of the extracted water increased in 1980 to support wheat production. Wheat is a water- intensive crop, and this farming effort required a tremendous amount of groundwater extraction, around 1.0 km³/year (e.g., Ferragina and Greco, 2008). Since 2000, extensive development has been recorded in the region with urban growth, improved transportation corridors, agricultural expansion, and associated irrigation projects. These developments have stressed the

groundwater resources of the Saq aquifer; in 2000's the reported groundwater extraction rates were estimated at 5.7 km³/year (BRGM, 2008).

The Saq is the largest of the shared KSA/Jordan aquifer systems. Unlike KSA, Jordan has access to renewable surface water via the Jordan River. Jordan has also planned to dam the Yarmouk, a tributary of the Jordan River, to form a reservoir with a total capacity of 0.9 km³/year (Ferragina and Greco, 2008). Jordan uses the Saq aquifer to supply water to the city of Aqaba and the surrounding areas. Total current Jordanian water consumption from the Saq aquifer is 0.075 km³/year (Ferragina and Greco, 2008). Jordan, however, plans to increase the exploitation of this aquifer system, with a project underway to construct a 325-km pipeline from a well field in the south to the capital city of Amman in the north, which will supply about 0.1 km³/year to the water- starved region (Ferragina and Greco, 2008).

3. Data and Methods

A flowchart summarizing the main processing steps applied to GRACE and other relevant datasets used in this study is shown in Figure 2. Generally, the soil moisture data were utilized to remove the non-groundwater storage components from TWSgrace data. Rainfall data used to explore the climatic controls on the temporal variations in TWSgrace. Groundwater levels and irrigated areas, among others, were used to validate GWSgrace results over the Saq aquifersystem.

3.1 GRACE-Derived Total Water Storage (TWSgrace) Data (see

Appendix A)

Three sources of GRACE data have been utilized in this study: spherical harmonics and mascons products of the University of Texas Center for Space Research (UT-CSR) and mascons solutions from the Jet Propulsion Laboratory (JPL) in USA. Compared to the spherical harmonic fields, the mascons solutions provide higher signal-to-noise ratio, higher spatial resolution, reduced error, and do not require spectral (e.g., de-striping) or spatial (e.g., smoothing) filtering (Watkins et al., 2015; Save et al., 2016; Wiese et al., 2016).

The spherical harmonics of UT-CSR GRACE solution (Level 2; Release 05; degree/order: 60) have been utilized in this study. The time-variable component of the gravity field was obtained by subtracting the temporal (April 2002 to April 2015) mean from each of the monthly spherical harmonics values. The systematic and the random errors in the GRACE datasets were then reduced by despiking and Gaussian (200 km) filters, respectively (Wahr et al., 1998; Swenson and Wahr, 2006). The GRACE spherical harmonics coefficients were then converted to a TWS_{grace} grid of equivalent water thickness (Wahr et al., 1998).

The JPL mascons data (version RL05M_1) provide monthly gravity field variations for 4,551 equal areas of 3° spherical caps. The Coastline Resolution Improvement (CRI) filtered data, utilized to determine the land and ocean fractions of mass inside every land/sea mascon, were used in this study (Watkins et al., 2015). The UT-CSR mascons solutions (version v01) approach uses the geodesic grid technique to model the surface of the

earth using equal area gridded representation of the earth via 40,962 cells (40,950 hexagons + 12 pentagons) (Save et al., 2016). The size of each cell is about equatorial 1° , the number of cells along the equator is 320, and the average area of each cell is 12,400 km². The average distance between cell centers is 120 km. The UT- CSR mascons do not suffer from over-sampling at the poles like an equiangular grid. No neighboring cells meet at a single point (Save et al., 2016).

After generating TWSgrace grids from GRACE spherical harmonics and mascons solutions, trend images were extracted from each of these solutions by fitting a time series at each grid point using annual and semiannual sines and cosines, means, and linear trends components (Figure 3). To examine the temporal variability in TWSgrace over the Saq aquifer, the TWSgrace grid points lying within the Saq aquifer were averaged to produce the Saq TWSgrace time series (Figure 4.a). This rescaling approach, described in Sultan et al. (2014), was used to minimize the attenuation in the amplitude of the TWSgrace time series due to the application of GRACE post-processing steps. The uncertainty associated with the monthly TWSgrace time series among all datasets and TWSgrace trends were then calculated following the approach advanced by Ahmed et al., (2016) and Tiwari et al. (2009). In this approach, monthly TWSgrace time series were fitted using annual, semiannual, and trend terms and residuals were calculated. These residuals were then smoothed using a 13-month moving average, a trend was removed, and another set of residuals were calculated. The standard deviation of the second set of residuals was

interpreted as the maximum uncertainty in monthly TWS_{grace} values. To calculate the TWS_{grace} trend errors, Monte Carlo simulations were performed by fitting trends and seasonal terms for many synthetic monthly datasets, each with values chosen from a population of Gaussian-distributed numbers having a standard deviation similar to that of the second set of residuals. The standard deviation of the extracted synthetic trends was interpreted as the trend error for TWS_{grace}. The generated TWS_{grace} trend data were then statistically analyzed by using the Student t-test to identify their significance levels.

3.2 Land Surface Model-derived TWS Data

Since GRACE has no vertical resolution, the TWS outputs of the GLDAS model (TWS_{gldas}) were utilized in this study to enhance the vertical resolution of TWS_{grace} data. Compared to other land surface models, the GLDAS model provides reasonable estimates of soil moisture over an arid environment of North Africa and Middle East (Ahmed et al., 2016). GLDAS is a land surface modeling system developed by NASA that incorporates field and satellite-based observations to drive detailed advanced simulations of climatic and hydrologic variables (Rodell et al., 2004). The GLDAS model simulates TWS_{gldas} (summation of soil moisture, snow, and canopy storages) through four model versions: VIC, Noah, MOSAIC, and CLM (Koster and Suarez, 1996; Liang et al., 1996; Koren et al., 1999; Dai et al., 2003). The four GLDAS versions (e.g., VIC, Noah, Mosaic, and CLM), were used in this study after subtraction of the temporal (April 2002 to April 2015) mean from each version. Given the

fact that the Saq aquifer is located in a hyper-arid region with minimal vegetation and no surface water reservoirs, the GLDAS-derived snow and canopy storages were neglected. The mean soil moisture estimates of the four TWSgldas simulations (e.g., VIC, Noah, Mosaic, and CLM), were calculated and then subtracted from TWSgrace estimates to quantify the GWSgrace variability over the Saq aquifer system. Errors in GLDAS-derived soil moisture (SMgldas) estimates were calculated as the standard deviations of the soil moisture values computed from the four GLDAS simulations. The final GWSgrace uncertainties were calculated by summing, in quadrature, the contributions from TWSgrace errors to SMgldas errors. The spatial variability in GWSgrace trends are shown in Figure 5.

3.3 Rainfall Data

Precipitation data were utilized to explore the climatic controls on the temporal variation in TWSgrace observed over the Saq aquifer system. The Climate Prediction Center (CPC) Merged Analysis of Precipitation (CMAP) dataset was utilized in this study. CMAP data provide global (88.75°N to 88.75°S) merged precipitation estimates from a variety of satellite and ground-based sources from January 1979 to June 2016 with spatial and temporal resolutions of 2.5° and one month, respectively (Xie and Arkin, 1997). The temporal difference in average annual precipitation (AAP), calculated from CMAP data, for the periods 2002-2015 and 1979-2001 was calculated and mapped over the entire Arabian Peninsula (Figure 6). AAP data were used to explore the climatic control on TWSgrace given

the fact that a rainfall value is already a rate, and so it corresponds to a trend (i.e., a mass/time) signal in the TWS_{grace}; a trend in rainfall corresponds to an increase in mass rate, and so to a quadratic function of time in the mass.

3.4 Field Data

Water level data of 15 monitoring wells distributed over the entire Saq aquifer system in the KSA (Figure 1) and maintained by Ministry of Environment, Water, and Agriculture in the KSA, over the period from 2002 through 2016, were used in this study. Water level data were used to validate the GWS_{grace} variability of the Saq aquifer system. The selection of these wells is justified by their particular characteristics and availability of data during the study period. Only the monitoring wells that show nearly continuous monthly water level records were selected.

These wells are located in two KSA provinces: The Tabuk Province (13 wells: 1T052S, 1T058S, 1H060S, 1T063S, 1T072S, 1T074S, 1T075S, 1T097S, 1T098S, 1T099, 1T107S, 1T114S, and 1T3053S; Figure 1) and the Al Jawf Province (2 wells, SK-624-T and SK-625-P; Figure 1). The Tabuk and Al Jawf areas represent the most irrigated provinces in KSA. In these provinces, modern irrigation (e.g., localized and sprinkler) represent about 89% of the irrigation activities, while the remaining 11% is under flood irrigation (GASTAT, 2016). Following the approach advanced by previous similar studies (e.g., Castle et al., 2014), given the lack of specific yield information from examined wells, the water level time series was normalized for each monitoring well by its standard deviation with the

following method: (1) the mean and the standard deviation for each well time series were calculated; (2) the mean was subtracted and the mean-removed water levels were divided by standard deviation to get the normalized water level value (Jutla et al., 2006) (Figure 7).

3.5 Normalized Difference Vegetation Index (NDVI)

The spatial distribution of irrigated areas (Figure 8a) extracted from the global map of irrigation areas (Siebert et al., 2017), as well as the spatial distribution in the NDVI trends (Figure 8b) and the NDVI time series (Figure 9) were used to validate GWSgrace results over the Saq aquifer.

The Moderate-resolution Imaging Spectroradiometer (MODIS)-derived NDVI products were used in this study. NDVI data were generated from global monthly level-3 MODIS Terra (MOD13C2; spatial resolution: 0.05°) (Justice et al. 1998; 2002).

4. RESULTS AND DISCUSSION

4.1 GRACE-derived TWS (TWSgrace) Trend

The TWSgrace secular trends over the Arabian Peninsula are displayed in Figure 3. The areas in the southern parts of the Arabian Peninsula exhibit minimal variations in TWSgrace (secular trend ~ 0 mm/year), whereas areas in the northern parts of the Arabian Peninsula coincide with the spatial distribution of the Saq aquifer in the KSA and Jordan, exhibiting strong negative TWSgrace trends (Figure 3). The TWSgrace anomalies decrease with time over the negative trend anomalies (shades of blue in Figure 3). The spatial distributions of negative TWSgrace trend anomalies vary slightly with the source of GRACE data. In the case of the UT-CSR

mascons solutions, the negative trend areas are closely centered over the Saq aquifer, whereas these areas extend beyond the spatial distribution of the Saq aquifer in the case of the JPL mascons and UT-CSR spherical harmonic solutions. This is probably related to the way that the TWSgrace products have been generated. Among others, JPL mascons were generated from 3° spherical caps, UT-CSR mascons were generated from 1° hexagons, and UT-CSR spherical harmonics were smoothed using 200 km Gaussian filter (spatial resolution ~ 125,000 km²).

Temporal variations in the TWSgrace time series generated over the Saq aquifer system shows a depletion in the TWSgrace estimates extracted from UT-CSR mascons, JPL mascons, and UT- CSR spherical harmonic solutions (Figure 4a). Depletion rates of -8.96 ± 0.27 mm/year (-4.79 ± 0.14 km³/year), -9.65 ± 0.26 mm/year (-5.16 ± 0.13 km³/year), and -8.60 ± 0.31 mm/year (-4.60 ± 0.16 km³/year) were observed in TWSgrace estimates of UT-CSR and JPL mascons, and UT- CSR spherical harmonic solutions, respectively. The average depletion rate over the entire Saq system, as calculated from the mean of the three solutions (black line; Figure 4.a), is estimated at -9.05 ± 0.25 mm/year (-4.84 ± 0.13 km³/year). All of the reported TWSgrace trends are significant at the < 0.001% significance level. Errors in the average of the three solutions (black line; Figure 4.a) were calculated by adding, in quadrature, errors associated with each solution.

The question of whether the observed TWSgrace negative trend anomalies over the Saq aquifer system (Figure 3) are caused by natural factors (such

as global warming and associated changes in the amounts, patterns, and frequencies of precipitation) and/or by anthropogenic factors (such as increased domestic groundwater withdrawal for urbanization and irrigation activities) are addressed by examining climatic data over the Arabian Peninsula. Recent studies (e.g., Bucchignani et al., 2015) have shown that, in arid and semi-arid areas, precipitation represents one of the primary climatic forcing parameters, whereas other climatic parameters such as specific humidity, wind speed, surface pressure, and solar radiation play a secondary role. Accordingly, the spatial and temporal variability in rainfall rates over the Arabian Peninsula were examined.

To check the mutual effects of variations in rainfall on the TWS_{grace}, the changes of the Annual Average Precipitation (AAP) over the last decade (2002-2015) were examined relative to that of the previous two decades (1979-2001) (Figure 6a). Areas that exhibit a decline in rainfall over 2002-2015 are shown in the shades of blue, whereas areas experiencing an increase in rainfall over 1979-2001 are shown in the shades of red. If the TWS_{grace} negative trend over the Saq aquifer is partially related to decline in rainfall, one would expect to see significantly reduced AAP rates throughout the examined time period (2002-2015) compared to the recorded precipitation for the preceding period (1979-2001) given the fact that the ground and soil are drying out. Figure 6a shows that the Saq aquifer system experienced a decline in rainfall over the past decade. The reduction in rainfall over the Saq aquifer system is also evident from the analysis of rainfall time series extracted from CMAP data) Figure 6b (.

Figures 6a and b indicate that the decline in rainfall rates is apparent in a comparison of AAP for the investigated period to that of the previous 23 years (AAP for 1979- 2001: 104 mm; AAP for 2002-2015: 60 mm; Figs. 6a, b). Declines are higher in the southern and the central parts of the Saq aquifer; this could be related to changes in wind regime and/or atmospheric circulations prevailing these areas (e.g., Alsharhan 2001). Figure 6a is correlated, to a more significant extent, with the TWS_{grace} trends extracted from UT-CSR mascons data (Figure 3a) and, to lesser extent, with TWS_{grace} trends extracted from UT-CSR spherical harmonics (Figure 3c). This might indicate that the observed TWS_{grace} depletions, seen in Figures 3a and 3c, are strictly related to climate change. However, Figure 6a doesn't seem to match well the TWS_{grace} trends extracted from JPL mascons data (Figure 3b). This might be consistent with the anthropogenic factors (e.g., groundwater extraction) as being a cause of TWS_{grace} depletion.

4.2 GRACE-derived GWS (GWS_{grace}) Trend

The observed TWS_{grace} depletions over the Saq aquifer are related to variations in both soil moisture storage and GWS since there are no surface water inputs. To quantify the GWS_{grace} variations over the Saq aquifer system (Figure 5), the SM_{gldas} estimates (average of VIC, Noah, Mosaic, and CLM versions) are subtracted from the TWS_{grace} (averaged from UT-CSR mascons, JPL mascons, and UT-CSR spherical harmonic solutions). The spatial distribution in GWS_{grace} (Figure 5) reveals that the entire Arabian Peninsula is witnessing GWS_{grace} depletion, except the

southwestern parts of Yemen (GWSgrace trend: > 1 mm/yr). Areas in the northern parts of the Arabian Peninsula coincide with the spatial distribution of the Saq aquifer in the KSA and Jordan, exhibiting strong negative GWSgrace trends of up to -8.85 mm/yr.

Errors in GWSgrace were calculated by adding, in quadrature, errors associated with GWSgrace and SMgldas estimates. Figure 4b shows a groundwater depletion rate of -6.52 ± 0.29 mm/year, equivalent to -3.49 ± 0.15 km³/year over the Saq aquifer system during the investigated (April 2002 to April 2015) period. The reported GWSgrace trend is significant at $< 0.001\%$ significance level. The GWSgrace depletion rate indicates that more than 70% of the TWSgrace variability over the Saq aquifer system is controlled by GWS variabilities.

To validate the GWSgrace variability, the normalized GWSgrace were compared with groundwater level observations of 15 monitoring wells (Figure 7) distributed throughout the Saq aquifer (locations shown in Figure 1). To the best of our knowledge, this is the first-time field data from water supply wells, within the vulnerable Saq aquifer region, has been used to directly validate TWSgrace and/or GWSgrace estimates. Comparisons indicated that the GWSgrace estimates generally capture the observed groundwater level depletion shown by the analysis of water level data (Figure 5). The observed GWSgrace depletions over the Saq aquifer are attributed to extensive groundwater extraction activities mainly from the Saq aquifer system. These activities were intended to develop agricultural communities in northern and northwestern parts of the Arabian

Peninsula.

Our interpretation is supported by the reported groundwater extraction rates as well as the observed variations in the areas and the spatial distribution of the irrigated regions and irrigation wells (Figure 8a). Figure 8a shows that areas that are witnessing GWS_{grace} depletion (Figure 5) coincide with a broad part of irrigation and intensive groundwater extraction (Figure 8a), suggesting that the negative GWS_{grace} trend is a result of that extraction. Moreover, in the 1960s, groundwater extraction from the Saq aquifer in the KSA was as small as 0.1 km³/year and increased to 2.0 km³ and in the 1980's and to 8.7 km³ in the 2000's (BRGM, 2008). In the KSA, extraction from the Saq aquifer itself represents 65% to 70% of the reported extraction rates (BRGM, 2008). The reported groundwater extraction rates from the Saq aquifer itself were estimated at 1.4 km³ in the 1980's and 5.7 km³ in the 2000's.

The spatial variations in the NDVI trends (Figure 8b), as well as the temporal changes in the NDVI (Figure 9), extracted from Landsat TM data, over the entire Saq aquifer system, supports the fact that the GWS_{grace} depletions are related to extensive groundwater extraction activities for agricultural purposes. Figure 8b reveals positive NDVI trends correlated with the heavily irrigated areas (Figure 8a) that are witnessing GWS_{grace} depletions (Figure 5). Figure 9 shows a moderate decrease in the NDVI values until the beginning of 2007, and then a bright switch to a positive trend, which coincides strongly, in trends, with the increase in TWS_{grace} and GWS_{grace} (Figure 4) depletion rates.

4.3. Factor driving TWS_{grace} and GWS_{grace} depletions

Freshwater resources in the Saq aquifer system are extremely vulnerable to both climatic and anthropogenic factors. The variations in total and groundwater storage (TWS_{grace} and GWS_{grace}) data over the past fourteen years (April 2002-April 2015) indicates the following:

(1) The Saq aquifer system is witnessing rapid TWS_{grace} and GWS_{grace} depletion rates of -9.05 ± 0.25 mm/year (-4.84 ± 0.13 km³/year) and -6.52 ± 0.29 mm/year (-3.49 ± 0.15 km³/year), respectively, related to both climatic and anthropogenic factors; (2) the observed TWS_{grace} depletion rate is partially related to a decline in rainfall as is evident from a comparison of AAP for the investigated period to the previous 23 years (AAP for 1979-2001: 104 mm; AAP for 2002-2015: 60 mm); (3) the observed TWS_{grace} depletion rate is largely attributed to groundwater extraction activities for irrigation; and (4) the observed GWS_{grace} depletion is correlated with the observed water level depletion rates in water supply wells within the aquifer region.

Our findings are in agreement with other researchers' results that indicate the Saq aquifer is witnessing TWS_{grace} depletion. However, the rates of, and the factors controlling, the observed TWS_{grace} and GWS_{grace} depletions are slightly different. For example, Sultan et al., (2014) indicated that only excessive groundwater extraction, not climatic changes, is responsible for the observed TWS_{grace} depletion (6.11 ± 1.83 km³/yr) over the Saq aquifer during the period from January 2003 to September 2012. Similarly, Joodaki et al., (2014) have concluded that during the

period from February 2003 to December 2012, the northern KSA region, has witnessed a decline in TWS_{grace} that is mainly due to a decline in GWS_{grace} ($6.0 \pm 3.0 \text{ km}^3/\text{yr}$). The observed differences between the previous and our findings could be, among others, attributed to the changes in the investigated time, investigated area, and the data source.

It is worth mentioning that, the mascons solutions, used in our study, provide higher signal to noise ratio, higher spatial resolution, reduced error, and do not require spectral and spatial filtering or any experimental scaling techniques. As a result, our results report far better accuracy and much smaller error margins (an order of magnitude lower) in the TWS and GWS estimates. Our GWS_{grace} depletion rates are highly correlated with the observed decline in water level measured in water supply wells within the investigated aquifer system.

The rapid declines in GWS_{grace} in this extremely arid, strategic, and geopolitically significant region needs to be carefully monitored and managed with competing uses within KSA and plans to use the Saq aquifer to supply freshwater to the Jordanian capital city of Amman. Our results indicate that the implications of unsustainable groundwater based irrigation and extraction practices are clear for these fossil aquifers, also warranting future investigation on the impacts on water quality changes in the valuable sources. Our study also demonstrates that global monthly GRACE

solutions can provide a practical, informative, and cost-effective method for monitoring aquifer systems in water-stressed regions across the globe.

5. Conclusion

Water is a valuable resource in the Arabian Peninsula's current hyper-arid conditions. In KSA, for example, there are no surface water rivers or reservoirs. To sustain its growing population, KSA is currently utilizing more of its groundwater resources and is planning to increase the groundwater extraction rates in the near future. The lack of an understanding of the available groundwater resources and the spatiotemporal depletion rates and locations along with the factors controlling these depletions are posing enormous challenges to the general population of KSA. This study included an integrated, cost-effective approach that combines the state-of-art GRACE data along with other relevant land surface models, remote sensing, geological, and hydrological data and GIS techniques to examine the spatiotemporal variations in the groundwater resources of the Saq aquifer system and to explore the natural and anthropogenic drivers of these variations. Results of this study will contribute to the effective and efficient utilization of the Saq aquifer water resources and will be used to promote the sustainable development of the Arabian Peninsula's natural resources in general. The study findings are being shared with decision-makers in relevant governmental agencies to develop sustainable management scenarios for the Saq aquifer water resources.

6. Acknowledgments

This research was supported, in part, by NASA Health and Air Quality grant (NNX15AF71G). The authors would like to thank the Ministry of Water and Electricity of the Kingdom of Saudi Arabia, Water Information Department for providing the field data to support this research.

7. References:

1. Abouelmagd A, Sultan M, Milewski A, Kehew AE, Sturchio NC, Soliman F, Krishnamurthy R V., Cutrim E. 2012. Toward a better understanding of palaeoclimatic regimes that recharged the fossil aquifers in North Africa: Inferences from stableisotope and remote sensing data. *Palaeogeography, Palaeoclimatology, Palaeoecology* 329–330: 137–149 DOI: 10.1016/j.palaeo.2012.02.024.
2. Abouelmagd A, Sultan M, Sturchio NC, Soliman F, Rashed M, Ahmed M, Kehew AE, Milewski A, Chouinard K. 2014. Paleoclimate record in the Nubian Sandstone Aquifer, Sinai Peninsula, Egypt. *Quaternary Research (United States)* 81 (1): 158–167 DOI: 10.1016/j.yqres.2013.10.017
3. Ahmed M, Sultan M, Wahr J, Yan E. 2014. The use of GRACE data to monitor natural and anthropogenic induced variations in water availability across Africa. *Earth-Science Reviews* 136: 289–300 DOI: 10.1016/j.earscirev.2014.05.009
4. Ahmed M, Sultan M, Wahr J, Yan E, Milewski A, Sauck W, Becker R, Welton B. 2011. Integration of GRACE (Gravity Recovery and Climate Experiment) data with traditional data sets for a better understanding of the time-dependent water partitioning in African watersheds. (5): 479–482 DOI: 10.1130/G31812.1
5. Ahmed M, Sultan M, Yan E, Wahr J. 2016. Assessing and

- Improving Land Surface Model Outputs over Africa using GRACE, Field, and Remote Sensing Data. *Surveys in Geophysics* 37 (3): 529–556 DOI: 10.1007/s10712-016-9360-8
6. Al-Zyoud S, Rühaak W, Forootan E, Sass I. 2015. Over Exploitation of Groundwater in the Centre of Amman Zarqa Basin—Jordan: Evaluation of Well Data and GRACE Satellite Observations. *Resources* 4 (4): 819–830 DOI: 10.3390/resources4040819
 7. Al Alawi, J., Abdulrazzak M. 1994. Water in the Arabian Peninsula: problems and perspectives. In *Water in the Arab World; Perspectives and Prognoses.*, Rogers, P., Lydon P (ed.). Harvard University Press; 171–202.
 8. Alsharhan AS. 2001. Hydrogeology of an arid region: the Arabian Gulf and adjoining areas. Elsevier.
 9. Alsharhan AS. 2003. Petroleum geology and potential hydrocarbon plays in the Gulf of Suez rift basin, Egypt. *AAPG Bulletin* 87 (1): 143–180 DOI: 10.1306/062002870143
 10. Alsharhan AS, Nairn AEM. 1997. Sedimentary basins and petroleum geology of the Middle East. Elsevier.
 11. Bayumi T. 2008. Quantitative Groundwater Resources Evaluation in the Lower Part of Yalamlam Basin, Makkah Al Mukarramah, Western Saudi Arabia. *Journal of King Abdulaziz University-Earth Sciences* 19: 35–56 DOI: 10.4197/Ear.19-1.3

12. Beaumont P. 1977. Water and Development in Saudi Arabia. *The Geographical Journal* 143 (1): 42 DOI: 10.2307/1796674
13. BRGM. 2008. Bureau de Recherches Géologiques et Minières: Investigations for updating the groundwater mathematical model(s) of the Saq and overlying aquifers (BRGM, ed.). Ministry of Water and Electricity: Kingdom of Saudi Arabia.
14. Bucchignani E, Cattaneo L, Panitz H-J, Mercogliano P. 2015. Sensitivity analysis with the regional climate model COSMO-CLM over the CORDEX-MENA domain. *Meteorology and Atmospheric Physics* DOI: 10.1007/s00703-015-0403-3
15. Castellazzi P, Martel R, Galloway DL, Longuevergne L, Rivera A. 2016. Assessing Groundwater Depletion and Dynamics Using GRACE and InSAR: Potential and Limitations. *Groundwater* 54 (6): 768–780 DOI: 10.1111/gwat.12453
16. Castle S, Thomas B, Reager J, Rodell M, Swenson S, Famiglietti J. 2014. Groundwater depletion during drought threatens future water security of the Colorado River Basin. *Geophysical Research Letters* 10: 5904–5911 DOI: 10.1002/2014GL061055. Received
17. Chinnasamy P, Agoramoorthy G. 2015. Groundwater Storage and Depletion Trends in Tamil Nadu State, India. *Water Resources Management* 29 (7): 2139–2152 DOI: 10.1007/s11269-015-0932-z

18. Chinnasamy P, Sunde MG. 2016. Improving spatiotemporal groundwater estimates after natural disasters using remotely sensed data – a case study of the Indian Ocean Tsunami. *Earth Science Informatics* 9 (1): 101–111 DOI: 10.1007/s12145-015-0238-y
19. Chinnasamy P, Maheshwari B, Prathapar S. 2015. Understanding groundwater storage changes and recharge in Rajasthan, India through remote sensing. *Water (Switzerland)* 7 (10): 5547–5565 DOI: 10.3390/w7105547
20. Dai Y, Zeng X, Dickinson RE, Baker I, Bonan GB, Bosilovich MG, Denning a. S, Dirmeyer P a., Houser PR, Niu G, et al. 2003. The common land model. *Bulletin of the American Meteorological Society* 84 (8): 1013–1023 DOI: 10.1175/BAMS-84-8-1013
21. Döll P, Müller Schmied H, Schuh C, Portmann FT, Eicker A. 2014. Global-scale assessment of groundwater depletion and related groundwater abstractions: Combining hydrological modeling with information from well observations and GRACE satellites. *Water Resources Research* 50 (7): 5698–5720 DOI: 10.1002/2014WR015595
22. Ellett KM, Walker JP, Western AW, Rodell M. 2006. A framework for assessing the potential of remote-sensed gravity to provide new insight on the hydrology of the Murray-Darling

- Basin. *Australasian Journal of Water Resources* 10: 125–138
23. Famiglietti JS. 2014. The global groundwater crisis. *Nature Climate Change* 4 (11): 945–948 DOI: 10.1038/nclimate2425
24. Famiglietti JS, Rodell M. 2013. Water in the balance. *Science* 340: 1300–1301 DOI: 10.1126/science.1236460
25. Feng W, Zhong M, Lemoine J-M, Biancale R, Hsu H-T, Xia J. 2013. Evaluation of groundwater depletion in North China using the Gravity Recovery and Climate Experiment (GRACE) data and ground-based measurements. *Water Resources Research* 49 (4): 2110–2118 DOI: 10.1002/wrcr.20192
26. Ferragina E, Greco F. 2008. The Disi project: an internal/external analysis. *Water International* 33 (4): 451–463 DOI: 10.1080/02508060802504412
27. GASTAT. 2016. General Authority for Statistics Available at <http://www.stats.gov.sa/en> [Accessed 24 December 2016]
28. Gonçalves J, Petersen J, Deschamps P, Hamelin B, Baba-Sy O. 2013. Quantifying the modern recharge of the ‘fossil’ Sahara aquifers. *Geophysical Research Letters* 40 (11): 2673–2678 DOI: 10.1002/grl.50478
29. Huang J, Pavlic G, Rivera A, Palombi D, Smerdon B. 2016. Mapping groundwater storage variations with GRACE: a case study in Alberta, Canada. *Hydrogeology Journal*: 1663–1680 DOI: 10.1007/s10040-016-1412-0

30. Huang Z, Pan Y, Gong H, Yeh PJF, Li X, Zhou D, Zhao W. 2015. Subregional-scale groundwater depletion detected by GRACE for both shallow and deep aquifers in North China Plain. *Geophysical Research Letters* 42 (6): 1791–1799 DOI: 10.1002/2014GL062498
31. Huo A, Peng J, Chen X, Deng L, Wang G, Cheng Y. 2016. Groundwater storage and depletion trends in the Loess areas of China. *Environmental Earth Sciences* 75 (16): 1–11 DOI: 10.1007/s12665-016-5951-4
32. Jiang Q, Ferreira VG, Chen J. 2016. Monitoring groundwater changes in the Yangtze River basin using satellite and model data. *Arabian Journal of Geosciences* 9 (7) DOI: 10.1007/s12517-016-2522-7
33. Joodaki G, Wahr J, Swenson S. 2014. Estimating the human contribution to groundwater depletion in the Middle East, from grace data, land surface models, and well observations Gholamreza. *Water Resources Research* 50: 1–14 DOI: 10.1002/2013WR014633.Received
34. Justice C., Townshend JR., Vermote E., Masuoka E, Wolfe R., Saleous N, Roy D., Morisette J. 2002. An overview of MODIS Land data processing and product status. *Remote Sensing of Environment* 83 (1): 3–15 DOI:10.1016/S0034-4257(02)00084-6
35. Justice CO, Vermote E, Townshend JRG, Defries R, Roy DP,

- Hall DK, Salomonson VV, Privette JL, Riggs G, Strahler A, et al. 1998. The Moderate Resolution Imaging Spectroradiometer (MODIS): land remote sensing for global change research. *IEEE Transactions on Geoscience and Remote Sensing* 36 (4): 1228–1249 DOI: 10.1109/36.701075
36. Kinzelbach W, Aeschbach W, Alberich C, Baba GI, Beyerle U, Brunner P, Chiang Wen- Hsing, Rueedi J, Zoellmann K. 2002. A survey of methods for groundwater recharge in arid and semi-arid regions | Protos. Nairobi UNEP - United Nations Environment Programme KE: Nairobi. Available at: <http://www.protos.ngo/en/survey-methods-groundwater-recharge-arid-and-semi-arid-regions> [Accessed 24 December 2016]
37. Koren V, Schaake J, Mitchell K, Duan Q, Chen F, Baker JM. 1999. A parameterization of snowpack and frozen ground intended for NCEP weather and climate models. *Journal of Geophysical Research* 104: 19569–19585 DOI: 10.1029/1999JD900232.
38. Koster RD, Suarez MJ. 1996. Energy and Water Balance Calculations in the Mosaic LSM. NASA Technical Memorandum 104606, 76
39. Lakshmi V. 2016. Beyond GRACE: Using Satellite Data for Groundwater Investigations. *Groundwater* 54 (5): 615–618 DOI:

10.1111/gwat.12444

40. Lenk O. 2013. Satellite-based estimates of terrestrial water storage variations in Turkey. *Journal of Geodynamics* 67 (March 2003): 106–110 DOI: 10.1016/j.jog.2012.04.010
41. Li B, Rodell M. 2015. Evaluation of a model-based groundwater drought indicator in the conterminous U.S. *Journal of Hydrology* 526: 78–88 DOI: 10.1016/j.jhydrol.2014.09.027
42. Liang X, Lettenmaier DP, Wood EF. 1996. One-dimensional statistical dynamic representation of subgrid spatial variability of precipitation in the two-layer variable infiltration capacity model. *Journal of Geophysical Research* 101 (D16): 21403 DOI: 10.1029/96JD01448
43. Long D, Chen X, Scanlon BR, Wada Y, Hong Y, Singh VP, Chen Y, Wang C, Han Z, Yang W. 2016. Have GRACE satellites overestimated groundwater depletion in the Northwest India Aquifer? *Scientific reports* 6 (April): 24398 DOI: 10.1038/srep24398
44. MEWA. 2016. Ministry of Environment, Water, and Agriculture Available at <http://www.mowe.gov.sa/en/index.aspx?AspxAutoDetectCookieSupport=1> [Accessed 25 December 2016]
45. Mohamed A, Sultan M, Ahmed M, Yan E, Ahmed E. 2016. Aquifer recharge, depletion, and connectivity: Inferences from

- GRACE, land surface models, geochemical, and geophysical data. GSA Bulletin: 1–13 DOI: 10.1130/B31460.1
46. Pedraza L, Heinrich M. 2016. Water Scarcity: Cooperation or Conflict in the MiddleEast and North Africa? Foreign Policy Journal Available at <http://www.foreignpolicyjournal.com/2016/09/02/water-scarcity-cooperation-or-conflict-in-the-middle-east-and-north-africa/> [Accessed 24 December 2016]
47. Richey AS, Thomas BF, Lo M-H, Reager JT, Famiglietti JS, Voss K, Swenson S, Rodell
48. M. 2015. Quantifying renewable groundwater stress with GRACE. Water Resources Research 51 (7): 5217–5238 DOI: 10.1002/2015WR017349
49. Rodell M, Houser PR, Jambor U, Gottschalck J, Mitchell K, Meng C-J, Arsenault K, Cosgrove B, Radakovich J, Bosilovich M, et al. 2004. The global land data assimilation system. Bulletin of the American Meteorological Society 85 (3): 381–394 DOI: 10.1175/BAMS-85-3-381
50. Rodell M, Velicogna I, Famiglietti JS. 2009. Satellite-based estimates of groundwater depletion in India. Nature 460 (7258): 999–1002 DOI: 10.1038/nature08238
51. Save H, Bettadpur S, Tapley B. 2016. High-resolution CSR GRACE RL05 mascons. Journal of Geophysical Research

52. Scanlon BR, Healy RW, Cook PG. 2002. Choosing appropriate techniques for quantifying groundwater recharge. *Hydrogeology Journal* 10 (1): 18–39 DOI: 10.1007/s10040-001-0176-2
53. Sultan M, Ahmed M, Wahr J, Yan E, Emil MK. 2014. Monitoring Aquifer Depletion from Space : Case Studies from the Saharan and Arabian Aquifers. In *Remote Sensing of the Terrestrial Water Cycle*, Lakshmi, V. (ed.).AGU Geophysical Monograph # 206; 349–366.
54. Sultan M, Metwally S, Milewski a., Becker D, Ahmed M, Sauck W, Soliman F, Sturchio N, Yan E, Rashed M, et al. 2011. Modern recharge to fossil aquifers: Geochemical, geophysical, and modeling constraints. *Journal of Hydrology* 403 (1–2): 14–24 DOI: 10.1016/j.jhydrol.2011.03.036
55. Sultan M, Sturchio N, Al Sefry S, Milewski a., Becker R, Nasr I, Sagintayev Z. 2008. Geochemical, isotopic, and remote sensing constraints on the origin and evolution of the Rub Al Khali aquifer system, Arabian Peninsula. *Journal of Hydrology* 356 (1–2): 70–83 DOI: 10.1016/j.jhydrol.2008.04.001
56. Swenson S, Wahr J. 2006. Post-processing removal of correlated errors in GRACE data. *Geophysical Research Letters* 33 (8): L08402 DOI: 10.1029/2005GL025285
57. Tapley BD, Bettadpur S, Ries JC, Thompson PF, Watkins MM. 2004a. GRACE measurements of mass variability in the Earth

- system. *Science* (New York, N.Y.) 305 (5683): 503–5 DOI: 10.1126/science.1099192
58. Tapley BD, Bettadpur S, Watkins M, Reigber C. 2004b. The gravity recovery and climate experiment: Mission overview and early results. *Geophysical Research Letters* 31 (9): 1– 4 DOI: 10.1029/2004GL019920
59. Tiwari VM, Wahr J, Swenson S. 2009. Dwindling groundwater resources in northern India, from satellite gravity observations. *Geophysical Research Letters* 36 (18):L18401 DOI: 10.1029/2009GL039401
- Veit E, Conrad CP. 2016. The impact of groundwater depletion on spatial variations in sea level change during the past century. *Geophysical Research Letters* 43 (7): 3351– 3359 DOI: 10.1002/2016GL068118
60. Voss K a, Famiglietti JS, Lo M, Linage C, Rodell M, Swenson SC. 2013. Groundwater depletion in the Middle East from GRACE with implications for transboundary water management in the Tigris-Euphrates-Western Iran region. *Water resources research* 49 (2): 904–914 DOI: 10.1002/wrcr.20078
61. Wada Y, Lo M-H, Yeh PJ-F, Reager JT, Famiglietti JS, Wu R-J, Tseng Y-H. 2016. Fate of water pumped from underground and contributions to sea-level rise. *Nature Climate Change* IN PRESS (May): 8–13 DOI: 10.1038/nclimate3001
62. Wagner W. 2011. Groundwater in the Arab Middle East. DOI:

10.1007/978-3-642-19351-4

63. Wahr J, Molenaar M, Bryan F. 1998. Time variability of the Earth's gravity field: Hydrological and oceanic effects and their possible detection using GRACE. *Journal of Geophysical Research* 103 (B12): 30205–30229 DOI: 10.1029/98JB02844
64. Watkins MM, Wiese DN, Yuan D, Boening C, Landerer FW. 2015. Improved methods for observing Earth's time-variable mass distribution with GRACE using spherical cap mascons. *Journal of Geophysical Research: Solid Earth* 120: 2648–2671 DOI: 10.1002/2014JB011547. Received
65. Wiese DN, Landerer FW, Watkins MM. 2016. Quantifying and reducing leakage errors in the JPL RL05M GRACE mascon solution. *Water Resources Research* 52 (9): 7490–7502 DOI: 10.1002/2016WR019344
66. Wouters B, Bonin J a, Chambers DP, Riva REM, Sasgen I, Wahr J. 2014. GRACE, time-varying gravity, Earth system dynamics and climate change. *Reports on Progress in Physics* 116801 DOI: 10.1088/0034-4885/77/11/116801
67. Xie P, Arkin P a. 1997. Global Precipitation: A 17-Year Monthly Analysis Based on Gauge Observations, Satellite Estimates, and Numerical Model Outputs. *Bulletin of the American Meteorological Society* 78 (11): 2539–2558 DOI: 10.1175/1520-0477(1997)078<2539:GPAYMA>2.0.CO;2

68. Yosri AM, Abd-Elmegeed MA, Hassan AE. 2016. Assessing groundwater storage changes in the Nubian aquifer using GRACE data. *Arabian Journal of Geosciences* 9 (10): 1–9 DOI: 10.1007/s12517-016-2593-5
69. Zaidi FK, Nazzal Y, Ahmed I, Naeem M, Jafri MK. 2015. Identification of potential artificial groundwater recharge zones in Northwestern Saudi Arabia using GIS and Boolean logic. *Journal of African Earth Sciences* 111: 156–169 DOI: 10.1016/j.jafrearsci.2015.07.008

Figure Legends:

Figure 1: (a) Location map showing the spatial distribution of major aquifer outcrops in the KSA and Jordan, spatial domain of the Saq aquifer system (red dashed polygon), and distribution of groundwater wells (black circles) within the KSA's borders

Figure 2: A flowchart showing the main processing steps applied to Gravity Recovery and Climate Experiment (GRACE) and other relevant datasets used in this study. JPL = Jet Propulsion Laboratory; NDVI = normalized difference vegetation index; TWS = terrestrial water storage; UT-CSR = University of Texas Center for Space Research

Figure 3: Secular trend images of TWS_{grace} estimates generated from (a) UT-CSR mascons, (b) JPL mascons, and (c) UT-CSR spherical harmonics over the Arabian Peninsula from April 2002 to April 2015.

Figure 4: (A) Temporal variation in TWS_{grace} estimates, along with the associated uncertainties, extracted from the UT-CSR mascons (blue line), JPL mascons (green line), UT-CSR spherical harmonics (red line), and average (black line) solutions over the Saq aquifer system. (b) Temporal variation in the GWS_{grace} estimates over the Saq aquifer system. All of the reported TWS_{grace} and GWS_{grace} trends are significant at $> 0.001\%$ significance level.

Figure 5: Secular trend in GWS_{grace} estimates generated over the Arabian Peninsula from April 2002 to April 2015.

Figure 6: Difference in Average Annual Precipitation (AAP, mm) between 2002-2015 period and 1979-2001 period over the Arabian Peninsula.

Figure 7: Validation of the Gravity Recovery and Climate Experiment-derived groundwater storage (GWS_{grace}) storage anomalies (black solid thick line) against the available monthly well observations (individual well: colored circles; average: blue thick line) over the Saq aquifer system

Figure 8: (a) Spatial distribution of areas equipped for irrigation with groundwater expressed as a percentage of the cell area (Siebert et al., 2017). Also shown is the distribution the irrigation wells (blue cross). (b) Secular trends in normalized difference vegetation index (NDVI) estimates over the irrigated areas

Figure 9: Temporal variations in the normalized difference vegetation index (NDVI) estimates (red line) along with their linear trend line (black line) over the Saq aquifer system

Figure 1.

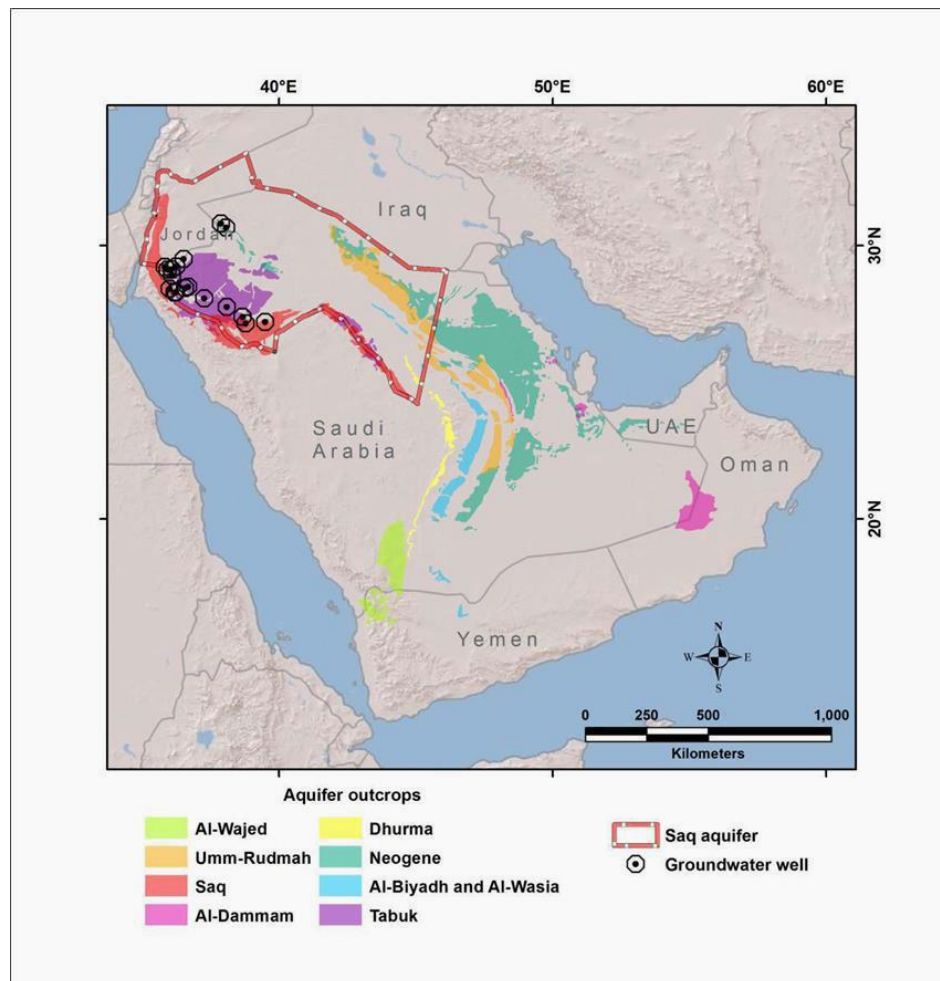


Figure 2.

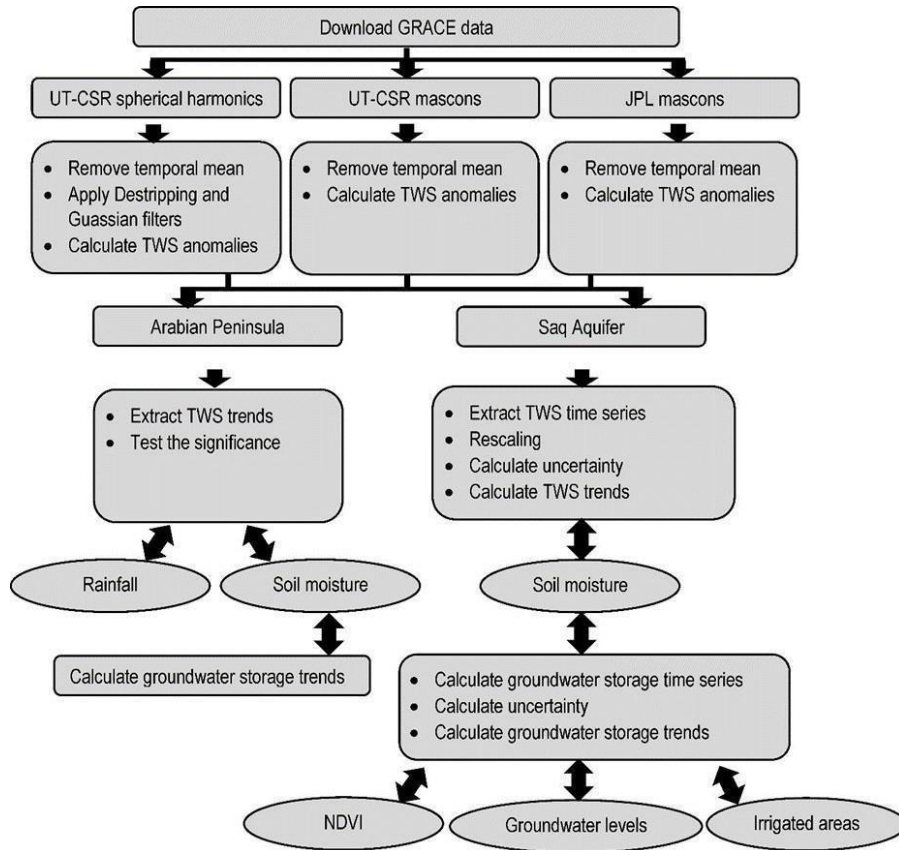


Figure 3.

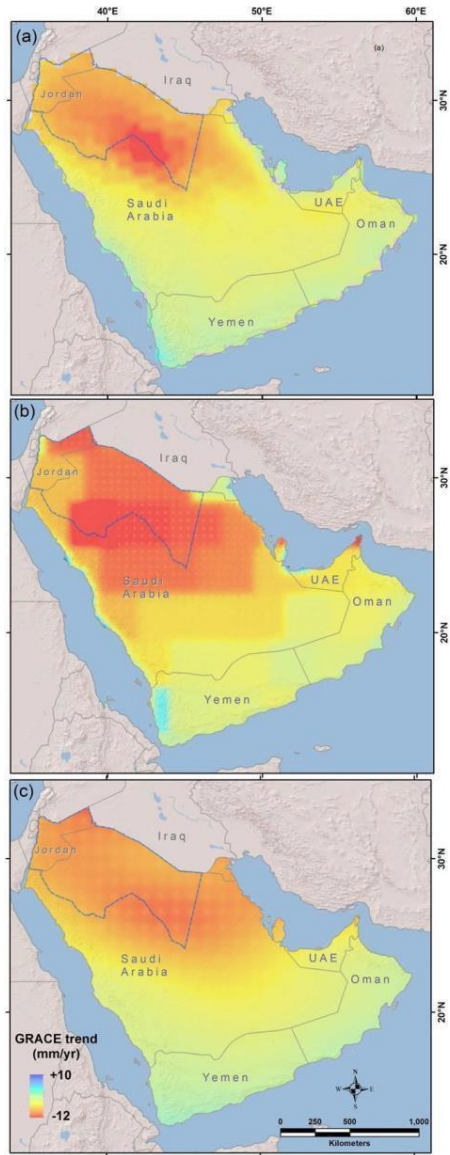


Figure 4.

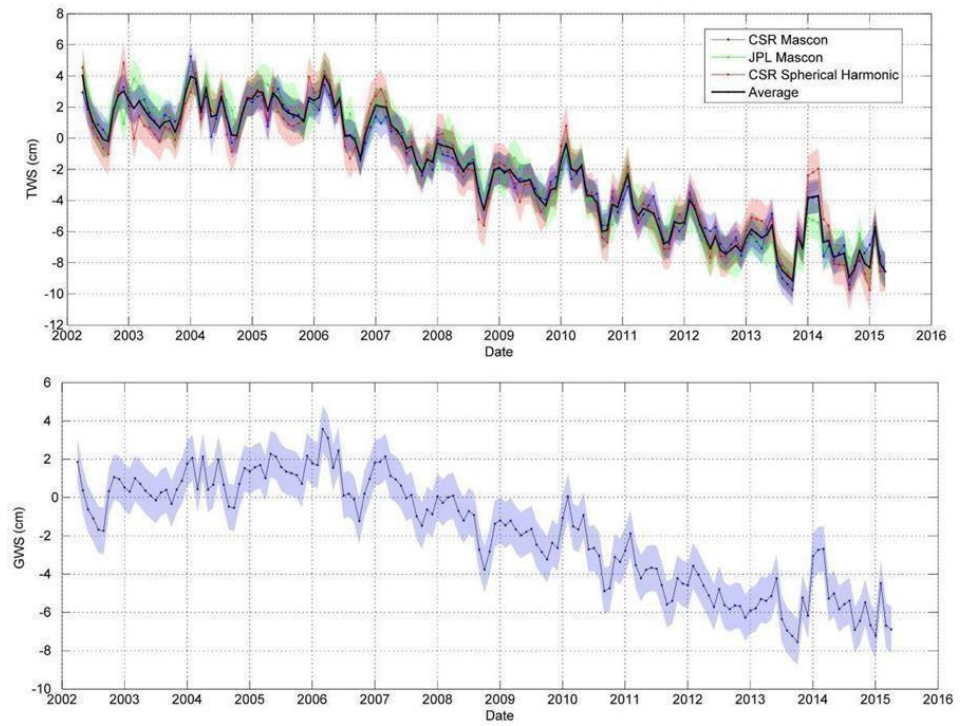


Figure 5.

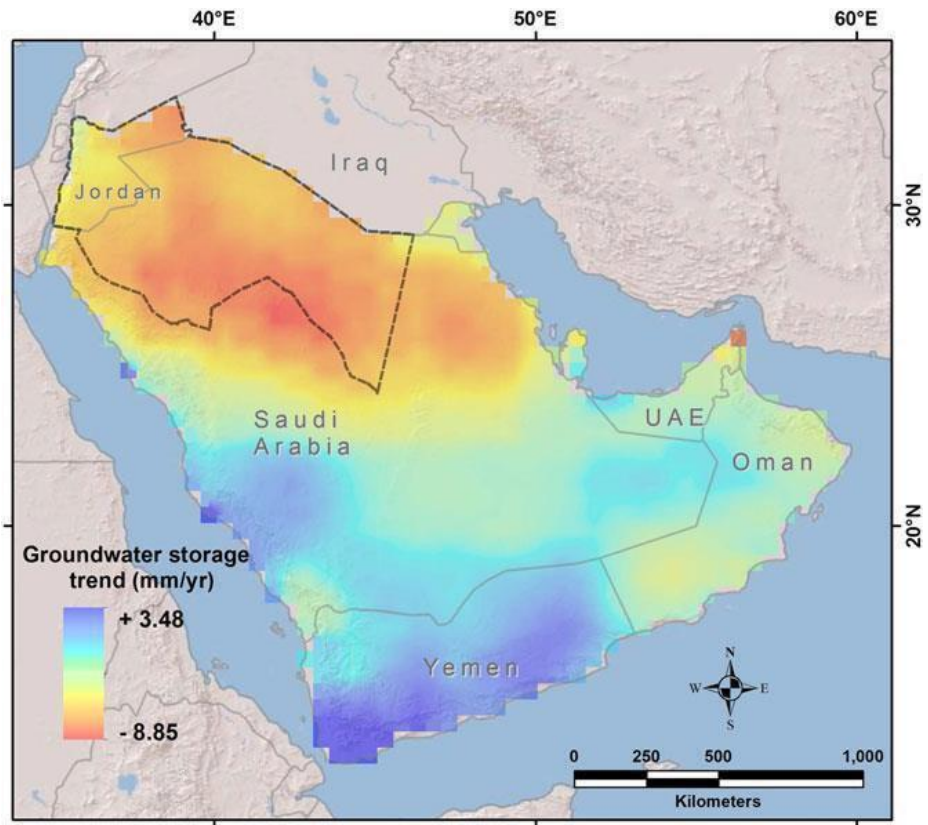


Figure 6.

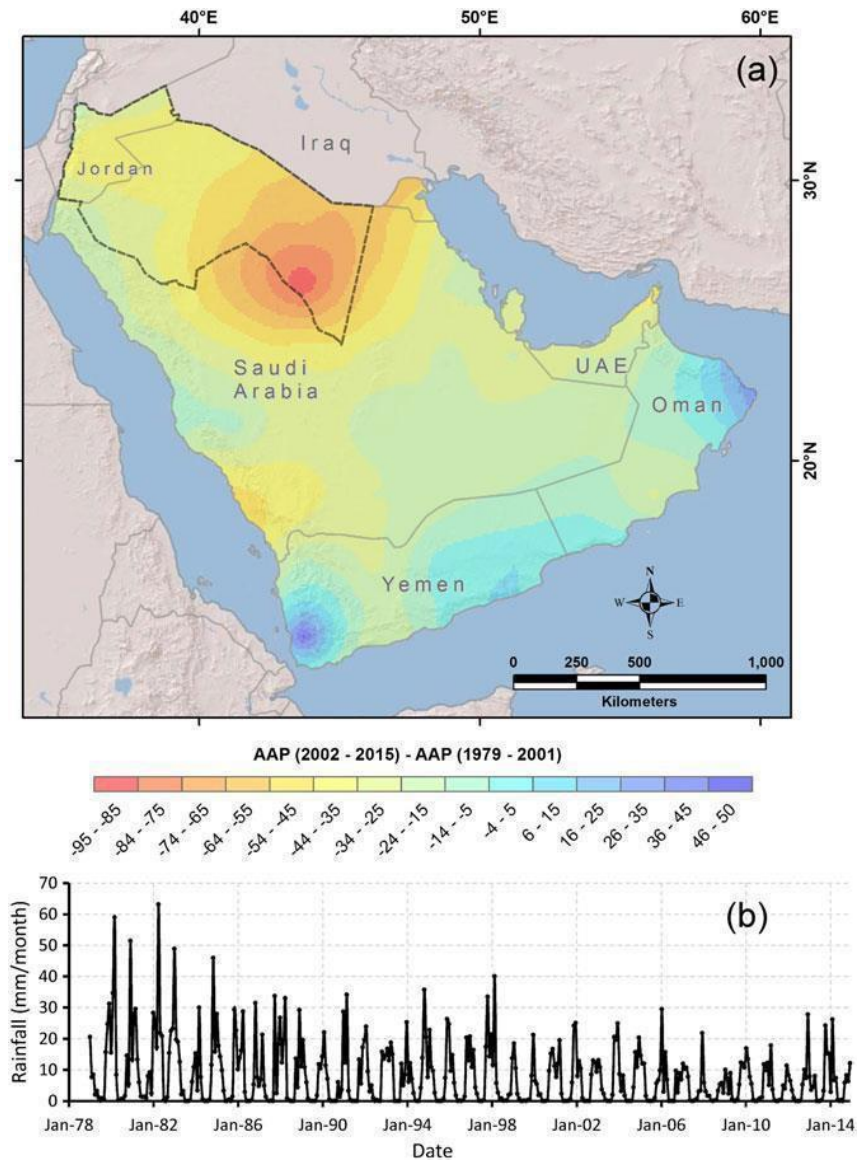


Figure 7.

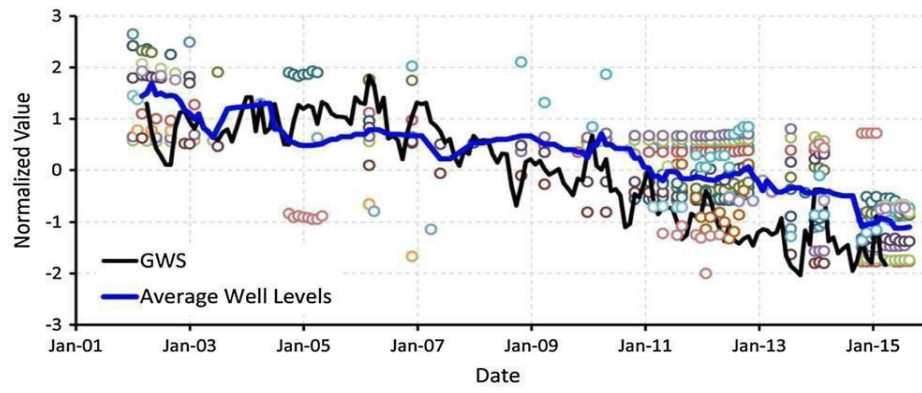


Figure 8:

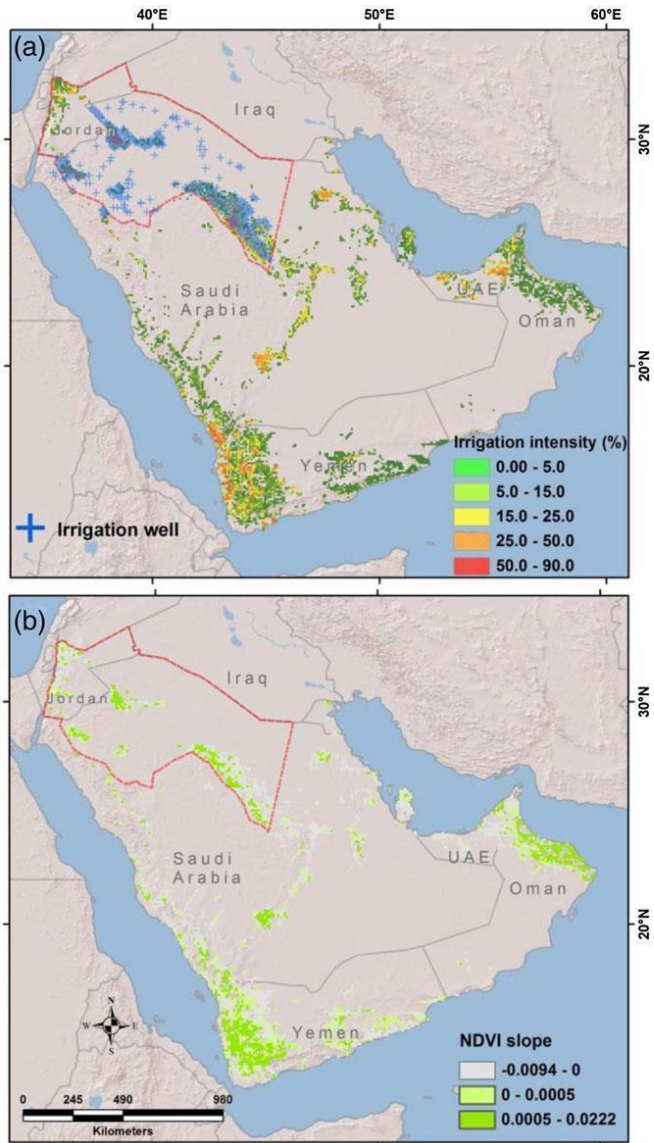
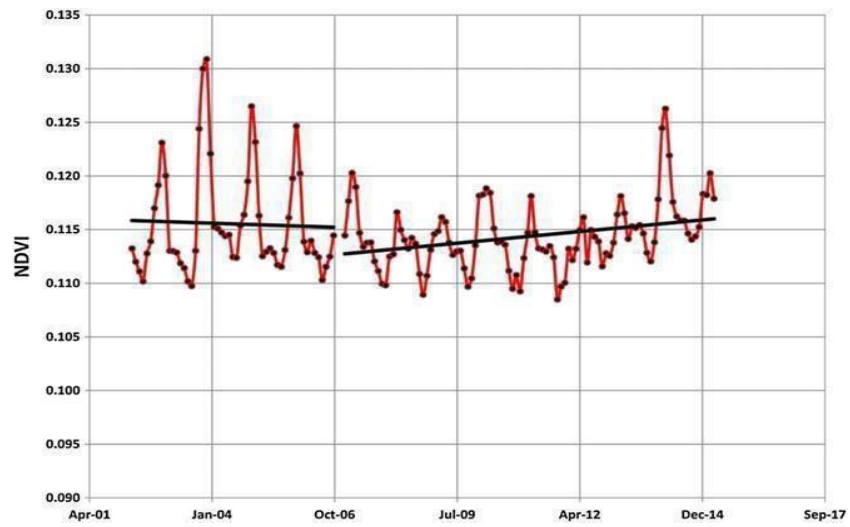


Figure 9



Manuscript II

Submitted to **Journal of Hydrology**, 2018

Assessment of Critical Modern Recharge to Arid Region Aquifer Systems Using an Integrated Geophysical, Geochemical, and Remote Sensing Approach

**Othman Abdurrahman Fallatah^{1, 2}, Mohamed Ahmed^{3, 4},
Dawn Cardace⁵, Thomas Boving^{1, 5}, Ali S. Akanda¹**

- 1) Department of Civil and Environmental Engineering, University of
Rhode Island, Kingston, Rhode Island 02881
- 2) Faculty of Engineering, Radiation Protection & Training Centre, King
Abdulaziz University,
P.O. Box 80204, Jeddah 21589, Saudi Arabia
- 3) Department of Geosciences, Western Michigan University, Kalamazoo,
Michigan 49008
- 4) Department of Geology, Faculty of Science, Suez Canal University,
Ismailia 41522, Egypt Department of Geosciences, University of Rhode
Island, Kingston, Rhode Island 02881

1. Abstract

The arid and semi-arid regions of the world are facing limited freshwater resources, minimal amounts of rainfall, and increasing population and water demands. These resources, often groundwater, are vulnerable to both natural variability and anthropogenic interventions. Here, we develop and apply an integrated approach using geophysical, geochemical, and remote sensing observations to quantify the recharge rates of arid region aquifers that are witnessing rapid groundwater depletion. Focusing on the Saq aquifer system in the Arabian Peninsula, our study was three-fold: (1) to examine the areal extent of the aquifer recharge domains using geologic, climatic, and remote sensing data; (2) to investigate the origin of, and modern contributions to the aquifer system by examining the isotopic composition of groundwater samples; and (3) to estimate the magnitude of contemporary recharge to the aquifer utilizing Gravity Recovery and Climate Experiment (GRACE) data and also applying a continuous rainfall-runoff model, the Soil and Water Assessment Tool (SWAT) model. Isotopic examination of the groundwater samples from Saq revealed that deeper aquifers (fossil water) are more depleted compared to shallow reserves (alluvial aquifer; mixed waters). Analysis of GRACE-derived Terrestrial and groundwater storage time series indicates that the aquifer system received an annual recharge rate of $5.21 \pm 0.10 \text{ km}^3/\text{yr}$ ($11.85 \pm 0.22 \text{ mm/yr}$), equal to about half of groundwater withdrawal rate from wells during the investigation

period (April 2002 – December 2016). Analysis of SWAT results indicates that, during the period from 1998 to 2014, the investigated watersheds received an average annual precipitation of 19.20 km³, of which approximately 51% is partitioned as potential recharge. The temporal variations in storage, depletion, and recharge rates are related to the changes in regional groundwater extraction, rainfall, and extent of irrigated areas.

Keywords: Saudi Arabia; Saq Aquifer; Recharge; Soil and Water Assessment Tool; Gravity Recovery and Climate Experiment; Depletion

2. Introduction

The arid and semi-arid parts of the world are currently facing more difficult problems than ever before when it comes to freshwater resources. The limited freshwater resources, minimal amounts of rainfall, drought, and increasing population and living standards are contributing to environmental and economic devastation in these areas. The freshwater resources of Saudi Arabia, for example, are primarily those found in groundwater aquifer systems; only about 5% comes from desalination plants (Ouda, 2013). These limited resources are extremely vulnerable to both natural interventions (e.g., rainfall/temperature patterns, duration, and magnitude) and anthropogenic ones (e.g., population growth, over-exploitation, and pollution). The average annual rainfall (AAR) over the entirety of Saudi Arabia decreased from 75 mm in 1930 to 65 mm in 1990, 52 mm in 2000, and 60 mm in 2015. Recent studies have projected that mean evaporation in that country will increase from 245 mm/yr in 2011 to 368 mm/yr by 2050 (Chowdhury and Al- Zahrani, 2015). On the other hand, the population growth of Saudi Arabia (1960: 4.0×10^6 ; 1975: 6.9×10^6 ; 2010: 27.3×10^6) has resulted in a significant increase in freshwater use. For example, the consumption of freshwater resources in Saudi Arabia was estimated at $17.9 \times 10^9 \text{ m}^3$ in 2010 but expected to be $19.5 \times 10^9 \text{ m}^3$ in 2050 (MEWA, 2016). To reduce the pressures on non-renewable groundwater resources, Saudi Arabia is currently adopting a strategy that

introduces advanced irrigation techniques, reduces water-intensive agricultural production, and uses more desalinated and treated wastewater and renewable groundwater resources. However, more actions are required to make use of the water resources of Saudi Arabia more sustainable. The most crucial task is to quantify the modern recharge to its principal aquifer systems.

The Saq aquifer represents one of the most significant transboundary aquifer systems that extends between northern parts of Saudi Arabia and southwestern Jordan. The Saq aquifer is witnessing groundwater overexploitation and is showing severe signs of groundwater decline. For example, a recent study by Fallatah et al., (2017), indicates that the Saq aquifer system in Saudi Arabia and Jordan is witnessing groundwater storage depletions of -6.52 ± 0.29 mm/year (-3.49 ± 0.15 km³/year). The observed depletion is highly correlated with increasing groundwater extraction for irrigation and observed water level declines (up to 15 m) in local supply wells. The major recharge events of the Saq aquifer occurred only during the past wet climatic periods in Pleistocene (Abouelmagd et al. 2012; Abouelmagd et al. 2014; Bayumi 2008; Sultan et al. 2008; Sultan et al. 2011; Wagner 2011; Zaidi et al. 2015). However, the Saq aquifer is currently receiving minimal recharge under present-day climatic conditions. Quantifying groundwater recharge of the Saq aquifer is thus key to the sustainable utilization of the groundwater resources in that system. Groundwater recharge is generally assessed either by direct or by indirect

methods (e.g., Scanlon et al., 2002). Some of the physical and chemical methods that are used to quantify the recharge are difficult to apply, given the sizeable areal extent of the Saq aquifer and the absence of field data that is required for implementing these methods.

In this manuscript, we develop and apply an integrated approach to quantify the recharge rates of the Saq aquifer system. Given the areal distribution of the Saq transboundary aquifer system, the interaction between the Saq aquifer and the overlying aquifers was also assessed. Specifically, we set out to accomplish the following: (1) examine the areal extent of the Saq aquifer recharge domains using geologic, climatic, and remote sensing data; (2) investigate the origin of, and modern contributions to, the groundwater in the Saq aquifer system by examining the isotopic compositions of groundwater samples collected from, and outside of, the Saq aquifer; and (3) estimate, to first order, the magnitude of modern recharge to the Saq aquifer utilizing data from the Gravity Recovery and Climate Experiment (GRACE) and applying the continuous rainfall- runoff model, the Soil and Water Assessment Tool (SWAT).

3. Saq Aquifer System

Saudi Arabia is divided mainly into the Arabian Shield and the Arabian Shelf. The Arabian Shield, an outcropping along the Red Sea, is principally composed of Precambrian igneous and metamorphic complexes. On the other hand, the Arabian Shelf is mainly formed of a sedimentary sequence lying unconformable on the Arabian Shield and dipping away towards the

Arabian Gulf (Fig. 1). The Saq aquifer system is situated in an arc directly over the Precambrian Arabian Shield, which dips and thickens towards the Arabian Gulf. This aquifer is characterized by a thick sedimentary succession of Cambro-Ordovician medium to coarse sandstone that is unconfined towards the recharge domains and becomes confined towards the discharge domains. Precipitation that falls along the foothills of the Red Sea hills feeds the Saq aquifer, and the groundwater flows from the west towards the east, draining naturally in and close to the Arabian Gulf (Alsharhan and Nairn 1997; Alsharhan 2001; Alsharhan 2003; Sultan et al. 2008). The water-bearing layer of the Saq aquifer exhibits a large thickness (400–1200 meters) and high storage capacity (storage: 258 km³; Abunayyan Trading Corporation and BRGM 2008). The Saq aquifer waters are believed to have originated, to a great extent, from paleo-precipitation during the previous wet climatic periods, which recharged the aquifers through outcrop locations at the foothills of the Red Sea hills (Beaumont 1977; Bayumi 2008; Sultan et al. 2008; Sultan et al. 2011; Wagner 2011; Abouelmagd et al. 2012; Abouelmagd et al. 2014; Zaidi et al. 2015).

4. Delineating the recharge domains of the Saq aquifer

Two main peak periods characterize seasonal rainfall patterns over Saudi Arabia. The first peak comes during March and April, followed by almost no rainfall during June to August, which in turn is followed by a second peak from October to January. These precipitation events act as the main sources of recharge to the underlying aquifer systems. Recharge domains of

the Saq aquifer system were defined as those areas that are witnessing annual rainfall and covered by the Saq outcrops. We examined the AAR data over the Saq aquifer using satellite-based rainfall estimates given the lack of rain gauges over the monitored area and the discontinuous nature of rainfall records of the existing stations. The Tropical Rainfall Measuring Mission (TRMM; version 3B43) dataset (available at <http://mirador.gsfc.nasa.gov/cgi-bin/mirador/presentNavigation.pl?project=TRMM&tree=project>) were used in this study. TRMM is a joint mission between NASA and the National Space Development Agency (NASDA) of Japan, launched in 1997. It provides near-global (50°N–50°S) data on rainfall every 3 hours with a spatial resolution of 0.25° × 0.25° (Huffman et al. 2007). Previous studies have demonstrated that, over arid and semi-arid regions, TRMM-derived rainfall estimates provide adequate spatial and temporal correspondence with steady rainfall and streamflow data (e.g., Adeyewa and Nakamura 2003; Dinku et al. 2007, 2008; Beighley et al. 2011; Sylla et al. 2013). The AAR over the entirety of Saudi Arabia is shown in Figure 2. Examination of Fig. 2 shows that the precipitation is mostly concentrated over the southern parts of the Red Sea Hills. Generally, over Saudi Arabia, the precipitation increases from north to south. For example, western and southwestern areas of Jizan, Asir, Al Bahah, and Makkah receive average rainfall of up to 300 mm. Al Qasim and the northern parts of the Ar Riyad and Ash Sharqiyah have an average rainfall of up to 125 mm.

Areas that receive average annual rainfall ≥ 15 mm within the Saq aquifer domains are believed to represent recharge domains of the Saq aquifer given the fact that individual precipitation events of < 5 mm over arid and semi-arid areas would produce negligible recharge and/or runoff events (Mohamed et al., 2016; Milewski et al., 2009). It is worth mentioning that the Saq aquifer could also receive recharge through the downward and upward flows from the overlying and underlying aquifer systems, respectively. The mechanism of this recharging process could, for example, be through different fault systems existing in the domain (e.g., Sultan et al., 2007). The recharge domain of the Saq aquifer is shown as the hatched area in Fig. 2.

5. Geochemical Constraints on the Modern Recharge of the Saq aquifer

The origin of the groundwater in the Saq aquifer, as well as the recharge timing, are determined from analysis of the isotopic composition of groundwater samples collected from the aquifer. Twenty-four groundwater samples, locations shown in Fig. 1, were collected in high-density polyethylene bottles, which were then tightly capped, and transported from Saudi Arabia to the United States. The hydrogen (H) and oxygen (O) isotopic ratios of water samples were analyzed by wavelength scanned cavity ring-down spectrometry on un-acidified samples by a Picarro L-1102i WS-CRDS analyzer (Lehmann et al., 2009) at the University of Massachusetts, Amherst. Samples were vaporized at 110°C . International reference standards (IAEA, Vienna, Austria) were used to calibrate the

instrument on the VSMOW-VSLAP scale, and working standards were used with each analytical run. Long-term averages of internal laboratory standard analytical results yield an instrumental precision of 0.51‰ for $\delta^2\text{H}$ and 0.08‰ for $\delta^{18}\text{O}$. The house reference standards for this particular run were an instrumental precision of 1.03‰ for $\delta^2\text{H}$ and 0.16‰ for $\delta^{18}\text{O}$. Hydrogen and oxygen stable isotope ratios are reported using conventional delta (δ) notation, in units of per mil (‰) deviation relative to the Vienna's standard mean ocean water (V-SMOW) and PeeDee Belemnite (PDB) standards (Coplen 1996), where:

$$\delta, \text{‰} = [(\text{R}_{\text{sample}} / \text{R}_{\text{standard}}) - 1] \times 1000 \quad (1)$$

and where $R = {}^2\text{H}/{}^1\text{H}$ or ${}^{18}\text{O}/{}^{16}\text{O}$ and the standard is Vienna Standard Mean Ocean Water (Coplen, 1996).

The isotopic analyses of the collected groundwater samples are listed in Table 1. Two of these samples are collected from irrigation wells; the remaining samples are collected from domestic wells. The examined wells are tapping the Saq and the alluvial aquifer systems. The O and H stable isotopic ratio of the collected groundwater samples are shown in Figure 3. Examination of Fig. 3 and Table 1 reveals two main groups of groundwater samples. Group (I) groundwater samples are collected from wells tapping the Saq aquifer system (sample ID: 1–12; well depth: 144–607 m), whereas the Group (II) samples are collected from wells tapping the alluvial aquifer

system (sample ID: 13–24; well depth: 12–150 m). The hydrogen ($\delta^2\text{H}$) and oxygen ($\delta^{18}\text{O}$) isotopic compositions of the groundwater samples collected from the Saq aquifer (Group I) are more depleted ($\delta^2\text{H}$: -16.92‰ to -46.37‰ ; $\delta^{18}\text{O}$: -3.64‰ to -6.05‰) compared to those collected from the alluvial aquifer system ($\delta^2\text{H}$: -10.36‰ to $+1.38\text{‰}$; $\delta^{18}\text{O}$: 2.96‰ to $+0.10\text{‰}$). Isotopic compositions of Group I samples could represent either high elevation recharge from mountainous areas or the Red Sea Hills, and/or recharge formed mainly of paleo-water "fossil water" precipitated during moist climate intervals of the late Pleistocene. The fossil water hypothesis is more acceptable to us given the fact that the isotopic composition of the most depleted sample (ID: 10; $\delta^2\text{H}$: -46.37‰ ; $\delta^{18}\text{O}$: -6.05‰) is similar to that of the fossil water samples collected from similar geological, environmental, and climatic settings ($\delta^2\text{H}$: -72‰ to -81‰ ; $\delta^{18}\text{O}$: -10.6‰ to -11.9‰ ; Sultan et al., 1997, 2011).

The $\delta^2\text{H}$ and $\delta^{18}\text{O}$ isotopic compositions of Group II samples and the rest of the Group I samples represent various degrees of mixing between two endmembers, one being fossil waters (ID: 10; $\delta^2\text{H}$: -46.37‰ ; $\delta^{18}\text{O}$: -6.05‰) and the other being modern precipitation ($\delta^2\text{H}$: $+16.70\text{‰}$; $\delta^{18}\text{O}$: $+0.37\text{‰}$). This hypothesis is supported by the observed progressive depletion in the isotopic composition with distance from the recharge areas. For example, within Group (I), the isotopic compositions of the groundwater samples collected from, and/or close to, the recharge areas cropping out at the foothills of the basement outcrops (e.g., sample 9) are

less depleted compared to those collected away from the recharge areas (e.g., sample 10).

6. Quantifying Modern Recharge to the Saq Aquifer

Two independent approaches were used to quantify the amounts and timing of modern recharge to the Saq aquifer. The first one is based on the analysis of GRACE data, whereas the second approach focused on rainfall-runoff modeling using the SWAT model was utilized.

(A) Modern Recharge to the Saq Aquifer: GRACE Constraints

GRACE is a joint NASA/DLR mission that was launched in March 2002 to map the Earth's static and temporal global gravity fields (Tapley et al. 2004). The variability in Earth's gravity field is directly related to the spatiotemporal variations in the total vertically integrated terrestrial water storage (TWS; Wahr et al., 1998). The GRACE-derived Terrestrial Water Storage (TWS) is used extensively in hydrology, oceanology, cryosphere, and solid Earth fields (e.g., Ahmed et al. 2011; Famiglietti and Rodell 2013; Ahmed et al. 2014; Wouters et al. 2014; Famiglietti 2014; Ahmed et al. 2016; Mohamed et al. 2016).

In this study, the monthly (April 2002 to December 2016) mass

concentration (mascons; release 05; version 1; $0.5^\circ \times 0.5^\circ$ grid), GRACE-derived TWS solutions generated by the University of Texas Center for Space Research (UT-CSR) were used. Previous work has demonstrated that the mascon solutions provide higher signal-to-noise ratio, higher spatial resolution, and reduced error compared to other solutions (e.g., spherical harmonics) and do not require spectral (e.g., describing) and spatial (e.g., smoothing) filtering or any empirical scaling techniques (Luthcke et al. 2013; Watkins et al. 2015; Save et al. 2016; Wiese et al. 2016; Scanlon et al. 2016). The UT-CSR mascon solutions approach uses the geodesic grid technique to model the surface of Earth using an equal area gridded representation of the planet via 40,962 cells (40,950 hexagons + 12 pentagons; Save et al. 2012; Save et al. 2016).

The GRACE-derived TWS time series, generated by spatially averaging all TWS results over the Saq aquifer, is shown in Figure 4a. Errors associated with monthly TWS as well as calculated trend values were then estimated (Tiwari et al. 2009; Scanlon et al. 2016). First, we fitted the monthly TWSGRACE time series using trend, and we calculated the seasonal terms and set residuals. We then smoothed these residuals using a 13-month moving average and removed the trend to calculate a second set of residuals. Next, we performed Monte Carlo simulations by fitting trends and seasonal terms for 10,000 synthetic monthly datasets, each with values chosen from a population of

Gaussian-distributed numbers having a standard deviation similar to that of the second set of residuals. Finally, the standard deviation of the extracted synthetic trends was interpreted as the trend error for the GRACE-derived TWS.

We estimated secular trends by simultaneously fitting a trend and seasonal terms (e.g., annual and semiannual) to the GRACE-derived TWS time series. The extracted trend values were then statistically tested adapting the Student's t-test. The GRACE-derived TWS trend for the entire period (April 2002 to December 2016) is estimated at -8.55 ± 0.22 mm/yr (-3.76 ± 0.10 km³/yr). Moreover, piecewise trend analysis of the GRACE-derived TWS is conducted over three distinctive periods: April 2002 to March 2006 (Period I), April 2006 to June 2012 (Period II), and July 2012 to December 2016 (Period III). The trend results, along with their statistical significance, are shown in Table 2. Examination of Fig. 4a and Table 2 shows that the Saq aquifer is witnessing a near-steady state in GRACE-derived TWS during Period I (Period I: -0.73 ± 0.95 mm/yr [-0.32 ± 0.42 km³/yr]), a severe decline in GRACE-derived TWS during Period II (Period II: -11.05 ± 0.44 mm/yr [-4.86 ± 0.19 km³/yr]), and a modest decrease in GRACE-derived TWS during Period III (Period III: -4.04 ± 1.62 mm/yr [-1.78 ± 0.71 km³/yr]). The temporal variability in GRACE-derived TWS is related to temporal variations in one or more of the TWS compartments (e.g., soil moisture and groundwater).

Given the fact that GRACE cannot distinguish between anomalies resulting from different components of TWS (e.g., soil moisture and groundwater), the contributions of soil moisture storage need to be quantified and removed from GRACE-derived TWS (Fig. 4a) to calculate groundwater storage (GWS). Soil moisture data were extracted from the Global Land Data Assimilation System (GLDAS). GLDAS is a NASA-developed land surface modeling system which performs advanced simulations of climatic and hydrologic variables using field and satellite-based observations (Rodell et al. 2004). The GLDAS model simulates soil moisture through four model versions: VIC, CLM, Noah, and Mosaic (Koster and Suarez 1996; Liang et al. 1996; Koren et al. 1999; Dai et al. 2003; Rodell et al. 2004). The soil moisture time series (Fig. 4b) over the Saq aquifer was calculated by averaging the soil moisture estimates from the four GLDAS model versions. The soil moisture monthly errors were calculated as the mean monthly standard deviation from the four GLDAS model simulations (e.g., Tiwari et al. 2009; Voss et al. 2013; Castle et al. 2014; Joodaki et al. 2014). Trends in soil moisture time series were quantified using the same approach used for GRACE-derived TWS data.

Fig. 4b shows that the GLDAS-derived soil moisture estimate is witnessing an overall depletion of -2.21 ± 0.07 mm/yr (-0.97 ± 0.03 km³/yr) during the entire investigated period (April 2002 to December 2016). Inspection of piecewise trend analysis results (Table 2) indicates

that the GLDAS-derived soil moisture estimate is always declining during the three investigated periods but at varying rates (Period I: -3.23 ± 0.27 mm/yr [-1.42 ± 0.12 km³/yr]; Period II: -2.13 ± 0.13 mm/yr [-0.94 ± 0.06 km³/yr]; Period III: -0.94 ± 0.23 mm/yr [-0.41 ± 0.10 km³/yr]).

The GRACE-derived GWS time series over the Saq aquifer (Fig. 4c) is generated by subtracting the GLDAS-derived soil moisture storage (Fig. 4b) from the GRACE-derived TWS (Fig. 4a). The monthly GWS uncertainties were calculated by summing, in quadrature, the contributions from GRACE-derived TWS errors to GLDAS-derived soil moisture errors. Trends in GWS time series were quantified using the same approach used for GRACE-derived TWS data.

Inspection of Fig. 4c shows that the Saq aquifer is witnessing an overall GWS decline of -6.34 ± 0.22 mm/yr (-2.79 ± 0.10 km³/yr). Piecewise trend analysis results (Table 2) shows that the Saq aquifer is experiencing a GWS increase ($+2.50 \pm 0.92$ mm/yr; $+1.10 \pm 0.40$ km³/yr) during Period I, followed by a sharp GWS decrease (-8.92 ± 0.41 mm/yr; -3.92 ± 0.18 km³/yr) during Period II, then a modest GWS decline during period III (-3.10 ± 1.59 mm/yr; -1.36 ± 0.70 km³/yr).

To quantify the recharge rates during the investigated periods, we added the summation of natural discharge and anthropogenic groundwater extraction to the GWS trends utilizing the following

equation:

$$\mathbf{Recharge} = \Delta\mathbf{GWS} + \mathbf{Discharge} \ (\mathbf{natural} + \mathbf{anthropogenic}). \quad (2)$$

The discharge rate of the Saq aquifer system over the last decade was estimated at ~8.00 km³/yr (18.20 mm/yr; Sultan et al. 2007; Mohamed et al. 2016). Following Equation 2, the recharge rate for the Saq aquifer is estimated at 5.21 ± 0.10 km³/yr (11.85 ± 0.22 mm/yr) during the entire investigated period. The recharge rate of the Saq aquifer during Periods I, II, and III is estimated at 9.10 ± 0.40 km³/yr, 4.08 ± 0.18 km³/yr, and 6.64 ± 0.70 km³/yr, respectively.

The temporal variations in GRACE-derived TWS and GWS are related to the temporal variations in groundwater extraction rates and irrigated areas (e.g., Fallatah et al., 2017; Ahmed et al., 2016). For example, the total areas for the irrigated lands decreased from 3.56 x 10⁶ hectares during the period from 2000 to 2006 to 2.76 x 10⁶ hectares during the period from 2006 to 2012 (MEWA, 2016). Moreover, the variations in recharge rates of the Saq aquifer during the investigated periods are related to the temporal variations in groundwater extraction and rainfall rates. The AAR was estimated at 79 mm, 51 mm, and 75 mm during Periods I, II, and III, respectively. Examination of AAR and recharge rates over the Saq Aquifer shows an obvious correspondence of the recharge rates on the rainfall amounts. It is worth mentioning that a one-to-one correspondence, in

magnitudes between recharge and AAR, is not to be expected, given that AAR could be redistributed as runoff and evapotranspiration that could affect the spatial and temporal distribution of the precipitated water, and hence the recharge locations and magnitudes.

(B) Modern Recharge to the Saq Aquifer: Modeling Constraints

The modern recharge of the Saq aquifer was quantified using SWAT, a catchment-based, semi- distributed hydrologic model that was developed for continuous simulation of surface runoff and potential recharge to the groundwater system. Among other things, the SWAT model simulates overland flow, channel flow, transmission losses, evaporation and evapotranspiration, and potential recharge (Arnold & Fohrer, 2005; Arnold, Srinivasan, Muttiah, & Williams, 1998). SWAT has been used to quantify the recharge rates in similar geologic environments and settings, including but not limited to the Eastern Desert (Milewski et al., 2009) and Sinai Peninsula (Sultan et al., 2011) of Egypt, the Saudi Red Sea watersheds (Sultan et al., 2015), and Kuwait (Aldosari et al., 2010).

In our simulations, the SWAT model used the US Department of Agriculture Soil Conservation Service method (SCS, 1972) to quantify the initial losses and direct overland flows. We estimated channel flows using the Muskingum routing method (McCarthy, 1938), and we used Manning's coefficient for uniform flow in a channel to calculate

the rate and velocity of flow in a reach segment for a given time step. Evaporation was estimated using the Penman-Monteith method (Monteith, 1981).

The SWAT model climatic inputs include rainfall, minimum and maximum temperature, solar radiation, relative humidity and wind speed. The climatic data were extracted from the Global Weather Data (GWD) for SWAT database (available at <http://globalweather.tamu.edu/>). The GWD-derived rainfall data was validated against available rain gauge records. A comparison between monthly GWD-derived rainfall records and the available rain gauges is shown in Figure 5. Locations of the selected rain gauges are

shown in Figure 6. Examination of Fig. 5 reveals satisfactory general correspondence (R^2 : 0.72 to 0.85) between the average monthly rainfall measured in the field and that obtained from GWD. We should note that a one-to-one correspondence between GWD and gauge-derived rainfall measurements is not expected given the fact that GWD integrates measurements over a large area ($\sim 38 \text{ km} \times 38 \text{ km}$).

The SWAT topographic data input was extracted from the Shuttle Radar Topography Mission (SRTM)-derived Digital Elevation Model (DEM; spatial resolution: 90 m; available at <http://dwtkns.com/srtm/>).

The SWAT model uses the DEM data to delineate watersheds, extract channel networks, and calculate the morphometric parameters (e.g., slope angle, channel slope, channel length and channel width, etc.).

The soil data inputs for SWAT model were extracted from Saudi Arabia geological maps (SGS, 1990). Five main soil types were recognized in the study area: alluvial sediments, sandstone, shale, limestone, and basement rocks. The land use data were extracted from the Global Land Cover 30-meter database (available at <http://www.globeland30.org/GLC30Download/index.aspx>).

SWAT simulations were performed at daily time steps for the period from 1998 to 2014 given the input GWD data availability. A manual calibration routine was applied to calibrate the SWAT model utilizing the model parameters used in Sultan et al. (2015). Several approaches have been applied to calculate the recharge rates out of the SWAT model in similar geologic, environmental, and climatic settings. For example, Al-Dousari et al. (2010) estimate the recharge as the summation of transmission losses and 5% of the initial losses; Milewski et al. (2009) and Sultan et al. (2011) used the transmission losses as a recharge rate; Milewski et al. (2014) assumed that the recharge rate equals the initial losses. In this study, we've adapted the approach of Sultan et al. (2015) to calculate potential recharge rates of the investigated watersheds.

Table 3 lists the model results for the four investigated watersheds. Streamflow was calculated by subtracting the transmission losses from the summation of surface runoff, lateral flow, and return flow. The potential recharge, however, was calculated by subtracting the

summation of amounts of water moving from shallow aquifers to plants/soil by re-evaporation (Revap) and return flow from the summation of percolation to shallow aquifer and transmission losses. Finally, the initial losses were estimated by subtracting the summation of potential recharge and streamflow from precipitation.

Examination of Table 3 indicates that, during the period from 1998 to 2014, the four investigated watersheds, Al Baten, Al Rumah, Al Sarhan, and Tabuk, shown in Fig. 6, received average annual precipitation of 19.20 km³. Of this precipitation, an average of 9.83 km³ (51% of the total rainfall) is partitioned as potential recharge. It is worth mentioning that by increasing the proportion of areas occupied by basement and/or rising precipitation amounts, the stream flow proportion is increased. Moreover, the higher the amount of precipitation and the stream flow, the higher the amount of potential recharge.

7. Sustainable Utilization and Management of the Saq Aquifer System

GRACE-based average annual groundwater recharge to the Saq aquifer system during the period from April 2002 to December 2016 was estimated at 5.21 ± 0.10 km³, assuming a constant average yearly groundwater extraction amount of 8.00 km³. Moreover, the SWAT-based average annual groundwater recharge during the period from

January 1998 to December 2014 was estimated at 9.83 km³. The difference between the recharge rates calculated from the two independent sources might be related to one or more of the following: (1) variation in the spatial extent of the examined areas (GRACE area: 0.43 x 10⁶ km²; SWAT area: 0.37 x 10⁶ km²), (2) difference in the monitored time periods (GRACE: April 2002 to December 2016; SWAT: January 1998 to December 2014), or (3) difference in the approach used to calculate recharge in each technique.

Sustainable utilization and management of the water resources of the Saq aquifer system could be achieved by adopting the following practices. First, groundwater extraction areas should be located at, or near to, the center of the aquifer; areas around the aquifer borders are expected to be depleted first as extraction increases with time. Second, groundwater extraction rates should be limited to maintain the GWS trend at ≥ 0 ; positive GWS trends means the extraction is less than the recharge, zero GWS trend implies extraction equals recharge, and negative GWS trends implies the extraction is greater than the recharge. Third, utilize the well spacing act such that the effects on the aquifer are not concentrated at any spot and well yields are sustained. The optimum well spacing is a function of a total number of wells, aquifer thickness, regional groundwater velocity, and pumping rate of an extraction well (Ahmed 1995), expressed as:

$$\textit{Optimum wellspacing} = \frac{\textit{Well pumping rate}}{\textit{Aquifer thickness} \times \textit{Groundwater velocity}} \times 0.4765. \quad (3)$$

8. Discussion and Conclusion

In Saudi Arabia, like in many other arid/semi-arid countries of the world, freshwater resources are crucial to improving human health and livelihoods, sustaining economic growth, and achieving sustainable development. Recent studies have shown that the Saq aquifer system, one of the most significant freshwater resources in Saudi Arabia, is not being used sustainably and is witnessing rapid groundwater depletion. Hence, actions are required to use the water resources of the Saq aquifer in Saudi Arabia sustainably. The most crucial of these is to quantify the modern recharge to their major aquifer systems.

In this study, we developed and applied an integrated approach to quantify the recharge rates of the Saq aquifer system. Our results indicate that throughout the recharge spatial domain of the Saq aquifer, the AAR was estimated to be over 15 mm. Examination of the groundwater samples collected from the Saq aquifer system reveals two main groups (Group I: well depths: 144–607 m; and Group II: well depths: 12–150 m). Group I (Saq aquifer; fissile water) isotopic compositions are more depleted ($\delta^{2}\text{H}$: -16.92‰ to -46.37‰ ; $\delta^{18}\text{O}$: -3.64‰ to -6.05‰) compared to Group II (alluvial aquifer; mixed waters) isotopic

compositions ($\delta^{2}\text{H}$: -10.36‰ to $+1.38\text{‰}$; $\delta^{18}\text{O}$: 2.96‰ to $+0.10\text{‰}$). Analysis of GRACE-derived TWS and GWS time series indicates that the Saq aquifer is receiving annual recharge $5.21 \pm 0.10 \text{ km}^3/\text{yr}$ ($11.85 \pm 0.22 \text{ mm/yr}$) during the entire investigated period (April 2002 to December 2016). Assuming constant groundwater extraction rates ($8 \text{ km}^3/\text{yr}$), the recharge rate of the Saq aquifer is witnessing a temporal variability. The temporal variations in GRACE-derived TWS, GWS, and recharge rates are related to the temporal variations in groundwater extraction rates, rainfall rates, and extent of irrigated regions. Analysis of SWAT results indicates that, during the period from 1998 to 2014, the four investigated watersheds (Al Baten, Al Rumah, Al Sarhan, and Tabuk) received average annual precipitation of 19.20 km^3 . Of this precipitation, an average of 9.83 km^3 (51% of the total rainfall) is partitioned as potential recharge.

Our results, we believe, will contribute to the effective and efficient utilization of the Saq aquifer water resources and will be used to promote the sustainable development of the Arabian Peninsula's natural resources in general. This study's findings are being shared with decision makers in relevant governmental agencies to develop sustainable management scenarios for the water resources of the Saq aquifer.

9. Acknowledgments

The authors are thankful Ministry of Environment Water and Agriculture in Saudi Arabia for providing the scientific data to improve this paper. Special acknowledgments are extended to Ministry of Water Tabuk Branch for providing all facilities needed to complete this work.

10. References

1. Abunayyan, BRGM (2008) Investigations for updating the groundwater mathematical model(s) of the Saq overlying aquifers. Ministry of Water and Electricity, Riyadh, Saudi Arabia. <https://www.scribd.com/document/16845648/Saq-Aquifer-Saudi-Arabia-2008>
2. Abouelmagd, A., Sultan, M., Milewski, A., Kehewa, A. E., Sturchio, N., Soliman, F., Krishnamurthy, R. V., & Cutrim, E. (2012). Toward a better understanding of palaeoclimatic regimes that recharged the fossil aquifers in North Africa: Inferences from stable isotope and remote sensing data. *Palaeogeography, Palaeoclimatology, Palaeoecology* 329–330, 137–149. doi: 10.1016/j.palaeo.2012.02.024
3. Abouelmagd, A., Sultan, M., Sturchio, N. C., ... Chouinard, K. (2014). Paleoclimate record in the Nubian Sandstone Aquifer, Sinai Peninsula, Egypt. *Quaternary Research* (United States) 81, 158–167. doi: 10.1016/j.yqres.2013.10.017
4. Adeyewa, Z. D., & Nakamura, K. (2003). Validation of TRMM radar rainfall data over major climatic regions in Africa. *Journal of Applied Meteorology* 42, 331–347. doi: 10.1175/1520-0450(2003)042<0331:VOTRRD>2.0.CO;2
5. Ahmed, M., Sultan, M., Wahr, J., & Yan, E. (2014). The

- use of GRACE data to monitor natural and anthropogenic induced variations in water availability across Africa. *Earth Science Reviews* 136:289–300. doi: 10.1016/j.earscirev.2014.05.009
6. Ahmed, M., Sultan, M., Wahr J, Yan, E., Milewski, A., Sauck, W., Becker, R., & Welton, B. (2011) Integration of GRACE (Gravity Recovery and Climate Experiment) data with traditional data sets for a better understanding of the time-dependent water partitioning in African watersheds. *Geology* 39:479–482. doi: 10.1130/G31812.1
 7. Ahmed, M., Sultan, M., Yan, E., & Wahr, J. (2016). Assessing and improving land surface model outputs over Africa using GRACE, field, and remote sensing data. *Surveys in Geophysics* 37, 529–556. doi: 10.1007/s10712-016-9360-8
 8. Ahmed, W. (1995). Optimum spacing of extraction wells. *Hydrogeology* 3, 64–74.
 9. Al-Dousari, A., Milewski, A., Din, S. U., & Ahmed, M. (2010). Remote sensing inputs to SWAT model for groundwater recharge estimates in Kuwait. *Advances in Natural and Applied Sciences*, 4(1), 71–77.
 10. Alsharhan, A. S., Rizk, Z. A., Nairn, A. E. M., Bakhit, D. W., & Alhajari, S. A. (Eds.). (2001). *Hydrogeology of an*

arid region: the Arabian Gulf and adjoining areas. Elsevier.

11. Alsharhan, A. S. (2003). Petroleum geology and potential hydrocarbon plays in the Gulf of Suez rift basin, Egypt. *AAPG bulletin*, 87(1), 143-180.
12. Arnold, J. G., & Fohrer, N. (2005). SWAT2000: current capabilities and research opportunities in applied watershed modeling. *Hydrological Processes*, 19(3), 563–572.
13. Arnold, J. G., Srinivasan, R., Mutiah, R. S., & Williams, J. R. (1998). Large area hydrologic modeling and assessment part I: model development. *Journal of the American Water Resources Association*, 34(1), 73–89.
14. Bayumi, T. (2008). Quantitative Groundwater Resources Evaluation in the Lower Part of Yalamlam Basin, Makkah Al Mukarramah, Western Saudi Arabia. *Journal of King Abdulaziz University of Science* 19, 35–56. doi: 10.4197/Ear.19–1.3
15. Beaumont, P. (1977). Water and Development in Saudi Arabia. *The Geographical Journal* 143, 42. doi: 10.2307/1796674
16. Beighley, R. E., Ray, R. L., He, Y., Shum, C. K.. (2011). Comparing satellite-derived precipitation datasets using the Hillslope River Routing (HRR) model in the CongoRiver Basin. *Hydrological Processes* 25, 3216–3229. doi:

10.1002/hyp.8045

17. Castle, S., Thomas, B., Reager, J., Rodell, M., Swenson, S. C., & Famiglietti, J. S. (2014). Groundwater depletion during drought threatens future water security of the Colorado River Basin. *Geophysical Research Letters* 10, 5904–5911. doi: 10.1002/2014GL061055. Received
18. Chowdhury, S., & Al-Zahrani, M. (2015). Characterizing water resources and trends of sector-wise water consumptions in Saudi Arabia. *Journal of King Saud University- of Engineering Sciences*, 27(1), 68–82
19. Coplen, T. B. (1996). New guidelines for reporting stable hydrogen, carbon, and oxygen isotope-ratio data. *Geochimica et Cosmochimica Acta* 60, 3359–3360. doi: 10.1016/0016-7037(96)00263-3
20. Dai, Y., Zeng, X., Dickinson, R. E., Yang, Z. L. (2003). The common land model. *Bulletin of the American Meteorological Society* 84, 1013–1023. doi: 10.1175/BAMS-84-8-1013
21. Dinku, T., Ceccato, P., Grover-Kopec, E., Lemma, M., Connor, S. J., & Ropelewski, C. F. (2007). Validation of satellite rainfall products over East Africa's complex topography. *International Journal of Remote Sensing* 28, 1503–1526. doi: 10.1080/01431160600954688

22. Dinku, T., Chidzambwa, S., Ceccato, P., Connor, S. J., & Ropelewski, C. F. (2008). Validation of high-resolution satellite rainfall products over complex terrain. *International Journal of Remote Sensing* 29, 4097–4110. doi: 10.1080/01431160701772526
23. Famiglietti, J. S. (2014). The global groundwater crisis. *Nature Climate Change* 4, 945– 948. doi: 10.1038/nclimate2425
24. Famiglietti, J. S., Rodell, M. (2013). Water in the balance. *Science* (80-) 340, 1300– 1301. doi: 10.1126/science.1236460
25. Fallatah, O. A., Ahmed, M., Save, H., & Akanda, A. S. (2017). Quantifying temporal variations in water resources of a vulnerable Middle Eastern transboundary aquifer system. *Hydrological Processes*. 2017;1–11. <https://doi.org/10.1002/hyp.11285>
26. Huffman, G. J, Bolvin, D. T., Nelkin, E. J., & Stocker, E. F. (2007). The TRMM multi- satellite precipitation analysis (TMPA): Quasi-global, multiyear, combined-sensor precipitation estimates at fine scales. *Journal of Hydrometeorology* 8, 38–55. doi: 10.1175/JHM560.1
27. Joodaki, G., Wahr, J., & Swenson, S. (2014). Estimating the human contribution to groundwater depletion in the Middle

- East, from GRACE data, land surface models, and well observations Gholamreza. *Water Resources Research* 50, 1–14. doi: 10.1002/2013WR014633. Received
28. Koren, V., Schaake, J., Mitchell, K., Duan, Q.-Y., Chen, F., & Baker, J. M. (1999). A parameterization of snowpack and frozen ground intended for NCEP weather and climate models. *Journal of Geophysical Research* 104, 19569–19585. doi: 10.1029/1999JD900232.
29. Koster, R. D., & Suarez, M. J. (1996). Energy and water balance calculations in the Mosaic LSM. National Aeronautics and Space Administration, Goddard Space Flight Center, Laboratory for Atmospheres, Data Assimilation Office: Laboratory for Hydrospheric Processes.
30. Lehmann, K. K., Berden, G., & Engeln, R. (2009). An introduction to cavity ring-down spectrometry, in Berden, G., and Engeln, R., eds., *Cavity Ring-Down Spectrometry Techniques and Applications*. London: John Wiley & Sons Ltd.
31. Liang, X., Lettenmaier, D. P., & Wood, E. F. (1996). One-dimensional statistical dynamic representation of subgrid spatial variability of precipitation in the two-layer variable infiltration capacity model. *Journal of Geophysical*

Research 101, 21403. doi: 10.1029/96JD01448

32. Luthcke, S. B., Sabaka, T. J., Loomis, B. D., Arendt, A. A., McCarthy, J. J., & Camp, J. (2013). Antarctica, Greenland, and Gulf of Alaska land-ice evolution from an iterated GRACE global mascon solution. *Journal of Glaciology* 59, 613–631. doi: 10.3189/2013JoG12J147
33. McCarthy, G.T. (1938). The unit hydrograph and flood routing. Conference of North Atlantic Division, US Army Corps of Engineers. Providence: Army Engineer District, Providence.
34. Milewski, A., Sultan, M., Al-Dousari, A., & Yan, E. (2014). Geologic and hydrologic settings for development of freshwater lenses in arid lands. *Hydrological Processes*, 28(7), 3185–3194.
35. Milewski, A., Sultan, M., Yan, E., Becker, R., Abdeldayem, A., Soliman, F., & Gelil, K. (2009). A remote sensing solution for estimating runoff and recharge in arid environments. *Journal of Hydrology*, 373(1), 1–14.
36. Ministry of Environment, W. a. A. (Jan 1, 2017). "Estimated Area and Production by Administrative Regions." <http://www.data.gov.sa/en/group/agriculture-and-fishing>
37. Mohamed, A., Sultan, M., Ahmed, M., Yan, E., & Ahmed,

- E. (2016). Aquifer recharge, depletion, and connectivity: Inferences from GRACE, land surface models, geochemical, and geophysical data. *GSA Bulletin* 1–13. doi: 10.1130/B31460.1
38. Monteith, J. L. (1981). Evaporation and surface temperature. *Quarterly Journal of the Royal Meteorological Society*, 107(451), 1–27.
39. Nairn, A. E. M., & Alsharhan, A. S. (1997). *Sedimentary basins and petroleum geology of the Middle East*. Elsevier.
40. Ouda, O. K. (2013). Towards an assessment of Saudi Arabia public awareness of water shortage problem. *Resources and Environment*, 3(1), 10–13.
41. Rodell, M., Houser, P. R., Jambor, U.,...Toll, D. (2004) The global land data assimilation system. *Bulletin of the American Meteorological Society* 85, 381–394. doi: 10.1175/BAMS-85-3-381
42. Save, H., Bettadpur, S., & Tapley, B. D. (2016). High-resolution CSR GRACE RL05 mascons. *Journal of Geophysical Research: Solid Earth*, 121(10), 7547-7569.
43. Save, H., Bettadpur, S., & Tapley, B. D. (2012). Reducing errors in the GRACE gravity solutions using regularization. *Journal of Geodesy* 86, 695–711. doi: 10.1007/S00190-012-0548-5

44. Scanlon, B. R., Healy, R. W., & Cook, P. G. (2002). Choosing appropriate techniques for quantifying groundwater recharge. *Hydrogeology Journal*, 10(1), 18–39.
45. Scanlon, B. R., Zhang, Z., Save, H., Wiese, D. N., Landerer, F. W., Long, D., Longuevergne, L., & Chen, J. (2016). Global evaluation of new GRACE mascon products for hydrologic applications. *Water Resources Research* 52, 9412–9429. doi: 10.1002/2016WR019494
46. Saudi Geological Survey (SGS). (1990). Geological map of the main sedimentary rock main types in the eastern and the northern parts of the kingdom of Saudi Arabia (<http://www.sgs.org.sa/English/Pages/Default.aspx>)
47. Sultan, M., Metwally, S., Milewski, A.,...Welton, B. (2011). Modern recharge to fossil aquifers: Geochemical, geophysical, and modeling constraints. *Journal of Hydrology* 403, 14–24. doi: 10.1016/j.jhydrol.2011.03.036
48. Sultan, M., Sefry, S., & AbuAbdallah, M. (2015). Impacts of climate change on the Red Sea region and its watersheds, Saudi Arabia. In *The Red Sea* (pp. 363–377). Springer: Berlin.
49. Sultan, M., Sturchio, N., Al Sefry, S., Milewski, A., Becker, R., Nasr, I., & Sagintayev,
50. Z. (2008). Geochemical, isotopic, and remote sensing

- constraints on the origin and evolution of the Rub Al Khali aquifer system, Arabian Peninsula. *Journal of Hydrology* 356, 70–83. doi: 10.1016/j.jhydrol.2008.04.001
51. Sultan, M., Yan, E., Sturchio, N., Wagdy, A., Abdel Gelil, K., Becker, R., Manocha, N., & Milewski, A. (2007). Natural discharge: A key to sustainable utilization of fossil groundwater. *Journal of Hydrology* 335, 25–36. doi: 10.1016/j.jhydrol.2006.10.034
52. Sylla, M. B., Giorgi, F., Coppola, E., & Mariotti, L. (2013). Uncertainties in daily rainfall over Africa: assessment of gridded observation products and evaluation of a regional climate model simulation. *International Journal of Climatology* 33, 1805–1817. doi: 10.1002/joc.3551
53. Tapley, B. D., Bettadpur, S., Ries, J. C., Thompson, P. F., & Watkins, M. M. (2004). GRACE measurements of mass variability in the Earth system. *Science* 305, 503–505. doi: 10.1126/science.1099192
- Tiwari, V. M., Wahr, J., & Swenson, S. (2009) Dwindling groundwater resources in northern India, from satellite gravity observations. *Geophysical Research Letters* 36, L18401. doi: 10.1029/2009GL039401
54. Voss, K. A., Famiglietti, J. S., Lo, M., de Linage, C., Rodell, M., & Swenson, S. C. (2013). Groundwater

- depletion in the Middle East from GRACE with implications for transboundary water management in the Tigris-Euphrates-Western Iran region. *Water Resources Research* 49, 904–914. doi: 10.1002/wrcr.20078
55. Wagner, W. (2011). *Groundwater in the Arab Middle East*. Springer Science & Business Media.
56. Wahr, J., Molenaar, M., & Bryan, F. (1998). Time variability of the Earth's gravityfield: Hydrological and oceanic effects and their possible detection using GRACE. *Journal of Geophysical Research* 103, 30205–30229. doi: 10.1029/98JB02844
57. Watkins, M. M., Wiese, D. N., Yuan, D., Boening, C., & Landerer, F. W. (2015). Improved methods for observing Earth's time-variable mass distribution with GRACE using spherical cap mascons. *Journal of Geophysical Research-Solid Earth* 120, 2648–2671. doi: 10.1002/2014JB011547. Received
58. Wiese, D. N., Landerer, F. W., & Watkins, M. M. (2016). Quantifying and reducing leakage errors in the JPL RL05M GRACE mascon solution. *Water Resources Research* 52, 7490–7502. doi: 10.1002/2016WR019344
59. Wouters, B., Bonin, J. A., Chambers, D. P., et al. (2014). GRACE, time-varying gravity, Earth system dynamics and

climate change. Reports Prog Phys. doi: 10.1088/0034-4885/77/11/116801

60. Zaidi, F. K., Nazzal, Y., Ahmed, I., Naeem, M., & KamranJafri, M. (2015). Identification of potential artificial groundwater recharge zones in Northwestern Saudi Arabia using GIS and Boolean logic. *Journal of African Earth Science* 111, 156–169. doi: 10.1016/j.jafrearsci.2015.07.008

Figure Legends:

Figure 1: Location map showing the aerial distribution of major aquifer outcrops in Saudi Arabia. Also shown are the spatial domain of the Saq aquifer system (*red polygon*) and the locations of the groundwater samples (*black crosses*) examined in this study.

Figure 2: AAR (mm) extracted from TRMM over Saudi. Also shown are the spatial domain of the administrative regions (*black dashed lines*), Saq aquifer system (*black polygon*), Saq outcrop (*black area*), and the recharge domains of the Saq aquifer system (*hatched area*).

Figure 3: $\delta^2\text{H}$ versus $\delta^{18}\text{O}$ plot for the groundwater samples collected from Saq aquifer system. Also shown are the isotopic composition of modern rainfall and the Global Meteoric Water Line.

Figure 4: Temporal variations in (a) GRACE-derived TWS estimates, (b) GLDAS-derived soil moisture estimates, and (c) GRACE-derived GWS estimates averaged over the Saq aquifer system in Saudi Arabia. Also shown are the error bars in each time series.

Figure 5: Comparison between average monthly rainfall estimates reported from rain gauges and GWD-derived estimates. The degree of fitness, R^2 , is also shown for each plot.

Figure 6: The spatial distribution of the four watersheds examined by the SWAT model overlying the SRTM-derived DEM. Also shown are the GWD network and the spatial distribution of the six rain gauges shown in Fig. 5.

Tables captions:

Table 1: Well information and O and H isotopic compositions for groundwater samples collected from the Saq aquifer system in Saudi Arabia.

Table 2: Trends in water budget components averaged over the Saq aquifer system during the investigated period (April 2002 to December 2016). Trends that are significant at $\geq 65\%$ level of confidence are underlined and at $\geq 95\%$ level of confidence are normal.

Table 3: SWAT model results for the four investigated watersheds during the period from 1998 to 2014.

Figure 1.

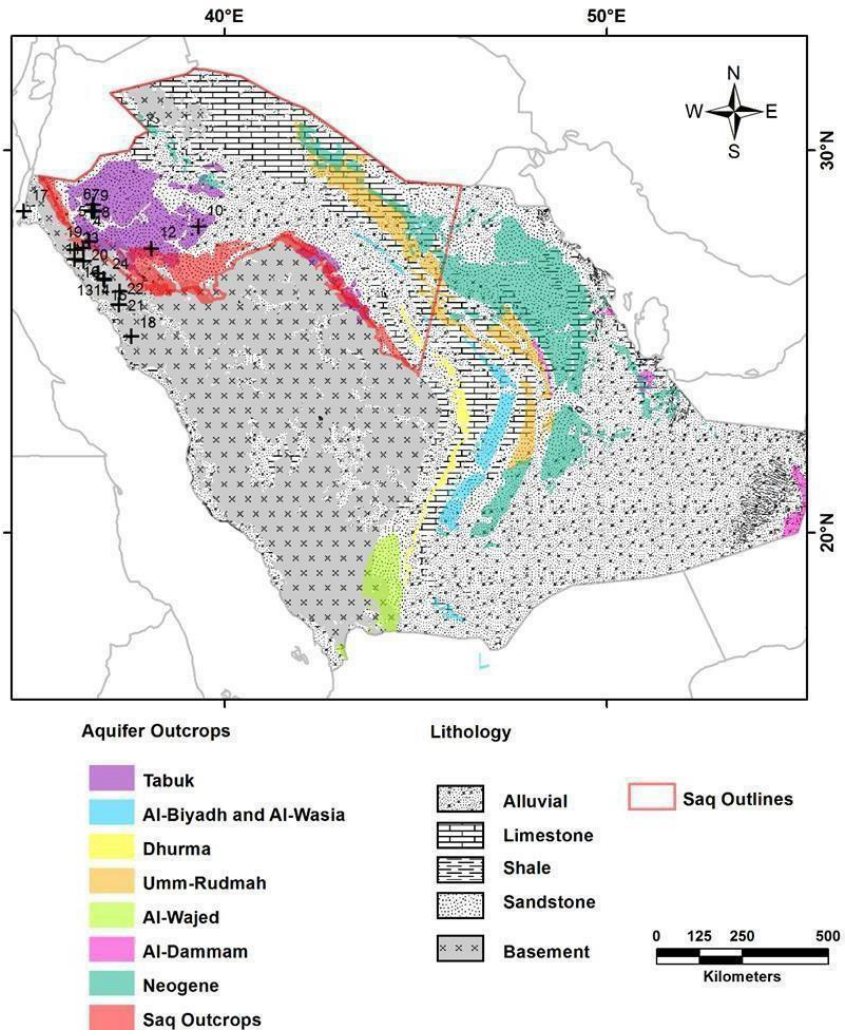


Figure 2.

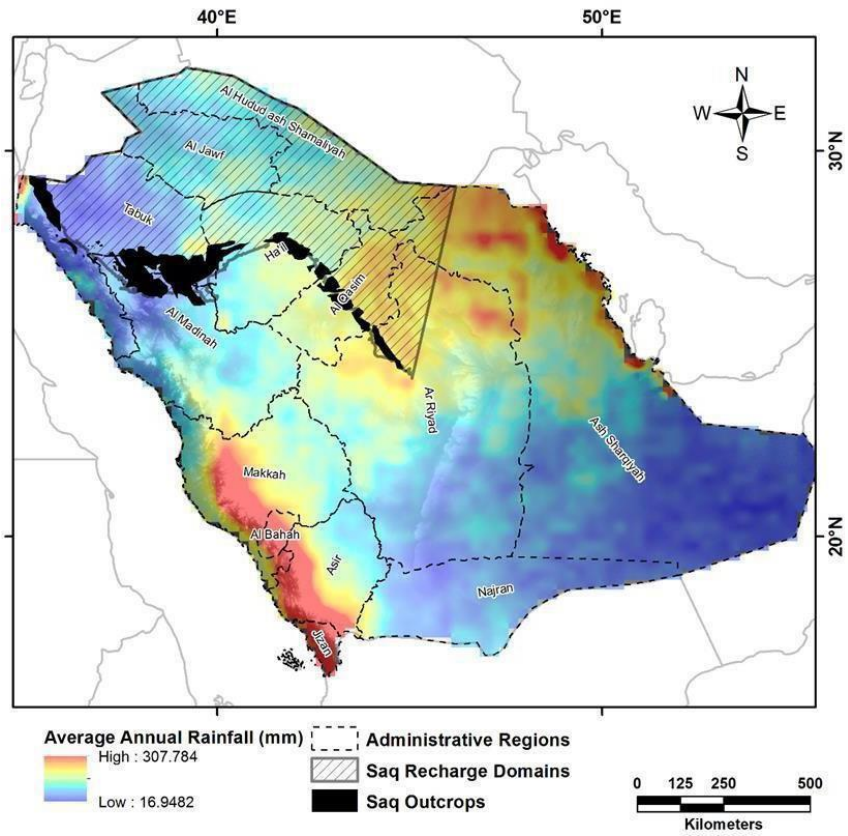


Figure 3.

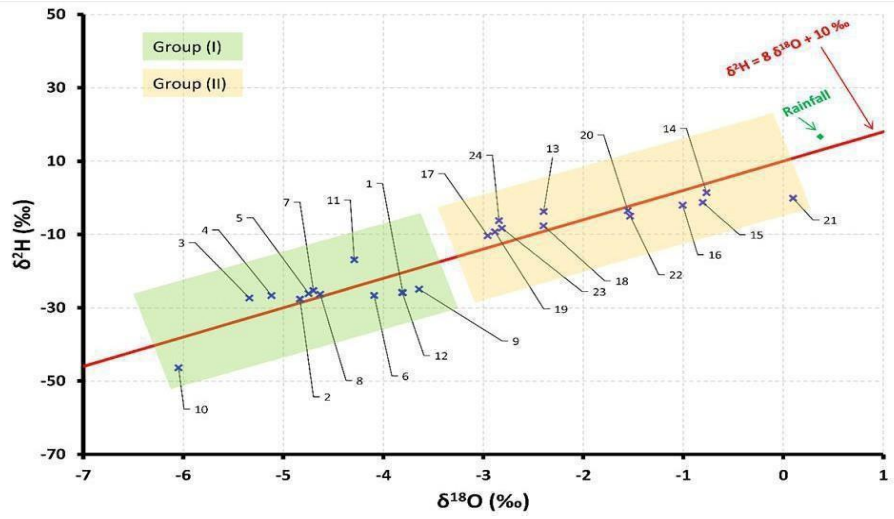


Figure 4.

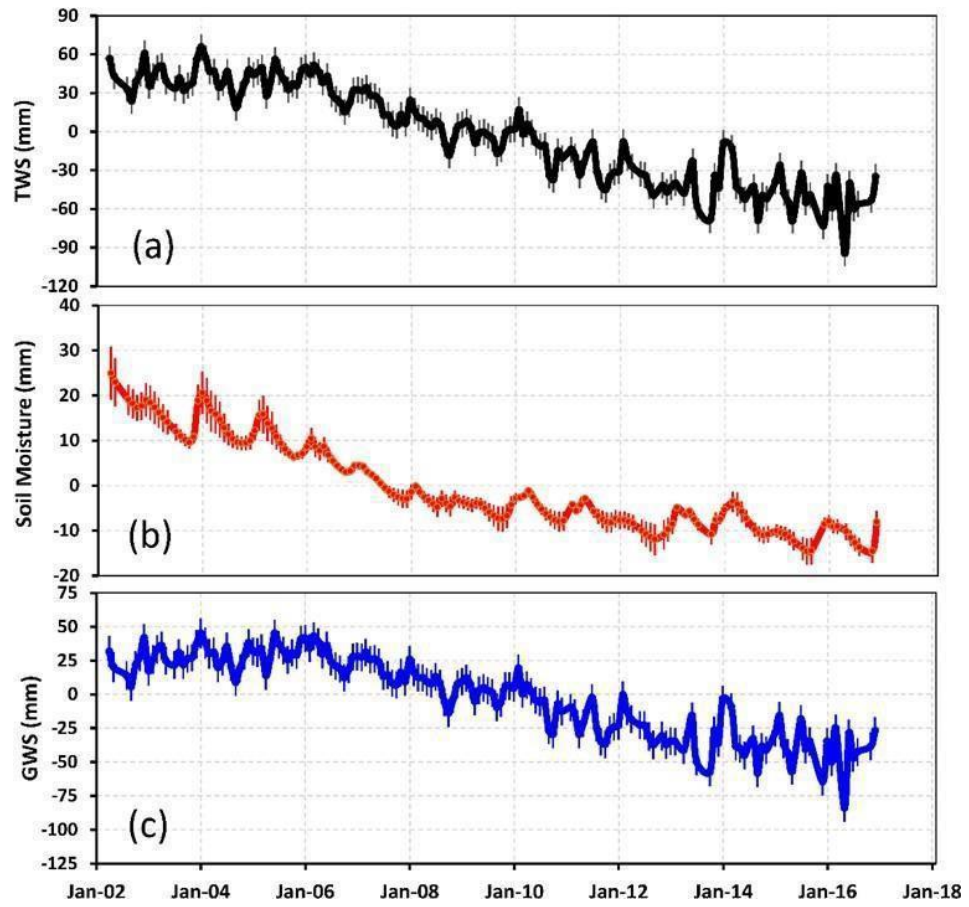


Figure 5.

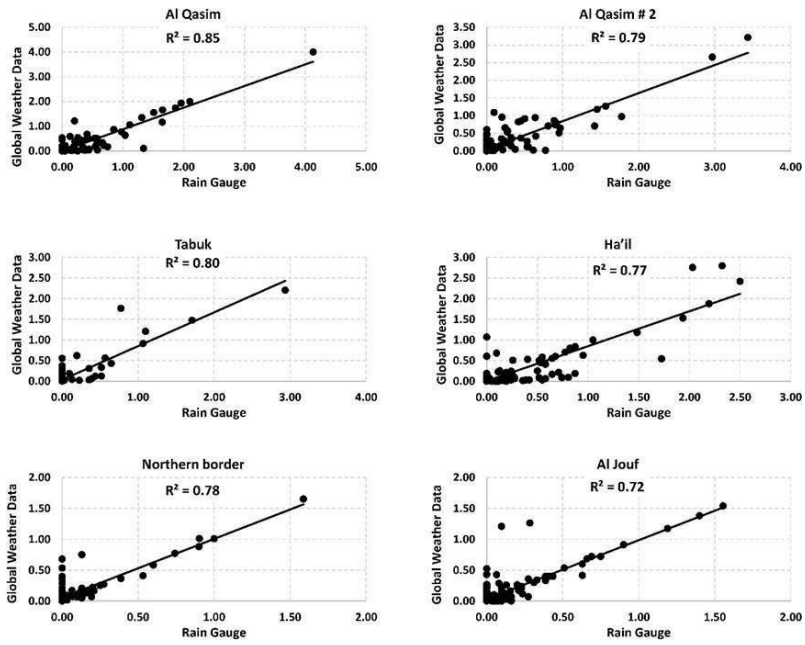


Figure 6.

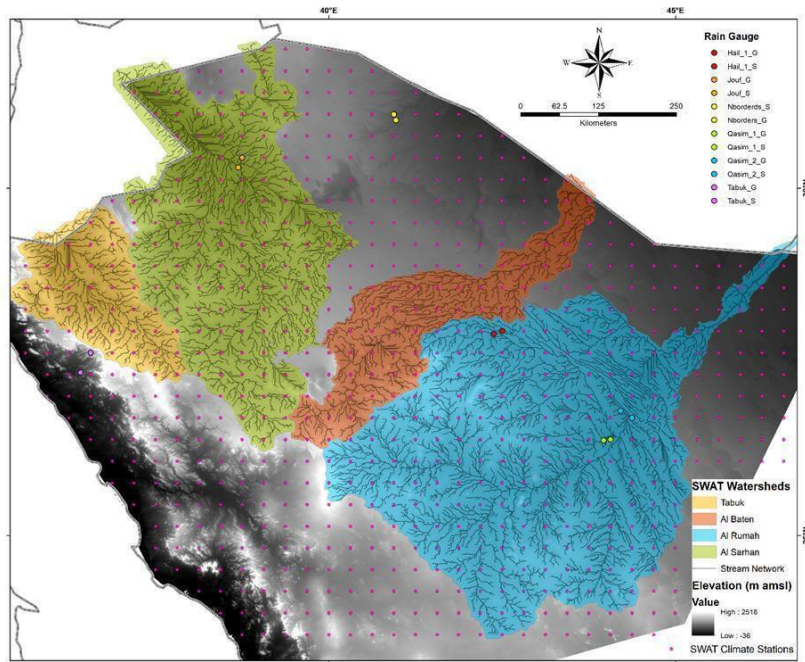


Table 1.

Well ID	log	lat	Well Use	Aquifer.N	Well.D	$\delta^{18}\text{O}(\text{‰})$	$\delta^2\text{H}(\text{‰})$	A	B
1	36.519	28.407	Demotic	Saq	607	-3.80	-25.89	0.05	0.21
2	36.558	28.413	Demotic	Saq	600	-4.83	-27.64	0.02	0.45
3	36.554	28.392	Demotic	Saq	604	-5.34	-27.32	0.04	0.1
4	36.561	28.575	Demotic	Saq	600	-5.12	-26.63	0.1	0.74
5	36.593	28.412	Demotic	Saq	605	-4.75	-26.11	0.04	0.44
6	36.519	28.424	Demotic	Saq	607	-4.09	-26.65	0.13	0.55
7	36.59	28.407	Demotic	Saq	603	-4.70	-25.33	0.07	0.33
8	36.577	28.397	Demotic	Saq	606	-4.63	-26.32	0.03	0.01
9	36.536	28.393	Demotic	Saq	605	-3.64	-24.94	0.04	0.41
10	39.321	28	Irrigation	Saq	600	-6.05	-46.37	0.38	0.96
11	36.45	27.611	Demotic	Saq	144	-4.29	-16.92	0.05	0.23
12	38.083	27.423	Irrigation	Saq	300	-3.81	-25.80	0.05	0.72
13	36.689	26.77	Demotic	Alluvial	45	-2.40	-3.76	0.07	0.3
14	36.689	26.77	Demotic	Alluvial	50	-0.77	1.38	0.02	0.15
15	36.833	26.629	Demotic	Alluvial	49	-0.80	-1.29	0.03	0.52
16	36.076	27.147	Demotic	Alluvial	-	-1.01	-2.04	0.07	0.17
17	34.742	28.398	Demotic	Alluvial	12	-2.96	-10.35	0.07	0.2
18	37.56	25.131	Demotic	Alluvial	50	-2.40	-7.63	0.06	0.72
19	36.299	27.437	Demotic	Alluvial	42	-2.88	-9.29	0.13	0.4
20	36.308	27.103	Demotic	Alluvial	-	-1.55	-3.51	0	0.84
21	37.254	26.295	Demotic	Alluvial	23	0.1	-0.12	0.09	0.02
22	37.239	25.953	Demotic	Alluvial	30	-1.53	-5.00	0.07	0.76
23	36.071	27.391	Demotic	Alluvial	34	-2.81	-8.32	0.01	0.08
24	36.852	26.607	Demotic	Alluvial	150	-2.84	-6.24	0.07	0.76

Log = longitude

Lat = latitude

Aquifer.N = Aquifer Name

A = $\delta^{18}\text{O}(\text{‰})$ st.dv

B = $\delta^2\text{H}(\text{‰})$ std.dv

Table 2.

Parameter	Unit	Period I	Period II	Period III	Entire period
		04/2002–03/2006	04/2006–06/2012	07/2012–12/2016	4/2002–12/2016
TWS _{GRACE}	mm/yr	-0.73 ± 0.95	-11.05 ± 0.44	-4.04 ± 1.62	-8.55 ± 0.22
	km ³ /yr	-0.32 ± 0.42	-4.86 ± 0.19	-1.78 ± 0.71	-3.76 ± 0.10
SMS	mm/yr	-3.23 ± 0.27	-2.13 ± 0.13	-0.94 ± 0.23	-2.21 ± 0.07
	km ³ /yr	-1.42 ± 0.12	-0.94 ± 0.06	-0.41 ± 0.10	-0.97 ± 0.03
GWS	mm/yr	$+2.50 \pm 0.92$	-8.92 ± 0.41	-3.10 ± 1.59	-6.34 ± 0.22
	km ³ /yr	$+1.10 \pm 0.40$	-3.92 ± 0.18	-1.36 ± 0.70	-2.79 ± 0.10
Recharge	km ³ /yr	$+9.10 \pm 0.40$	$+4.08 \pm 0.18$	$+6.64 \pm 0.70$	$+5.21 \pm 0.10$

Table 3.

Watershed	Area	Precipitation			Stream flow			Potential recharge			Initial losses			Soil (%)			
	km ²	mm	km ³	m	km ³	%	mm	km ³	%	mm	km ³	%	A	B	C	D	
Al Baten	27,496	55.77	1.53	2.18	0.06	3.91	34.46	0.95	61.79	19.14	0.53	34.32	79	0	20	1	
Al Rumah	215,521	59.79	12.89	11.71	2.52	19.59	29.84	6.43	49.91	18.25	3.93	30.52	28	49	8	14	
Al Sarhan	113,723	37.23	4.23	3.75	0.43	10.07	19.90	2.26	53.45	13.58	1.54	36.48	35	3	17	44	
Tabuk	20,341	26.72	0.54	8.15	0.17	30.50	9.10	0.19	34.06	9.47	0.19	35.44	24	12	0	64	
Total	377,080	180	19	26	3		93	10		60	6						

A: Alluvium

B: Basement

C: Limestone

D: Sandstone

Manuscript III

**Groundwater Quality Patterns and Spatio-temporal
Change in the Depletion Regions of Arabian Shield and
Arabian Shelf: Implications of Public Health**

**Othman Abdurrahman Fallatah^{1, 2}, Dawn Cardace¹, Ali S
Akanda¹**

1) Department of Civil and Environmental Engineering, University of
Rhode Island, Kingston, RI 02881, USA

2) Faculty of Engineering, Radiation Protection & Training Centre,
King Abdul-Aziz University,

P.O. Box 80204, Jeddah 21589, Saudi Arabia

1. Abstract:

Groundwater quality is a critical issue in the arid and semi-arid countries, where it is one of the most reliable sources on which people depend. Water quality is a vital concern in the Kingdom of Saudi Arabia (KSA) affecting as it affects the health of its people, the growth of its agriculture, and its economic development. In this study: the objectives were to (1) investigate the depletion rate of Groundwater storage (GWS) in the studying area by using art of Gravity Recovery and Climate Experiment (GRACE) solution during (2002-2016); (2) determine the ionic composition of cations and anions for 24 samples, 12 samples from Arabian Shield, and 12 from Arabian Shelf in Saudi Arabia. (3) Assess the characterization of the water quality of the aquifer by using Piper diagram. The results show GRACE-derived GWS depletion ($-2 \pm 0.13 \text{ km}^3/\text{year}$). The results of ionic composition reveal two main groups (Group I: well depths: 144 m – 607 m; Group II: well depths: 12 m – 150 m). The de Group I (Saq aquifer; fossil water), ionic composition results within limits for all samples, compared to Group II (alluvial aquifer; mixed water). The classification of groundwater was done by using Piper diagram, where most of the samples in Arabian Shelf (85 %) falls in the type of (Mix Ca-Mg-Cl-SO₄). In the Arabian Shield, 50% of the samples falls in the type of (Ca-Cl). Where most of the samples (98%) are

from domestic wells, and the people use it as drinking water, it is essential to assess the radioactive analysis and the water quality for those samples which is higher than Water Health Organization (WHO) standard and understanding its impacts on public health.

KEYWORDS

Groundwater quality, Arabian Shield, Arabian Shelf, GRACE, Hydro chemical, Cations, Anions

2. Introduction

Freshwater resources in the Kingdom of Saudi Arabia (KSA) are extremely vulnerable to both climate change and human interventions (Sultan et al., 2014; Ahmed et al., 2014). During the dry and wet seasons, the recharge rates of the underlying aquifer systems vary significantly; increases in the wet climatic period and groundwater levels fall in the dry period (Sultan et al., 2011). There are several reasons for human intervention on a given hydrologic system: for example, construction of dams (reservoirs) to expand the use and utilization of a surface water resource; a lack of development programs for the evaluation of alternative renewable water resources; or the unofficial pumping of fossil groundwater without knowing how this artificial recharge process could affect these groundwater systems on a regional scale. The management and development of these resources are important to sustain population growth and grow the agricultural, industrial, and tourism sectors. The population of the KSA is on the rise (population in 1960: 4×10^6 ; 1980: 9.8×10^6 ; 2010: 27.3×10^6 ; 2050 estimate: 59.5×10^6 ; GASTAT, 2015) and its annual consumption of freshwater resources is as well (2010: 17.9×10^9 m³; 2050 estimate: 19.5×10^9 m³; MWA, 2012). The population study area (Arabian Shelf in 2010: 571,717; Arabian Shield in 2010: 224,708; GASTAT, 2015).

In order to minimize the overexploitation of freshwater resources and

to maintain the livelihood of the population in a sustainable manner, we need to understand the natural phenomena (e.g., rainfall/temperature patterns, duration, and magnitude) together with human-related factors (e.g., population growth, over- exploitation, and pollution). In spite of the significance of the Saq aquifer system in the KSA, there are some major difficulties associated with using the groundwater system. The most critical of these difficulties are the unsustainable over- exploitation of the aquifer, which also significantly influences the water quality.

The water demand in Saudi Arabia increased 2,352 million cubic meters (MCM) in 1980 to more than 20,000 MCM in 2004 (FAO 2009). 88% of this demand is for irrigated agriculture, 9% for domestic use, and 3% for industrial. The present study focuses on the evaluated water quality of groundwater samples from Arabian Shield and Arabian Shelf and its suitability as drinking water and domestic purposes by compare it with WHO.

3. Study Area

3.1 Arabian Shield

The Arabian Shield occupies the west-central one-third of the Kingdom and is part of a higher Afro-Arabian Shield (Al-Sayari et al., 1978; Brown et al., 1960). It is the geologic base of the central Najd, Hijaz, and Asir regions, and extends from 50 to 700 kilometers inland from the Red Sea toward Riyadh (Fig. 1). This is an ancient landmass consisting of igneous and metamorphic rocks of Precambrian age (the oldest of them about 1,170 million years old). Basalts of mid- Tertiary and Quaternary age, 26 million years old or younger, are spread over western parts of the Shield and form the harrat (Al-Sayari et al., 1978; MPMR, 1972). Sedimentary rocks of Paleozoic age, between 570 million and 225 million years old and modern alluvium partly overlie the Shield itself. A narrow strip of Tertiary to Quaternary age sedimentary rocks, including alluvium and related surficial deposits, also mantles the Precambrian age rocks between the base of the mountain and the Red Sea Coast where the relations among them rocks are much complicated by faults connected with the Red Sea rift. For the most part, the rock of the shield is relatively impermeable therefore are not significant sources now or in the future (Greenwood et al., 1977). Locally small yields of water might be found in joining or fractured crystalline rock of the shield, or in the younger basalt. The Shield influences the water

resources in other ways as well. Such, it forms the highest parts of the Kingdom and substantially controls the distribution of rainfall, which runs off through the wadis and is available to recharge the groundwater. Because the rocks of the Shield are commonly impermeable, they shed most of the rain that falls on them, shunting relatively large percentages of the rainfall to the adjacent bodies of sedimentary rocks, which can take in and may store some of the water (MAW, 1984).

3.2 Arabian Shelf

When the vast mass of crystalline rocks that forms the eastward extension of the Shield was slowly and progressively tilted downward to the northeast by movements of the Earth's crust, a shallow sea occupied the eastern part of the Arabian Peninsula and received layer after layer of sedimentary deposits (MAW, 1984). The deposition of these sediments began during the Cambrian Period (more than 500 million years ago) and continued, with several interruptions, until about the Pliocene Epoch, which ended some 1.8 million years ago (MAW, 1984). Subsequent geologic events resulted in the folding and emergence of this part of the peninsula. Erosion by wind and water has since sculpted the land into its present form called Arabian Shelf. The character of the sedimentary rocks is known from data accumulated over many years from geologic and geophysical surveys, from test holes, and from production wells for the extraction

of petroleum, or water. The sedimentary rocks consist mainly of limestone, sandstone, and shale. They have an aggregate thickness as high as 5,500 meters, 1-5 thinning toward the west as the basement rocks become shallower. The critical water controlling role of the geological framework is seen in the fact that this sequence of sedimentary rocks virtually all the naturally occurring fresh water that is available in the kingdom (Greenwood et al., 1977). Some of the sedimentary rock layers, mainly sandstone and limestone, have considerable interconnected pore space or other openings that are filled with fresh water and, they are capable of transmitting the water readily to wells (Al-Sayari et al., 1978; Brown et al., 1960; Greenwood et al., 1977; MPMR, 1972; Brown et al., 1978; MacDonald et al., 1975).

4. Data and Methods:

4.1 Groundwater depletion from GRACE

GRACE is a joint between National Aeronautics and Space Administration (NASA) and the German Aerospace Center (DLR) mission that was launched in March 2002 to map the Earth's static and temporal global gravity fields (Tapley et al. 2004). The variability in Earth's gravity field is directly related to the

spatiotemporal variations in the total vertically integrated terrestrial water storage (TWS; Wahr et al., 1998). The GRACE-derived Terrestrial Water Storage (TWS) is used extensively in hydrology, oceanology, cryosphere, and solid Earth fields (e.g., Ahmed et al. 2011; Famiglietti and Rodell 2013; Ahmed et al. 2014; Wouters et al. 2014; Famiglietti 2014; Ahmed et al. 2016; Mohamed et al. 2016).

In this study GRACE, solution from University of Texas Center of Space Research (UT-CSR) was used to quantify Terrestrial Water Storage (TWS). The CSR mascons solutions approach uses the geodesic grid technique (Save et al., 2015) to model the surface of the earth using equal area gridded representation of the earth via 40,962 cells (40,950 hexagons + 12 pentagons). The size of each cell is about equatorial 1°, the number of cells along the equator is 320, the average area of each cell is 12,400 km², and the average distance between cell centers is 120 km. These mascons do not suffer from over-sampling at the poles like an equiangular grid. No neighboring cells meet at a single point (Save et al., 2015). The change in GWS determined using following equation:

$$\Delta GWS = \Delta TWS - \Delta SMS \quad (1)$$

where ΔGWS and ΔSMS represent the change in groundwater and soil moisture storage, respectively. Four versions of the Global Land Data Assimilation System (GLDAS): VIC, Noah, MOSAIC, and

CLM (Dai et al., 2003; Koren et al., 1999; Koster & Suarez, 1996; Liang, Lettenmaier, & Wood, 1996); were used to extract the soil moisture. The trend error in σ_{GWS} was calculated using standard error propagation equation:

$$\sigma_{GWS} = \sqrt{(\sigma_{TWS})^2 + (\sigma_{SM})^2} \quad (2)$$

Where (σ_{SM}) the error of soil moisture that calculated from standard deviation of the trends that were computed from the four GLDAS simulations, (σ_{TWS}) the error of terrestrial water storage that were calculated using procedures described in Scanlon et al. (2016).

4.2 Ionic composition of Cations and Anions of GW samples

All the water samples were stored in bottles that were kept at a temperature between 1 and 5°C. The water samples for trace element analyses were collected using sterile 100ml bottles designed for bacteriological examinations. The specific sampling conditions are described in Table 1, and the methods used for the chemical analyses are shown in Table 2. Unstable parameter hydrogen ion concentration (pH), and electrical conductivity (EC) were determined at the sampling sites by using of a pH-meter, a portable EC-meter.

4.3 Piper's Diagram

Hydro chemical classification and groundwater assessment have been

discussed using Piper's diagram. The Piper plot data should be in mill equivalents per liter which is converted from milligrams per liter to mill equivalents per liter.

4.4 Radioactive analysis

Radioactive materials were discussed to measure of gross α and gross β activities. Following the method of Salonen (1989) and Sanchez-Cabeza et al. (1993), an aliquot of the water sample (about 60 mL) was filtered using 0.45 μm membrane filter, and then warmed on a hot plate stirrer for 1 h at about 60 C with stirring in a narrow neck conical flask to remove radon. The sample was cooled to room temperature, and any change in volume due to evaporation was corrected by adding a few drops of distilled water. Gross α and gross β determinations were performed by direct measurement of 8 mL of the Rn-free sample and 12 mL of liquid scintillation cocktail in a 20-mL polyethylene vial for 500 minutes. The sample was vigorously shaken and cooled for 3 hours before start counting by a liquid scintillation spectrometer using the pulse-shape analyzer for α/β discrimination. Immediate counting reduces Rn-ingrowth interference to a minimum. Two control samples (blank and standard samples) were prepared and measured as the unknown samples. The blank sample was de-ionized water whereas the standard was a standard solution composed of a mixture of ^{241}Am and ^{90}Sr , in equilibrium with its daughter ^{90}Y , in de-ionized water. The obtained results are

compared to the World Health Organization (WHO) guidance levels, to show a preliminary assessment of the radiological risk attached to groundwater use.

5. Results

5.1 GWS from GRACE

The observed GRACE-derived TWS depletions over the study area are related to variations in both soil moisture storage and GWS since GRACE has no vertical resolution. To quantify the GRACE-derived GWS variations over the Saq aquifer system, the GLDAS-derived soil moisture estimates are subtracted from the GRACE-derived TWS averaged from UT-CSR mascons equation (1). Figure 4 shows the temporal variations in the GRACE-derived groundwater estimates over the Saq aquifer. Examination of (Figure 4) reveals a groundwater depletion rate of $-2.11 \pm 0.13 \text{ km}^3/\text{yr}$.

5.2 TDS

Table 3 shows the summary of the ionic composition in Arabian shelf and Arabian shield. The water samples are somewhat acidic to neutral with PH values ranging 6.40 to 7.80 in Arabian Shelf, and from 7.10 to 8 in the Arabian Shield. Electrical conductivity (EC) ranges from 460 to 1100 $\mu\text{S}/\text{cm}$, with an average of 766.64 $\mu\text{S}/\text{cm}$ in Arabian Shelf. On the other side, 95% of the samples are crossing the maximum permissible limit of EC (1,500 $\mu\text{S}/\text{cm}$) in the Arabian

Shield. The total dissolved solids (TDS) were measured through summing up all major ions concentrations, which range from 253 to 660 mg/l in Arabian Shelf with an average value of 479.92 mg/l. Only 20 % of the samples have TDS value <500 mg/l, which is below the stander 1200 mg/l from WHO. The water samples from Arabian Shield has high TDS, which is the max 5417.5 mg/l, and the minimum 942.7 mg/l around 95% of the samples is exceeding the permeation limit in water use. These high TDS values are probably linked to a local source of contamination of the aquifer, such as inadequate well completion and leading to pollution from the soil surface into the considered well through non-cemented or poorly cemented annular space (MWA, 2012). TDS distribution shows that the highest values, i.e., from 1,200 to 5,000 mg/l, are observed in areas where the geological formations contain aquifers outcrops. The TDS in deeper groundwater samples is generally below 1,200 mg/l, and in some places less than 500 mg/l. (MWA, 2012).

5.3 Ionic composition of Arabian Shelf and Arabian Sheild

Investigation focused on cations and anions distributions of Na⁺, Ca⁺⁺, Mg⁺⁺, K⁺ and Cl⁻, SO₄⁻², HCO₃, NO₃ respectively. Investigation Table.3 shows most of the cations and anions in Arabian Shield are exceeding the stander of WHO due several reasons that affect the water quality in that region such high evaporation, high abstraction which is affect the gradients of the

aquifer, and industrial activities. On other side, the ionic composition of Arabian Shelf are within the stander of WHO, but the radioactive materials of gross alpha and beta are exceeding WHO's guidance level.

5.4 Hydrochemical classification

The classification of groundwater analysis was done using Piper's diagram (Piper 1944). The ternary diagrams (Fig. 4) are showed three types of groundwater signed in this study, type (I) in the confined section near to the outcrops all over the study area, type (II) in the basaltic area, in the confined section, and to the north of the east part, and type (III) in the outcrops and shallow wells in the west part of the study area and in some deep wells near the outcrops in the east part.

Most of the samples falls in-group I and II, which show evolved (Ca-Cl) and (Mix Ca-Mg-Cl- SO₄) type where unique chemical masking is achieved through rock-water interaction, ion exchange, and reverse ion exchange; reactions within unsaturated zones; increased resident time; and anthropogenic influences. The group III water type (Ca-HCO₃) representing meteoric signatures or fresh recharged water constitutes only 5 % of the total samples.

5.5 Comparison of groundwater quality in the depletion regions between 2006 and 2016

As part of the investigation, we also compared groundwater quality in

the depletion regions between groundwater quality data in 2006 that was provided by MEWA and in 2016 tested in our lab from water samples directly collected from the area (Fig. 2). The statistical distributions in the Arabian Shelf of TDS are very similar, and no significant changes are identified between 2006 and 2016 (Fig. 3). However, in Arabian Shield samples, there is a significant increase of TDS in 2016, and that might be related to reverse pumping the hydraulic gradients resulting increasing dissolved mineral concentration especially in the coastal aquifers. Therefore most of the samples located on Arabian Shield have high ionic composition above drinking water standards (MWA, 2012)

5.6 Radio analysis results

We also performed radiological analysis of the Saq aquifer system and adjoining waters to investigate links with groundwater patterns and radioactive quality. Twelve wells samples are located in basement granite, and related alluvium, along with the edge; and other 12 wells samples are located in the unconfined sector of the Saq aquifer. The results showed most of the samples that located in Saq aquifer area have a high value of Gross α and Gross β exceeding WHO limit (Table 3). The basement is located below the Saq aquifer and laterally limits its extension westwards. The Saq aquifer is overlain by Hanadir shale. The radiological activity of the different rock types as mentioned in literature (Alabdula'aly, 1999; Iyengar et

al., 1990; Michel, 1991; Molinari et al., 1990; Aoudeh, 1994) are summarized as follows:

- Granite basement with an average content of 3 mg/kg of uranium: 1-190 Bq/kg of Ra-226.
- Sandstones are not known for their high radionuclide concentration: about 1 mg/kg of uranium and activity of less than 60 Bq/kg of Ra-226.
- Shale with an average content of 3.7 mg/kg of uranium: 10-2,300 Bq/kg of Ra-226.

Therefore, the origin of radioactivity in the Saq aquifer water seems more likely related to adjacent layers.

6. Conclusion

The quality of groundwater in the Kingdom of Saudi Arabia plays a significant role in maintaining the health of people, which is the most critical source of drinking water in the Kingdom. Therefore, it is imperative to monitor groundwater quality continuously and make sure that it meets the standard of drinking water is necessary for the safety and health of the people.

This study focused on examining the quality of water in two regions with different geological characteristics, and we found the difference in water quality used in those regions. Most of the samples collected

from the Arabian Shield, from wells used for domestic and drinking purposes, show that the percentage of TDS is very high and above the limit allowed globally. According to the WHO, this water is not suitable for drinking but can be used for others purposes; the high proportion of salinity in this water related to saltwater encroachment occur in coastal aquifers where pumping reverses the hydraulic gradients resulting in increasing dissolved mineral concentrations. Because of that, most of the cations and anions in the samples have a high concentration, above the standard limit for drinking water. The water type for this region was tested by using Piper diagram to explain the characterization of water quality; most of the water were related to (Ca-Cl) and (Mix Ca-Mg-Cl-SO₄) which is the samples are in the confined section near to the outcrops all over the study area, and other falls in the water type of (Ca-HCO₃) representing recharged water.

The results of the radioactive analysis in this region were average and within the standard limits for drinking water.

The samples collected from Arabian Shelf have a good quality of ionic compositions of cations and anions and within the standard limit of drinking water. Piper diagram shows the majority of samples in Arabian Shelf falls in the type of (Mix Ca-Mg-Cl-SO₄) and show evolved groundwater type that related to the different periods of climate conditions. Our investigation in this region for radioactive

analysis revealed most of the samples that located in Saq aquifer area have a high value of Gross α and Gross β exceeding the WHO limit. According to WHO, there is no health concern for using these samples from both regions in the short term. These study findings are being shared with decision makers in relevant governmental agencies and decision makers to manage and develop groundwater quality in these regions.

7. Acknowledgments

The authors would like to sincerely thank the Ministry of Water and Environment Tabuk branch for their efforts to analyze the water quality of the samples that was used in this project. Also great thanks to King Abdulaziz University for their help and advice on radiochemical analysis.

8. References

1. Ahmed, M., Sultan M., Wahr, J., Yan, E., Milewski, A., Sauck, W., Welton, B. (2011).
Integration of GRACE (Gravity Recovery and Climate Experiment) data with traditional data sets for a better understanding of the time- dependent water partitioning in African watersheds. (5): 479–482.
<https://doi.org/10.1130/G31812.1>
2. Ahmed, M., Sultan, M., Wahr, J., & Yan, E. (2014). The use of GRACE data to monitor natural and anthropogenic induced variations in water availability across Africa. *Earth- Science Reviews*, 136, 289–300.
<https://doi.org/10.1016/j.earscirev.2014.05.009>
3. Ahmed, M., Sultan, M., Yan, E., & Wahr, J. (2016). Assessing and improving land surface model outputs over Africa using GRACE, field, and remote sensing data. *Surveys in Geophysics*, 37(3), 529–556. <https://doi.org/10.1007/s10712-016-9360-8>
4. Al-Sayari, S.S., and Zotl, J.G., eds., 1978, *Quaternary Period in Saudi Arabia*: Wien- New York, Springer-Verlag, 334 p.
5. Alabdula'aly, A. I. (1999). Occurrence of radon in the central region groundwater of Saudi Arabia. *Journal of environmental radioactivity*, 44(1), 85-95. ISO 690

6. Aoudeh S.M. and Al-Hajri S.A. (1994). Regional distribution and chronostratigraphy of the Qusaiba Member of the Qalibah Formation in the Nafud Basin, northwestern Saudi Arabia. *Geo '94, The Middle East Petroleum Geosciences*. Vol. 1. pp 143-154. April 25- 27, 1994, Bahrain. Edited by M.I. Al-Husseini, published by GulfPetrolLink, Bahrain.
7. Brown, G.F., 1960, *Geomorphology of Western and Central Saudi Arabia: International Geological Congress, 21st, Copenhagen, 1960, Proceedings, sec. 9, p. 150-159.*
8. Brown, G.F., and Jackson, R.O., 1978, *an Overview of the Geology of Western Arabia: U.S. Geological Survey, Saudi Arabian Project Report 250, 23 p.*
9. F. Schonhofer, K. Pock, H. Friedmann, "Radon surveys with charcoal and liquid scintillation counting," *J. Radioanal. Nucl. Chem. Articles*, 193, 337-346 (1995).
10. Famiglietti, J. S. (2014). The global groundwater crisis. *Nature Climate Change*, 4(11), 945–948. <https://doi.org/10.1038/nclimate2425>
11. Famiglietti, J. S., & Rodell, M. (2013). Water in the balance. *Science*, 340, 1300–1301. <https://doi.org/10.1126/science.1236460>
12. Greenwood, W.R., Anderson, R.E., Fleck, R.S., and Roberts

- R. S., 1977, Precambrian Geologic History and Plate Tectonic Evolution of the Arabian Shield: U.S. Geological Survey, Saudi Arabian Project Report 222, 97 p.
13. GASTAT. (2016). General authority for statistics Available at <http://www.stats.gov.sa/en> [Accessed 24 December 2016]
 14. Iyengar, M. A. R. (1990). The natural distribution of radium. The environmental behavior of radium, 1, 59-128.
 15. MacDonald, M., and Partners, 1975, Final Report V., Regional Geology and Geophysical Investigation: Ministry of Agriculture and Water, Riyadh, Saudi Arabia, no. 18, p. 70-73.
 16. (MAW) Ministry of Agriculture and Water (1984). Water Atlas of Saudi Arabia. 112 pp.
 17. MEWA. (2016). Ministry of environment, water, and agriculture Available at <http://www.mowe.gov.sa/enindex.aspx?AspxAutoDetectCookieSupport=1>
 18. (MPMR) Ministry of Petroleum and Mineral Resources (1972), Tectonic Map of the Arabian Peninsula: Saudi Arabian Deputy Ministry for Mineral Resources, Ministry of Petroleum and Mineral Resources, Arabian Peninsula Map AP-2, scale
 19. Michel, J. (1991). Relationship of radium and radon with

- geological formations. In: “Radon, Radium, and Uranium in drinking water,” eds. Richard Cothorn C. and Rebers P.A.
20. Mohamed, A., Sultan, M., Ahmed, M., Yan, E., & Ahmed, E. (2016). Aquifer recharge, depletion, and connectivity: Inferences from GRACE, land surface models, geochemical, and geophysical data. *GSA Bullitin*, 1–13. <https://doi.org/10.1130/B31460.1>
21. Molinari J., and Snodgrass W.J. (1990). The chemistry and radiochemistry of radium and the other elements of the uranium natural decay series, in: “The environmental behavior of radium,” Vol.1, IAEA.
22. Piper, A. M. (1944). A graphical procedure in the geochemical interpretation of water analyses, *transactions. American Geophysical Union*, 25, 914–928.
23. S. Chalupnik, J.M. Lebecka, “Determination of ^{226}Ra , ^{228}Ra and ^{224}Ra in water and aqueous solutions by liquid scintillation counting”, “Liquid scintillation spectrometry 1992”, Edited by J.E. Noakes, F. Schonhofer and H.A. Polach, *RADIOCARBON* 1993, pp. 397-403.
24. Scanlon BR, Zhang Z, Save H et al. (2016) Global evaluation of new GRACE mascon products for hydrologic applications. *Water Resour Res* 52:9412–9429
25. Save, H., Bettadpur, S., & Tapley, B. (2016). High-resolution

- CSR GRACE RL05 mascons. *Journal of Geophysical Research*.
26. Schmidt, D.L., Hadley, D.G., Greenwood, W.R., Gonzalez, Lewis, Coleman, R.G., and Brown, G.F., 1972, *Stratigraphy and Tectonism of the Southern Part of the Precambrian Shield of Saudi Arabia*: U.S. Geological Survey, Saudi Arabian Project Report 139, 36 p.
 27. Sharaf, M. A., & Hussein, M. T. (1996). Groundwater quality in the Saq aquifer, Saudi Arabia. *Hydrological sciences journal*, 41(5), 683-696.
 28. Sultan, M., Metwally, S., Milewski, A.,...Welton, B. (2011). Modern recharge to fossil aquifers: Geochemical, geophysical, and modeling constraints. *Journal of Hydrology* 403, 14–24. doi: 10.1016/j.jhydrol.2011.03.036
 29. Sultan, M., Ahmed, M., Wahr, J., Yan, E., & Emil, M. K. (2014). Monitoring aquifer depletion from space: Case studies from the Saharan and Arabian aquifers. In V. Lakshmi (Ed.), *AGU Geophysical Monograph # 206. Remote sensing of the terrestrial water cycle* (pp. 349–366).
 30. Wahr, J., Molenaar, M., & Bryan, F. (1998). Time variability of the Earth's gravity field: Hydrological and oceanic effects and their possible detection using GRACE. *Journal of Geophysical Research*, 103(B12), 30205–30229.

31. Wouters, B., Bonin, J. A., Chambers, D. P., Riva, R. E. M., Sasgen, I., & Wahr J. (2014). GRACE, time-varying gravity, Earth system dynamics and climate change. Reports on Progress in Physics 116801.
<https://doi.org/10.1088/0034-4885/77/11/116801>

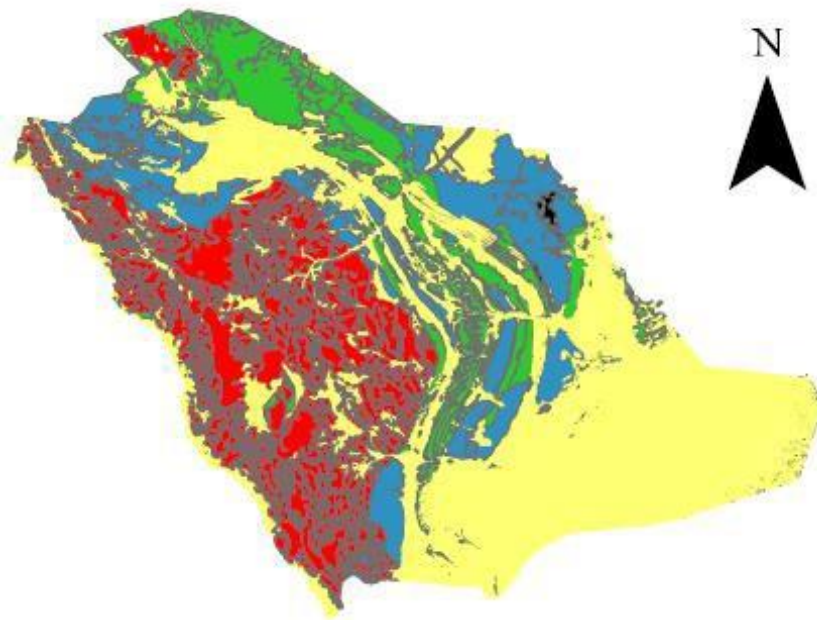
Figure Legends:

- Fig. 1 Geological map for Arabian Shield and Arabian Shelf.
- Fig. 2 the differences in TDS between 2006 and 2016, showed clearly the change in TDS of the samples those located in the Arabian shield
- Fig.3 Secular trend in Gravity Recovery and Climate Experiment derived groundwater storage estimates generated over the Arabian Peninsula from April 2002 to April 2016, and samples locations
- Fig.4 Piper diagram: Arabian Shelf and Arabian Shield

Table captions:

- Table. 1 Preservation conditions of water samples
- Table. 2 Analytical methods
- Table. 3 Summaries results of water quality data in Arabian Shelf and ArabianShield

Figure. 1



Geological map of KSA

- Shale
- Alluvial sediments
- Basement
- Limestone
- Sandstone

0 100 200 Miles

Figure. 2

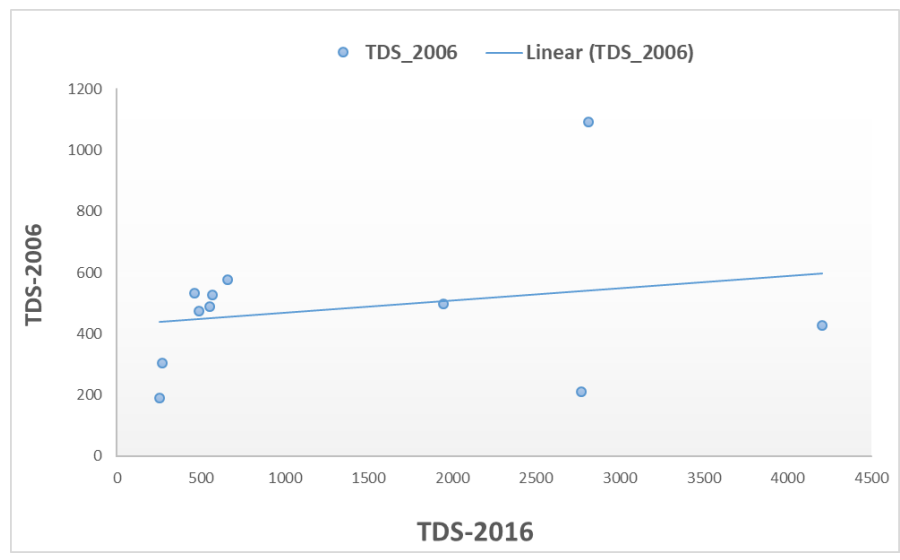


Fig. 3

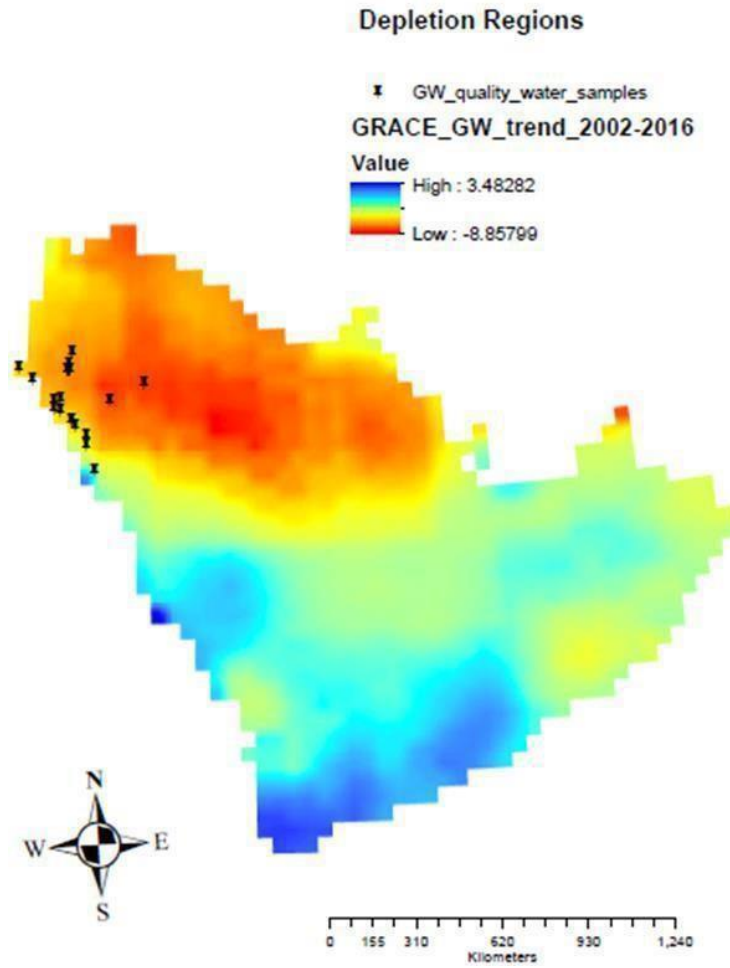


Figure. 4

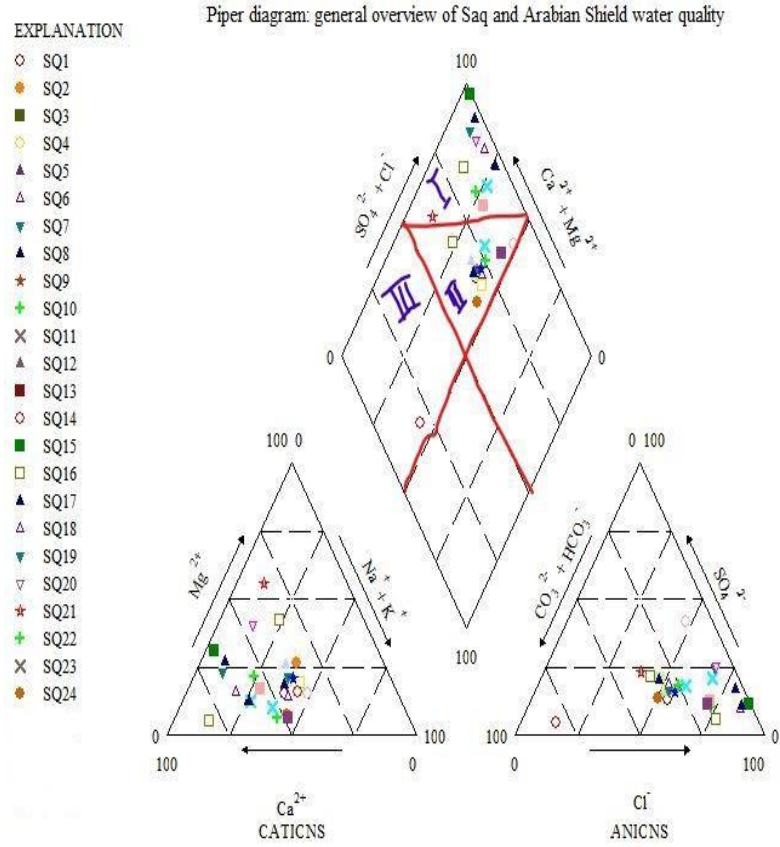


Table. 1

Species	Preservation conditions
Cl, NO ₂ , NO ₃ , SO ₄ , and PO ₄)	Refrigerate between 1 and 5°C
(Ca), Lithium (Li), Potassium (K), Sodium (Na)	Add HNO ₃ until 1<pH<2
Magnesium (Mg), Manganese (Mn), Selenium	ttle washed with acid solution. Add HNO ₃ until 1<pH<2.

Table.2

Measurement	Method	Quantification limit or uncertainty
SiO ₂	Colorimetry	1 mg/l
Ca, Mg, Fe	Flame	0.1
tot	atomic	mg/l
Na, K	absorption	0.1
HCO ₃	Flame	mg/l
Cl	photometry	mg/l
SO ₄	Acid titration	0.5 mg/l
NO ₃	with coloured	0.5 mg/l
B	indicator	0.5 mg/l
Trace elements	Specific electrode	0.05 mg/l
	Nephelometry	0.1 to 1 µg/l
	Colorimetry after reduction	
	Colorimetry	
	Furnace atomic absorption	

Tabl.3

Arabian					
Shelf					
	Min	Max	Average	Std.dv	WHO
Temp	26.5	38.8	30.96	3.59	
Depth	300	607	576.09	91.61	
EC(μ S/cm)	460	1100	766.64	178.92	1600
TDS(mg/l)	253	660	479.92	121.79	1200
pH	6.4	7.8	7.14	0.43	8.5 - 6.5
Alkalinity	54	180	125.36	37.5	200
Ca (mg/l)	51.2	82	64.36	10.05	200
Mg (mg/l)	8.64	24.96	17.78	4.95	150
Na (mg/l)	39.5	87	64.27	14.54	200
Cl (mg/l)	64	196	145.82	32.61	250
SO4(mg/l)	43	97	62.36	15.59	500
NO3(mg/l)	2.2	10	5.62	2.06	45
Gross α (Bq/L)	0.93	2.45	1.63	0.45	0.1
Gross β (Bq/L)	0.32	5.15	3.49	1.1	1
Arabian					
Shield					
	Min	Max	Average	Std.dv	WHO
Temp	25.8	38.6	29.05	3.37	
Depth	12	150	57.18	46.03	
EC	1714	9850	4912.62	2407.86	1600
TDS	942.7	5417	2702.02	1324.35	1200
pH	7.1	8	7.68	0.25	8.5 - 6.5
Alkalinity	84	1344	416.83	430.9	200
Ca (mg/l)	110.4	1200	459.32	329.37	200
Mg (mg/l)	16.3	170.9	71.92	47.81	150
Na (mg/l)	40	1357	318.38	342.13	200
Cl (mg/l)	360	4520	1445.54	1233.16	250
SO4	100	570	381.15	153.29	500
NO3	10.6	44.6	22.72	10.41	45
Gross α	0.14	0.62	0.37	0.17	0.1
Gross β	0.03	1.2	0.61	0.35	1

In conclusion

Groundwater monitoring includes both groundwater quantity (e.g., groundwater level and recharge rates) and quality monitoring (analysis of selected physical and chemical variables). The purposes of groundwater monitoring are to manage and develop the policy of the groundwater resources and to predict the groundwater quality and quantity due to natural processes and human impacts in time and space. Therefore, in this situation we need to have a useful database for assessment of the current state, anticipating changes and forecasting trends in the future. My results in this dissertation will contribute to the effective and efficient utilization of the Saq aquifer water resources and will be used to promote the sustainable development of the Arabian Peninsula and Middle East's natural resources in general. The findings have been and will be shared with stakeholders and decision makers in relevant governmental agencies to develop viable management scenarios for the water resources of the Saq aquifer.

Future work

- ❖ Mentoring groundwater quality and quantity characteristics on other main and secondary aquifers in AP along with water usage, demand, and demographics data.
- ❖ To incorporate new data from GRACE-FO satellite, land surface model, and rainfall data linked with water level data from the distribution wells temporal variations of groundwater.

- ❖ Development groundwater resources to support socio economic, agricultural and industrial developments.

APPENDIX A
Gravity Recovery and Climate
Experiment (GRACE) Introduction

GRACE Mission:

1.1 Earth's Gravity Field:

The Earth's gravity field is a product of its mass distribution. The mass included deep within the Earth, at the surface of the Earth and above the Earth's surface. That mass distribution is continually changing. Examples include, but not limited to: (1) tides in the ocean and solid Earth cause large mass variations at 12-hour and 24-hour periods, (2) atmospheric disturbances associated with synoptic storms or seasonal climatic differences may lead to variations in the distribution of mass in the atmosphere, the ocean, and the water stored on land, (3) mantle convection causes mass (Wahr, 2002).

The temporal variations in the mass distribution are responsible for the variations in the Earth's gravity field with time. The time-variable gravity field is successfully measured using either ground-based instrumentation or satellites. These measurements could be used to study a wide variety of geophysical processes that involve changes in mass (Dickey et al., 1997). Most of the time variable signal comes from the oceans, the atmosphere, the polar ice sheets, and the variations storage of water and snow on land.

1.2 Time-Variable Gravity Field:

The gravity signals detected from the satellite are due entirely to the underlying mass distribution. Until the launch of CHAMP

(Challenging Microsatellite Payload) in 2001 satellite time-variable gravity solutions were based entirely on Satellite Laser Ranging (SLR) observations. The most useful SLR measurements have involved LAGEOS (launched by NASA

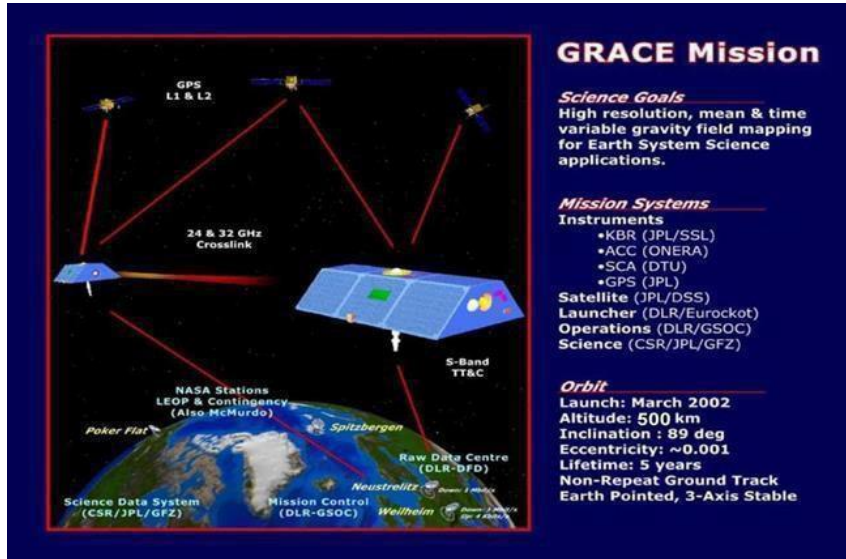


Fig. 1 GRACE flight configuration

1.3 GRACE Instrumentation:

The critical components of the GRACE twin satellites (Fig. 2) are listed below:

- 1- K-Band Ranging (KBR) system: Provides precise (up to 1 micrometer) measurements of the distance change between the two satellites.
- 2- Accelerometer: Measures the non-gravitational forces on the two satellites.
- 3- Star Camera: Provides the attitude of the spacecraft.
- 4- GPS Receivers: Provide continuous measurements regarding satellites position, orbit determination, timing, and atmospheric contributions.

1.4 GRACE Mission:

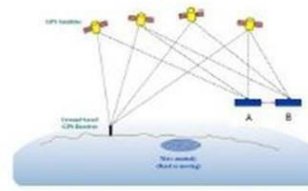
The GRACE mission consists of twin (GRACE A and GRACE B) satellites flying in a polar orbit with an inclination of 89.5° and altitude of 500 km (at launch) and approximately 200 km apart from each other (Fig.1). The satellite altitude decays naturally (~ 30 m/day) so that the ground track does not have a fixed repeat pattern (Tapley et al., 2004b). The two satellites follow the same path and are interconnected by a K-band (frequency: 12 to 63 GHz) microwave link (Bettadpur, 2006; Flechtner, 2005). The orbits of the two spacecraft are affected differently due to the spatial and temporal

variations in the Earth's gravity field, which can increase or decrease the distance between them. These distance variations affect the traveling time of the microwave signals, which are continually being transmitted and received between satellites. The accuracy of the measured separation distance is as small as 1 micron, about one over 100th the thickness of a human hair. When approaching an area of higher gravity/mass, the front satellite, GRACE A, speeds up and then slows down when flying above it. The second satellite, GRACE B, on the trail of GRACE A will have the same fate. The GRACE mission concept is summarized in Figure 3.

The disadvantage of having such a low (500 km) altitude is that GRACE experiences greater atmospheric drag, which can cause significant and unpredictable changes in the inter-satellite range distance (Wahr, 2002). Each GRACE satellite has an onboard accelerometer to measure non-gravitational accelerations. Those measurements are transmitted to the ground where they are used to correct the inter-satellite distance measurements (Wahr, 2002). Each spacecraft also has an onboard GPS receiver, used to determine the orbital motion of each spacecraft in the global GPS reference frame and to improve the gravity field solutions at global-scale wavelengths (Bettadpur, 2006; Flechtner, 2005; Tapley et al., 2004b).

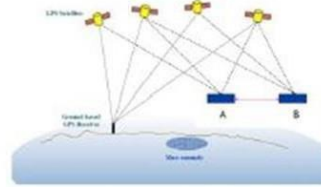
Stage 1: Normal Separation

→ No mass anomalies



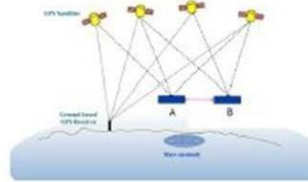
Stage 2: Separation Increased

→ As the satellite (A) approaching the anomaly and feels a greater gravitational attraction.



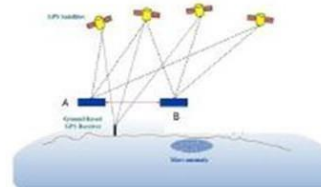
Stage 3: Separation Decreased

→ The satellite (B) also approaching the anomaly accelerates and catches up.



Stage 4: Separation Increased

→ As the satellite (A) not affected by the anomaly while (B) tugged backward by the anomaly.



Stage 5: Normal Separation

→ The satellite (B) leaves the anomaly and catches up.

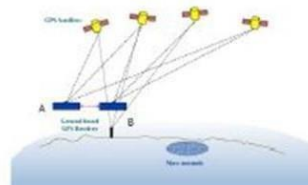


Figure 3: Gravity Recovery and Climate Experiment

(GRACE) mission concept.

1.5 GRACE Applications:

GRACE data has many applications, among others:

- Tracking water movement
- Tracking changes in ice sheets
- Tracking changes in the solid Earth.

Over the last decade, GRACE data has been successfully used to monitor the individual components of the TWS. GRACE has been widely used for:

- (1) Estimating regional water storage variations in the Amazon (Syed et al., 2005), Mississippi (Rodell et al., 2004; Syed et al., 2005), Oklahoma (Swenson et al., 2008), Ob (Frappart et al., 2006), and the Yangtze (Hu et al., 2006) River basins;
- (2) Monitoring the elements of hydrologic cycles on sub-basin scale in Africa (Ahmed et al., 2011);
- (3) Characterizing terrestrial moisture changes in the Canadian Prairie (Yirdaw et al., 2008);
- (4) estimating the groundwater withdrawal rates in India (Tiwari et al., 2009; Rodell et al., 2009) and California's Central Valley (Famiglietti et al., 2011);
- (5) Detecting water storage variations in the Three Gorges (Wang

et al., 2011) and Lake Victoria (Swenson and Wahr, 2009) reservoirs;

(6) Detecting flooding (Reager and Famiglietti, 2009) and drought (Andersen et al., 2005; Yirdaw et al., 2008; Leblanc et al., 2009; Agboma et al., 2009; Chen et al., 2010) potentials;

(1) Estimating the glacier melting rates in Alaska (Chen et al., 2006), and ice sheet mass loss in Greenland (Velicogna and Wahr, 2005, 2006) and Antarctica (Velicogna et al., 2006; Chen et al., 2009).

1.1 GRACE Partners:

Here we are listing the main GRACE partners:

(1) The University of Texas at Austin-Center for Space Research (UT-CSR), (2) GeoForschungsZentrum (GFZ), (3) National Aeronautics and Space Association, Earth System Science Pathfinder Project, (4) Deutschen Zentrum für Luft-und Raumfahrt (DLR), (5) Amarillo Independent School District, (6) Analytical Mechanics Associates, (7) Johns Hopkins University, Applied Physics Laboratory, (8) Astrium, (9) DJO, DASA, Jena-Optronik, Gm, (10) Elizabeth Board of Education, (11) Eurockot Launch Services, (12) European Space Agency, Earth Sciences Division, (13) French Aeronautics and Space Research Center (ONERA), (14) Killeen Independent School District, (15) Llano Independent School District, (16) Massachusetts Institute of Technology, Department of Earth, Atmospheric & Planetary

Sciences, (17) Messalonskee School System, (18) Mid Prairie Community School District, (19) NASA/Goddard Space Flight Center, (20) NASA Headquarters, (21) NASA/Jet Propulsion Laboratory, (22) NASA/Kennedy Space Center, (23) NASA/Langley Research Center, (24)Ohio State University, (25) Civil & Environmental Engineering and Geodetic Science, (26) Space Systems Loral, (27) Stanford Telecon, (28) Sunray Independent School District, (29) Technical University of Denmark, (30) Texas Space Grant Consortium, and (31) University of Colorado, Physics Department.

2. GRACE Data Products:

2.1 GRACE Data Levels:

As we discussed earlier, the long-term average distribution of the mass within the Earth system determines its mean "static" gravity field. The mean and time-variable gravity fields of the Earth affect the motion of all Earth satellites. The motion of twin GRACE satellites (A and B) are affected slightly differently since they occupy different positions in space. These differences cause small relative motions between these satellites (NASA, 2012, GRACE Mission. from <http://www2.csr.utexas.edu/grace/asdp.html>). "The distance changes are manifested as the change in time-of-flight of microwave signals between the two satellites, which in turn is measured as the phase

change of the carrier signals. The influence of non-gravitational forces on the inter-satellite range is measured using an accelerometer, and the orientation of the spacecraft in space is measured using star cameras” (NASA, 2012, GRACE Mission. from <http://www2.csr.utexas.edu/grace/asdp.html>). The onboard GPS receivers provide Science Data System (SDS) is responsible for extraction of Earth gravity models is with the GRACE project (Fig. 4). The SDS is distributed between University of Texas-Center of Space Research (UT- CSR), Jet Propulsion Laboratory (JPL), and GeoForschungsZentrum (GFZ). The SDS delivers monthly models of Earth gravity field. At present, the GRACE data is divided into four levels.

The raw data, collected from satellites, is calibrated and time-tagged in a non-destructive (or reversible) sense and labeled Level-1A. Level-1A data products are not distributed to the public (NASA, 2012, GRACE Mission. from <http://www2.csr.utexas.edu/grace/asdp.html>). These data undergo extensive and irreversible processing, and are converted to edited and cleaned data products are 1-5 second rates.

The products labeled Level- 1B, include among others, the inter-satellite range, range-rate, range-acceleration, the non- gravitational accelerations from each satellite, the pointing estimates, the orbits, etc. The Level- 1B products are processed to produce the monthly gravity field estimates in the form of spherical harmonic coefficients. GRACE

project also delivers Level-2 data products which consist of complete sets of harmonic coefficients out to maximum degree and order averaged over monthly intervals (Bettadpur, 2007; Dunn et al., 2003; Tapley et al., 2004b). Occasionally, several months of data are combined to produce an estimate of the mean "static" gravity field from Level-2 data. For the convenience of GRACE users who would prefer to access GRACE data products as for mass anomalies (e.g., water layer), the GRACE project also provide Level-3 data products in the form of equivalent water thicknesses (NASA, 2012, GRACE

Mission. from <http://www2.csr.utexas.edu/grace/asdp.html>).

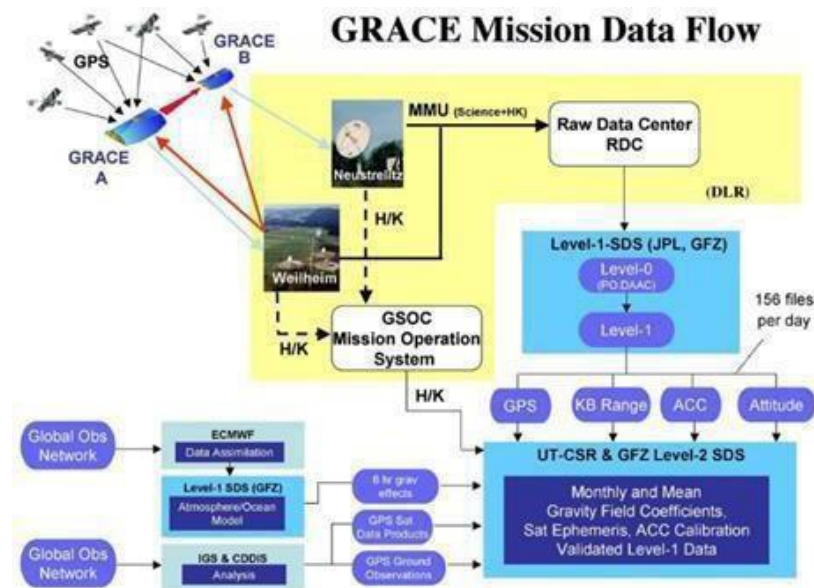


Figure 4: Gravity Recovery and Climate Experiment (GRACE) mission data flow

2.1 Accessing GRACE Data:

2.1.1 Level-1B and Level-2:

Level-1B, Level-2 data, and GRACE Documentations are available at

1- <ftp://podaac.jpl.nasa.gov/allData/grace>

2.1.1 Level-3:

Level-3 data are available at:

1- <http://grace.jpl.nasa.gov/data/>

2- <http://geoid.colorado.edu/grace/grace.php>

3- <http://icgem.gfz-potsdam.de/ICGEM/ICGEM.html>

2.2 GRACE Data Format:

Level-2 GRACE data are represented as a complete set of harmonic coefficients out to maximum degree and order averaged over monthly intervals. These data represent the GRACE anomalies after subtracting the background models (Fig. 5). The Background Model consists of mathematical models and the associated parameter values, which are used along with numerical techniques to predict the best-known value for the observable (in this case, the inter-satellite range or its derivatives). The Background Model encompasses both satellite dynamics and measurements. This model changes with the evolution of processing methods. The spherical harmonic coefficient at a given time is given by:

$$G^*(t) = \overset{1}{\overline{G}^*} + \overset{2}{G'(t-t_0)} + \overset{3}{\delta G^{st}(t)} + \overset{4}{\delta G^{ot}(t)} + \overset{5}{\delta G^{pt}(t)} + \overset{6}{\delta G^{a+o}(t)}$$

Where: (1) Coefficient value at time (t), (2) A priori knowledge of the static geopotential, (3) Secular variations of the harmonics, (4) Solid tides, (5) Ocean tides, (6) Pole tides, and (7) Atmospheric and oceanic non-tidal variability.

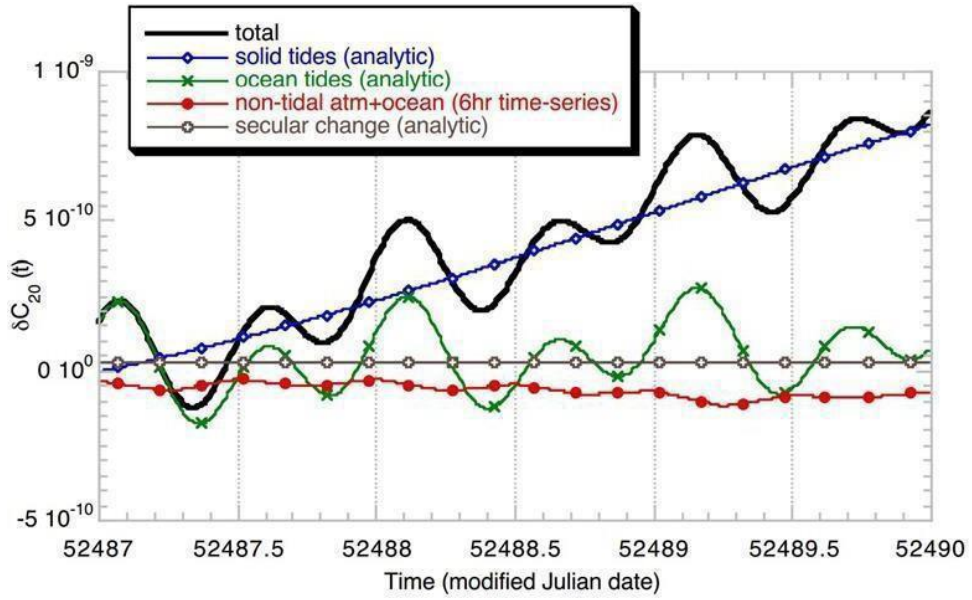


Figure 5: Components of the background model contributions to the C20 harmonic.

A GRACE Level-2 gravity field product is a set of spherical harmonic coefficients of the exterior geopotential. Level-2 data are produced by CSR, JPL and GFZ centers. A product name is specified as:

PID-2_YYYYDOY-YYYYDOY_dddd_ssss_mmmm_rrrr Where:

PID: is 3-character product identification mnemonic

-2: denotes a GRACE Level-2 product

YYYYDOY-YYYYDOY: specifies the date range (in year and day-of-year format) of the data used in creating this product.

dddd is the (leading-zero-padded) number of calendar days from which data was used in creating the product.

ssss is an institution-specific string.

mmmm is a 4-character free string (e.g., used for distinguishing constrained from unconstrained solutions).

rrrr: is a 4-digit (leading-zero-padded) release number (0000, 0001, ...)

The Product Identifier mnemonic (PID) is made up of one of the following values for each of its three characters:

1st Character:

- = G: Geopotential coefficients. 2nd Character:
- = S: Estimate made from only GRACE data.

- =C: Combination estimate from GRACE and terrestrial gravity information.

- = E: Any background model specified as a time-series.

- = A: Average of any background model over a period. 3rd Character:
- = M: Estimate of the Static field.

- = U: Geopotential estimate relative to the background gravity model.

- = T: Total background gravity model except for static background model.

- = A: non-tidal atmosphere.

- = B: non-tidal Oceans.

- = C: combination of non-tidal atmosphere and ocean.

- = D: bottom-pressure over oceans, zero over land. Example of the GSM file is shown in Figure 6

```
1 FIRST GSM-2_2003001-2003031_0025 UTCRR_0040_0005 SSM UT-CBR 20120910
2 COMMENT /acraatch/0079/Ryaa/05/graw/R05_03-01/ltw/ltw/GSM-2_2003001-2003031_0025 UTCRR_0040_0005
3 COMMENT Dusted days: 21,24,26,27,29,30
4 COMMENT Insert comments here
5 START 0.3984004418E+5 0.4378136300E+07
6 SSM 60 60 1.00 fully normalized inclusive permanent tide
7 COMMENT reported standard deviations are formal (not calibrated)
8 GRCP2 0 0 0.100000000000E+00 0.00000000000E+00 0.0000E+00 20030101.0000 20030201.0000 mman
9 GRCP2 1 0 0.00000000000E+00 0.00000000000E+00 0.0000E+00 20030101.0000 20030201.0000 mman
10 GRCP2 2 0 -0.48416231460E-03 0.00000000000E+00 0.0000E+00 20030101.0000 20030201.0000 yman
11 GRCP2 3 0 0.95715376302E-06 0.00000000000E+00 0.0000E+00 20030101.0000 20030201.0000 yman
12 GRCP2 4 0 0.54002114916E-06 0.00000000000E+00 0.0000E+00 20030101.0000 20030201.0000 yman
13 GRCP2 5 0 0.68478488520E-07 0.00000000000E+00 0.0000E+00 20030101.0000 20030201.0000 yman
14 GRCP2 6 0 -0.18952054282E-06 0.00000000000E+00 0.0000E+00 20030101.0000 20030201.0000 yman
15 GRCP2 7 0 0.90522217878E-07 0.00000000000E+00 0.0000E+00 20030101.0000 20030201.0000 yman
16 GRCP2 8 0 0.48471238444E-07 0.00000000000E+00 0.0000E+00 20030101.0000 20030201.0000 yman
17 GRCP2 9 0 0.28020077422E-07 0.00000000000E+00 0.0000E+00 20030101.0000 20030201.0000 yman
18 GRCP2 10 0 0.53398354897E-07 0.00000000000E+00 0.0000E+00 20030101.0000 20030201.0000 yman
19 GRCP2 11 0 -0.50746141421E-07 0.00000000000E+00 0.0000E+00 20030101.0000 20030201.0000 yman
20 GRCP2 12 0 0.36434547885E-07 0.00000000000E+00 0.0000E+00 20030101.0000 20030201.0000 yman
21 GRCP2 13 0 0.41727142394E-07 0.00000000000E+00 0.0000E+00 20030101.0000 20030201.0000 yman
22 GRCP2 14 0 -0.22644904449E-07 0.00000000000E+00 0.0000E+00 20030101.0000 20030201.0000 yman
23 GRCP2 15 0 0.21941272567E-08 0.00000000000E+00 0.0000E+00 20030101.0000 20030201.0000 yman
24 GRCP2 16 0 -0.47108599331E-08 0.00000000000E+00 0.0000E+00 20030101.0000 20030201.0000 yman
25 GRCP2 17 0 0.19187825309E-07 0.00000000000E+00 0.0000E+00 20030101.0000 20030201.0000 yman
26 GRCP2 18 0 0.60989438551E-08 0.00000000000E+00 0.0000E+00 20030101.0000 20030201.0000 yman
27 GRCP2 19 0 -0.336205931E-08 0.00000000000E+00 0.0000E+00 20030101.0000 20030201.0000 yman
28 GRCP2 20 0 0.21533458037E-07 0.00000000000E+00 0.0000E+00 20030101.0000 20030201.0000 yman
```

Figure 6: Print screen shows the format of the GRACE Level-2 GSM file.

2.1 Spherical Harmonics:

GRACE level-2 data are in the form of spherical harmonics.

Spherical harmonics are used to express values that vary sinusoidally in both latitude and longitude direction. Examples of these include the gravity and magnetic fields of the Earth, the geoid, earth topography, electron distribution around the atom, ..). The spherical harmonic coefficients are given regarding degree (ℓ) and order (m). m is the number of nodes (great circles) in the longitudinal direction, where, angle (ϕ) increases East from the Greenwich, and it ranges between 0 and 2π . The value ($\ell - m$) gives the number of nodes in the latitudinal sense. Where the angle (θ) increases from the North Pole, and it ranges from 0 to π (Fig. 7). Visualizations of the spherical harmonics are given at the GFZ website: <http://icgem.gfz-potsdam.de/ICGEM/potato/Tutorial.html>.

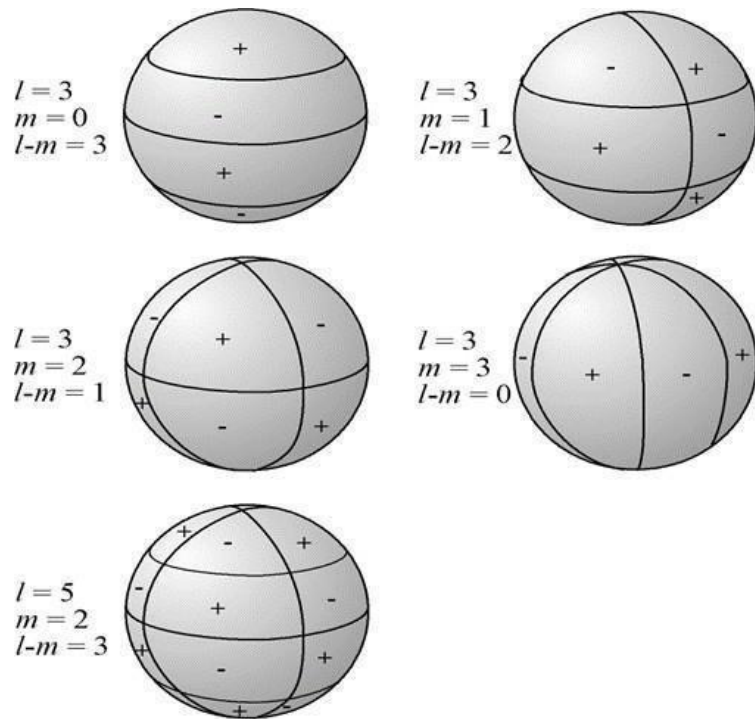


Figure 7: Schematic representation of the spherical harmonics on the unit sphere and its nodal lines. m is the number of nodes (great circles) in the longitudinal direction, where, angle ϕ increases East from the Greenwich, and it ranges between 0 and 2π . The value $(l-m)$ gives the number of nodes in the latitudinal sense. Where the angle θ increases from the North Pole, and it ranges from 0 to π .

3. Processing of GRACE Data:

In this section, we are introducing, in brief, the general steps that most of the researchers are using in processing of GRACE level-2 data.

3.1 Removal of the Temporal Mean:

The GRACE level-2 solutions are represented regarding fully normalized spherical harmonic decompositions up to degree (l) and order (m) of 60. The time-variable component of the gravity field solutions should be calculated by removing the long-term mean ($C_{lm}(t)$, $S_{lm}(t)$) of the Stokes coefficients from each monthly ($C_{lm}(t)$, $S_{lm}(t)$) value to get the temporal variations in these coefficients ($\delta C_{lm}(t)$, $\delta S_{lm}(t)$). The reason for removing the mean field is that it is dominated by the static density distribution inside the solid Earth (Wahr et al., 1998).

3.2 Spectral Filtering (Destripping):

After the temporal mean removal, the correlated errors (long, linear, north to south oriented features) also called “stripes” should be reduced by applying despiking methods developed by Swenson and Wahr (2006). The presence of stripes implies spatial correlations in the gravity field coefficients at higher degree (short wavelength components). Swenson and Wahr (2006) show how, at a single higher ($m > 8$) order, the even (or odd) coefficients values at each

degree tend to form smooth curves. Their filter, a moving window quadratic polynomial, was used to isolate and remove smoothly varying coefficients of the same parity. In this study, the least square method was used to fit a 4th order polynomial for the odd degree and the even degree separately, then to subtract those polynomials from the original coefficients to leave the residuals ($C^{\text{lm}}(t)$, $C^{\text{lm}}(t)$).

3.3 Spatial Averaging (Gaussian Smoothing):

At this point, we have a set of gravity coefficient anomalies for each month ($\Delta C^{\text{lm}}(t)$, $\Delta C^{\text{lm}}(t)$) that have been described and ready to compute mass anomalies. Several studies have used GRACE monthly solutions to make estimates of water storage variability, both on land and in the oceans (Chambers et al., 2004; Chen et al., 2005; Ramillien et al., 2005; Swenson and Milly, 2006; Tamisiea et al., 2005; Tapley et al., 2004b; Velicogna and Wahr, 2005; Wahr et al., 2004).

We will compute maps of water storage anomalies over the land ($\Delta\sigma(\theta, \phi, t)$) directly as:

Where ρ is the average density of the Earth (5517 kg m^{-3}), a_e is the mean equatorial radius of the Earth, θ is the geographic latitude, ϕ is the longitude, P_{lm} are the fully-normalized Associated Legendre Polynomials of degree l and order m and r is the Gaussian averaging radius, and k_l are elastic/load Love numbers of degree l . The later was calculated via linear interpolation of the original data computed by Han and Wahr (1995).

The spatial averaging, or smoothing, of GRACE data, is necessary to reduce the contribution of noisy short wavelength components of the gravity field solutions. We will generate $0.5^\circ \times 0.5^\circ$ equivalent water thickness grids using a Gaussian averaging radius of 200 km.

3.4 GRACE Errors:

Errors in GRACE-derived TWS fall into two main categories (Wahr et al., 2006): (1) Errors in monthly GRACE solutions. These include measurement and processing errors, aliasing errors related to the short-period (sub-monthly) variations and errors in the European Centre for Medium-Range Weather Forecasts (ECMWF) models used for atmospheric corrections of

GRACE data; (2) Errors due to changes caused by factors other than continental water storage (i.e., leakage errors). The leakage errors can come from time-variable mass anomalies either vertically above or

below, or from mass anomalies off to the side of the area of interest. The time variable gravity below the area of interest might include the gravity signal related to un-modeled mass variations in the Earth's interior while that above the area of interest might be related to errors in the atmospheric models (ECMWF). Leakage errors can also come from continental water storage signals where it comes from water storage outside of the region of interest. The measurement errors in GRACE data (type 1) exhibits a zonally banded pattern and varies with the Gaussian smoothing function used and with the latitude. At lower latitudes, a maximum error of ~36 mm (equivalent water thickness) was obtained with a Gaussian radius of 300 km whereas an error of ~28 mm was obtained when using a Gaussian radius of 750 km was adopted.

Poleward, the error decreases to <15 mm (Landerer and Swenson, 2012; Wahr et al., 2006).

Estimates of TWS variations suffer from signal degradation due to noise. The noise is manifested as (1) random errors that increase as a function of spherical harmonic spectral degree (Wahr et al., 2006), and (2) systematic errors that are correlated within a particular spectral order (Swenson and Wahr, 2006).

Several filtering techniques are used to damp or isolate and remove the GRACE-derived TWS errors. The problem with most of those

techniques is that the filters also modify the actual geophysical signal that the researchers are interested in. The following section explains the methods used to scale GRACE TWS data to account for the effect of the filter on the GRACE signal.

3.5 Scaling GRACE TWS Data

The scaling process is supposed to take care of the GRACE TWS errors that result from applying the following filters and/or truncations: (1) destriping filter designed to remove systematic errors that are characterized by correlations between certain spherical harmonic coefficients (Swenson and Wahr, 2006); (2) Gaussian smoothing filter when applied, it smoothes, but reduces the spatial resolution of GRACE observations by damping the higher degree coefficients (Wahr et al., 1998); and (3) truncation of the monthly GRACE solutions where GRACE gravity solutions are typically truncated at a spectral degree ($l_{max} \leq 60$; wavelength of ~ 330 km). This truncation means that GRACE cannot resolve signals with spatial variability finer than 330 km (Wahr et al., 1998; Wahr et al., 2006).

References:

- Bettadpur, S., 2006, GRACE level-2 gravity field product user handbook: Center for Space Research, The University of Texas at Austin.
- Bettadpur, S., 2007, GRACE Product Specification Document: Center for Space Research The University of Texas at Austin.
- Chambers, D.P., Wahr, J., and Nerem, R.S., 2004, Preliminary observations of global ocean mass with GRACE: Geophysical Research Letters, v. 31, L13310.
- Chen, J., Wilson, C., Famiglietti, J., and Rodell, M., 2005, Spatial sensitivity of the Gravity Recovery and Climate Experiment (GRACE) time-variable gravity observations: Journal of Geophysical Research, v. 110, B08408, doi: 10.1029/2004JB003536.
- Dunn, C., Bertiger, W., Bar-Sever, Y., Desai, S., Haines, B., Kuang, D., Franklin, G., Harris, I., Kruizinga, G., Meehan, T., Nandi, S., Nguyen, D., Rogstad, T., Thomas, J.B., Tien, J., Romans, L., Watkins, M., Wu, S.-C., Bettadpur, S., and Kim, J., 2003, Instrument of GRACE: GPS Augments Gravity Measurements: GPS World, v. 14, p. 16-28.
- Flechtner, F., 2005, GFZ Level-2 Processing Standards Document for Level-2 Product Release 0003: GeoForschungszentrum

Potsdam: Geodesy and Remote Sensing.

- Han, D., and Wahr, J., 1995, The viscoelastic relaxation of a realistically stratified Earth, and a further analysis of postglacial rebound: *Geophysical Journal International*, v. 120, p. 287– 311.
- Ramillien, G., Frappart, F., Cazenave, A., and Gnter, A., 2005, Time variations of land water storage from an inversion of 2 years of GRACE geoids: *Earth and Planetary Science Letters*, v. 253, p. 283– 301.
- Schmidt, R., Flechtner, F., Meyer, U., Neumayer, K.H., Dahle, C., König, R., and Kusche, J., 2008, Hydrological Signals Observed by the GRACE Satellites: *Survey in Geophysics*, v. 29, p. 319-334, doi: 10.1007/s10712-008-9033-3.
- Swenson, S.C., and Milly, P.C.D., 2006, Climate model biases in seasonality of continental water storage revealed by satellite gravimetry: *Water Resources Research*, v.42, W03201.
- Tamisiea, M.E., Leuliette, E.W., Davis, J.L., and Mitrovica, J.X., 2005, Constraining hydrological and cryospheric mass flux in southeastern Alaska using space-based gravity measurements: *Geophysical Research Letters*, v. 32, L20501.
- Tapley, B.D., Bettadpur, S., Ries, J.C., Thompson, P.F., and Watkins, M.M., 2004a, GRACE Measurements of Mass Variability in the Earth System: *Science*, v. 305, p. 503–505, doi:

10.1126/science.1099192.

- Tapley, B.D., Bettadpur, S., Watkins, M., and Reigber, C., 2004b, The Gravity Recovery and Climate Experiment: Mission overview and early results: *Geophysical Research Letters*, v. 31, L09607.

- Velicogna, I., and Wahr, J., 2005, Ice mass balance in Greenland from GRACE: *Journal of Geophysical Research*, v. 32, L18505, doi: 10.1029/2005GL023955.

APPENDIX B

Scientific Methods

Gravity Recovery and Climate Experiment (GRACE)

Methodologies

Download GRACE Level-2 Data:

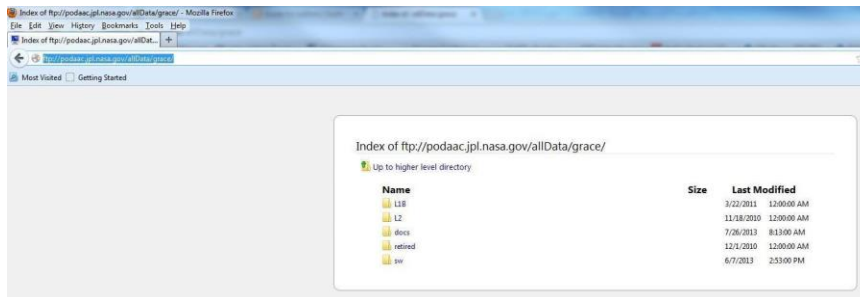
Below are the steps for downloading GRACE Level-2 data (e.g., Spherical harmonic coefficients):

1.1. Navigate to this website:

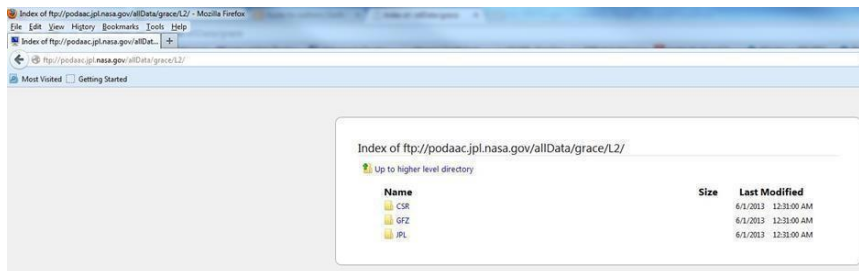
<ftp://podaac.jpl.nasa.gov/allData/grace/>

1.2. Click “L2”.

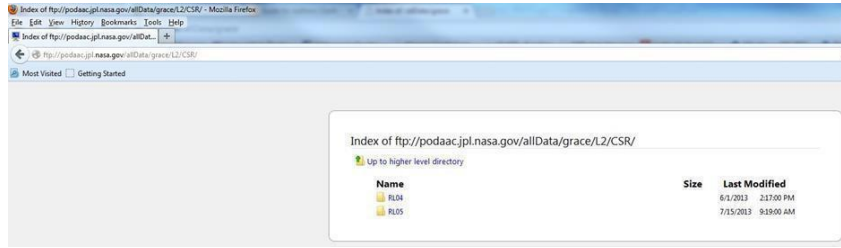
1.3. Select the “Data Center”: CSR, GFZ or JPL. In this



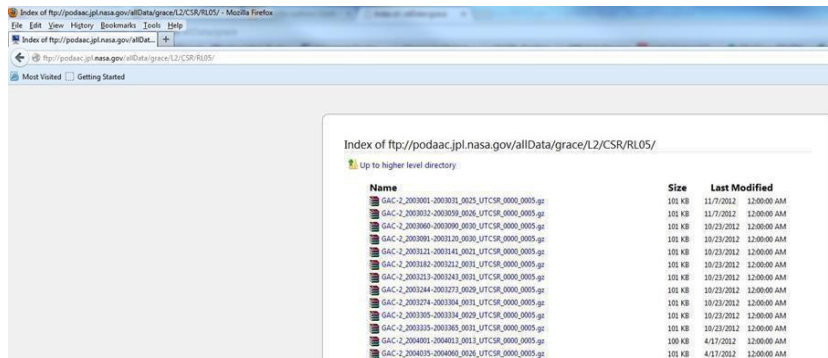
exercise, we will use CSRdata. Click “CSR.”



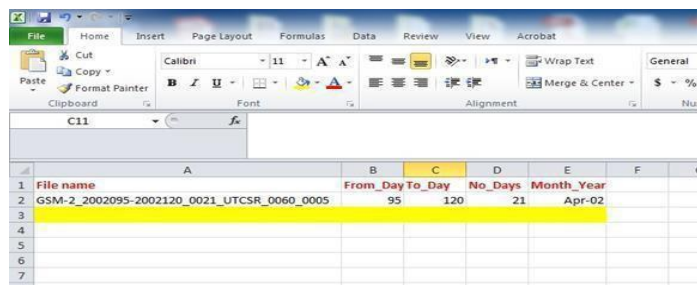
1.4. Select the “Data Release.” Click “RL05”.



1.5. Navigate to the “GSM” file. Click to download and place all file in one folder.



1.6 Dump the “file names,” “days from,” “days to,” “number of days,” and “month-year” for each file in one excel sheet (see below). Name this excel sheet as "CSR_Month_Index.xls." Insert a blank row for missing file(s) if any!



2. Explore GRACE Level-2 Data:

2.1. Open this file “GSM-2_2003001-2003031_0025_UTCSR_0060_0005”

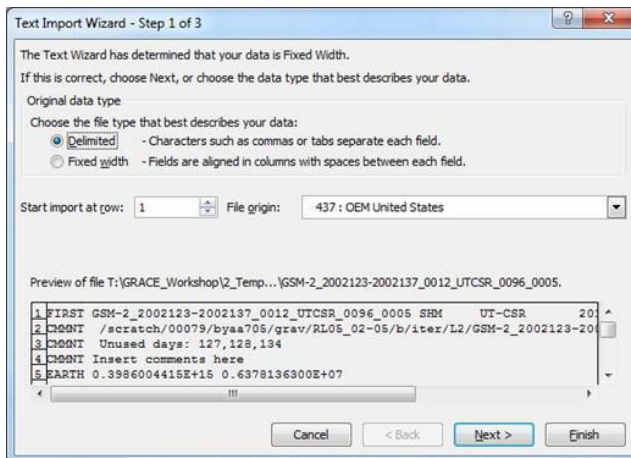
```
1 FIRST GSM-2_2003001-2003031_0025_UTCSR_0060_0005 SHM UT-CSR 20120910
2 COMMENT /scratch/00079/byaa705/grav/RL05_02-05/b/itez/L2/GSM-2_2003001-2003031_0025_UTCSR_0060_0005
3 COMMENT Unused days: 22,24,26,27,29,30
4 COMMENT Insert comments here
5 EARTH 0.3986004415E+15 0.6378136300E+07
6 SHM 60 45 1.61 fully normalized inclusive permanent tide
7 COMMENT Reported standard deviations are formal (not calibrated)
8 GRCOF2 0 0 0.1000000000E+01 0.0000000000E+00 0.000E+00 0.000E+00 20030101.0000 20030201.0000 mmns
9 GRCOF2 1 0 0.0000000000E+00 0.0000000000E+00 0.000E+00 0.000E+00 20030101.0000 20030201.0000 mmns
10 GRCOF2 2 0 -0.48149214440E-03 0.0000000000E+00 0.000E+00 0.000E+00 20030101.0000 20030201.0000 ymas
11 GRCOF2 3 0 0.97191761929E-06 0.0000000000E+00 0.000E+00 0.000E+00 20030101.0000 20030201.0000 ymas
12 GRCOF2 4 0 0.54802114914E-04 0.0000000000E+00 0.000E+00 0.000E+00 20030101.0000 20030201.0000 ymas
13 GRCOF2 5 0 0.48748484828E-07 0.0000000000E+00 0.000E+00 0.000E+00 20030101.0000 20030201.0000 ymas
14 GRCOF2 6 0 -0.14952056282E-04 0.0000000000E+00 0.000E+00 0.000E+00 20030101.0000 20030201.0000 ymas
15 GRCOF2 7 0 0.30522121787E-07 0.0000000000E+00 0.000E+00 0.000E+00 20030101.0000 20030201.0000 ymas
16 GRCOF2 8 0 0.49712359436E-07 0.0000000000E+00 0.000E+00 0.000E+00 20030101.0000 20030201.0000 ymas
17 GRCOF2 9 0 0.28020774217E-07 0.0000000000E+00 0.000E+00 0.000E+00 20030101.0000 20030201.0000 ymas
18 GRCOF2 10 0 0.31339434817E-07 0.0000000000E+00 0.000E+00 0.000E+00 20030101.0000 20030201.0000 ymas
19 GRCOF2 11 0 -0.50744814111E-07 0.0000000000E+00 0.000E+00 0.000E+00 20030101.0000 20030201.0000 ymas
20 GRCOF2 12 0 0.34164814911E-07 0.0000000000E+00 0.000E+00 0.000E+00 20030101.0000 20030201.0000 ymas
21 GRCOF2 13 0 0.41727142343E-07 0.0000000000E+00 0.000E+00 0.000E+00 20030101.0000 20030201.0000 ymas
22 GRCOF2 14 0 -0.22448644878E-07 0.0000000000E+00 0.000E+00 0.000E+00 20030101.0000 20030201.0000 ymas
23 GRCOF2 15 0 0.21141272587E-08 0.0000000000E+00 0.000E+00 0.000E+00 20030101.0000 20030201.0000 ymas
24 GRCOF2 16 0 -0.47108913611E-08 0.0000000000E+00 0.000E+00 0.000E+00 20030101.0000 20030201.0000 ymas
25 GRCOF2 17 0 0.18187131948E-07 0.0000000000E+00 0.000E+00 0.000E+00 20030101.0000 20030201.0000 ymas
26 GRCOF2 18 0 0.40789483851E-08 0.0000000000E+00 0.000E+00 0.000E+00 20030101.0000 20030201.0000 ymas
27 GRCOF2 19 0 -0.30623205319E-08 0.0000000000E+00 0.000E+00 0.000E+00 20030101.0000 20030201.0000 ymas
28 GRCOF2 20 0 0.21534580373E-07 0.0000000000E+00 0.000E+00 0.000E+00 20030101.0000 20030201.0000 ymas
29 GRCOF2 21 0 0.42519232462E-08 0.0000000000E+00 0.000E+00 0.000E+00 20030101.0000 20030201.0000 ymas
30 GRCOF2 22 0 -0.10786449714E-07 0.0000000000E+00 0.000E+00 0.000E+00 20030101.0000 20030201.0000 ymas
31 GRCOF2 23 0 -0.22325232737E-07 0.0000000000E+00 0.000E+00 0.000E+00 20030101.0000 20030201.0000 ymas
32 GRCOF2 24 0 -0.70178197515E-10 0.0000000000E+00 0.000E+00 0.000E+00 20030101.0000 20030201.0000 ymas
33 GRCOF2 25 0 0.30382449848E-08 0.0000000000E+00 0.000E+00 0.000E+00 20030101.0000 20030201.0000 ymas
34 GRCOF2 26 0 0.29792424219E-08 0.0000000000E+00 0.000E+00 0.000E+00 20030101.0000 20030201.0000 ymas
35 GRCOF2 27 0 0.38139149717E-08 0.0000000000E+00 0.000E+00 0.000E+00 20030101.0000 20030201.0000 ymas
36 GRCOF2 28 0 -0.77421621948E-08 0.0000000000E+00 0.000E+00 0.000E+00 20030101.0000 20030201.0000 ymas
37 GRCOF2 29 0 -0.52792135630E-08 0.0000000000E+00 0.000E+00 0.000E+00 20030101.0000 20030201.0000 ymas
38 GRCOF2 30 0 -0.77421621948E-08 0.0000000000E+00 0.000E+00 0.000E+00 20030101.0000 20030201.0000 ymas
39 GRCOF2 31 0 0.47980301194E-08 0.0000000000E+00 0.000E+00 0.000E+00 20030101.0000 20030201.0000 ymas
40 GRCOF2 32 0 -0.48191331817E-08 0.0000000000E+00 0.000E+00 0.000E+00 20030101.0000 20030201.0000 ymas
41 GRCOF2 33 0 -0.83224282705E-08 0.0000000000E+00 0.000E+00 0.000E+00 20030101.0000 20030201.0000 ymas
42 GRCOF2 34 0 -0.43131814197E-08 0.0000000000E+00 0.000E+00 0.000E+00 20030101.0000 20030201.0000 ymas
```

3. Processing GRACE Level-2 Data:

3.1. Calculate temporal mean of GRACE L2 data:

3.1.1. Unzip all GRACE L2 files downloaded in step (1.5).

3.1.2. Open each of the unzipped files in MS Excel. Use “Space Delimited” option.



A	B	C	D	E	F	G	H	I	J	K	L	M
1	FIRST	GSM-2_20 SHM	UT-CSR	20120910								
2	CMMNT	/scratch/00079/byaa705/grav/RL05_03-01/b/iter/L2/GSM-2_2003001-2003031_0025_UTCSR_0060_0005										
3	CMMNT	Unused days:	22,24,26,27,29,30									
4	CMMNT	Insert comment: here										
5	EARTH	3.99E+14	6.38E+06									
6	SHM	60	60	1	fully	normalize inclusive	permaner tide					
7	CMMNT	Reported standard deviation: are	formal (not calibrated)									
8	GRCOF2	0	0	1.00E+00	0.00E+00	0.00E+00	0.00E+00	20030101	20030201	nnnn		
9	GRCOF2	1	0	0.00E+00	0.00E+00	0.00E+00	0.00E+00	20030101	20030201	nnnn		
10	GRCOF2	2	0	-4.84E-04	0.00E+00	0.00E+00	0.00E+00	20030101	20030201	ynnn		
11	GRCOF2	3	0	9.57E-07	0.00E+00	0.00E+00	0.00E+00	20030101	20030201	ynnn		
12	GRCOF2	4	0	5.40E-07	0.00E+00	0.00E+00	0.00E+00	20030101	20030201	ynnn		
13	GRCOF2	5	0	6.87E-08	0.00E+00	0.00E+00	0.00E+00	20030101	20030201	ynnn		
14	GRCOF2	6	0	-1.50E-07	0.00E+00	0.00E+00	0.00E+00	20030101	20030201	ynnn		
15	GRCOF2	7	0	9.05E-08	0.00E+00	0.00E+00	0.00E+00	20030101	20030201	ynnn		
16	GRCOF2	8	0	4.95E-08	0.00E+00	0.00E+00	0.00E+00	20030101	20030201	ynnn		
17	GRCOF2	9	0	2.80E-08	0.00E+00	0.00E+00	0.00E+00	20030101	20030201	ynnn		
18	GRCOF2	10	0	5.33E-08	0.00E+00	0.00E+00	0.00E+00	20030101	20030201	ynnn		
19	GRCOF2	11	0	-5.08E-08	0.00E+00	0.00E+00	0.00E+00	20030101	20030201	ynnn		
20	GRCOF2	12	0	3.64E-08	0.00E+00	0.00E+00	0.00E+00	20030101	20030201	ynnn		
21	GRCOF2	13	0	4.17E-08	0.00E+00	0.00E+00	0.00E+00	20030101	20030201	ynnn		
22	GRCOF2	14	0	-2.27E-08	0.00E+00	0.00E+00	0.00E+00	20030101	20030201	ynnn		
23	GRCOF2	15	0	2.19E-09	0.00E+00	0.00E+00	0.00E+00	20030101	20030201	ynnn		
24	GRCOF2	16	0	-4.71E-09	0.00E+00	0.00E+00	0.00E+00	20030101	20030201	ynnn		
25	GRCOF2	17	0	1.92E-08	0.00E+00	0.00E+00	0.00E+00	20030101	20030201	ynnn		
26	GRCOF2	18	0	6.10E-09	0.00E+00	0.00E+00	0.00E+00	20030101	20030201	ynnn		
27	GRCOF2	19	0	-3.31E-09	0.00E+00	0.00E+00	0.00E+00	20030101	20030201	ynnn		

3.1.3 Organize the data columns in MS Excel in suchway: Organize the data columns in MS Excel in such way:

1st column = Coefficient

2nd column = Degree

3rd column = Order

4th column = Clm_first_month

5th column = S1m_first_month

6th column = Clm_second_month

7th column = S1m_second_month

The image shows a screenshot of the Microsoft Excel interface. The ribbon at the top includes File, Home, Insert, Page Layout, Formulas, Data, Review, and View. The Home ribbon is active, showing options for Cut, Copy, Paste, Format Painter, Font (Calibri, size 11), and Alignment. The active cell is D16, containing the formula -0.0000000226649066497 . Below the ribbon is a table with the following data:

	A	B	C	D	E	F
1	Coefficient	Degree	Order	Clm_Jan_2003	SIm_Jan_2003	
2	GRCOF2	0	0	1.00E+00	0.00E+00	
3	GRCOF2	1	0	0.00E+00	0.00E+00	
4	GRCOF2	2	0	-4.84E-04	0.00E+00	
5	GRCOF2	3	0	9.57E-07	0.00E+00	
6	GRCOF2	4	0	5.40E-07	0.00E+00	
7	GRCOF2	5	0	6.87E-08	0.00E+00	
8	GRCOF2	6	0	-1.50E-07	0.00E+00	
9	GRCOF2	7	0	9.05E-08	0.00E+00	
10	GRCOF2	8	0	4.95E-08	0.00E+00	
11	GRCOF2	9	0	2.80E-08	0.00E+00	
12	GRCOF2	10	0	5.33E-08	0.00E+00	
13	GRCOF2	11	0	-5.08E-08	0.00E+00	
14	GRCOF2	12	0	3.64E-08	0.00E+00	

	A	B	C	D	E	F	G	H
1	Coefficient	Degree	Order	Clm_Jan_2003	SIm_Jan_2003	Clm_Feb_2003	SIm_Feb_2003	
2	GRCOF2	0	0	1.00E+00	0.00E+00	1.00E+00	0.00E+00	
3	GRCOF2	1	0	0.00E+00	0.00E+00	0.00E+00	0.00E+00	
4	GRCOF2	2	0	-4.84E-04	0.00E+00	-4.84E-04	0.00E+00	
5	GRCOF2	3	0	9.57E-07	0.00E+00	9.57E-07	0.00E+00	
6	GRCOF2	4	0	5.40E-07	0.00E+00	5.40E-07	0.00E+00	
7	GRCOF2	5	0	6.87E-08	0.00E+00	6.86E-08	0.00E+00	
8	GRCOF2	6	0	-1.50E-07	0.00E+00	-1.50E-07	0.00E+00	
9	GRCOF2	7	0	9.05E-08	0.00E+00	9.05E-08	0.00E+00	
10	GRCOF2	8	0	4.95E-08	0.00E+00	4.95E-08	0.00E+00	
11	GRCOF2	9	0	2.80E-08	0.00E+00	2.80E-08	0.00E+00	
12	GRCOF2	10	0	5.33E-08	0.00E+00	5.33E-08	0.00E+00	
13	GRCOF2	11	0	-5.08E-08	0.00E+00	-5.08E-08	0.00E+00	
14	GRCOF2	12	0	3.64E-08	0.00E+00	3.64E-08	0.00E+00	
15	GRCOF2	13	0	4.17E-08	0.00E+00	4.17E-08	0.00E+00	
16	GRCOF2	14	0	-2.27E-08	0.00E+00	-2.27E-08	0.00E+00	
17	GRCOF2	15	0	2.19E-09	0.00E+00	2.20E-09	0.00E+00	
18	GRCOF2	16	0	-4.71E-09	0.00E+00	-4.71E-09	0.00E+00	
19	GRCOF2	17	0	1.92E-08	0.00E+00	1.92E-08	0.00E+00	
20	GRCOF2	18	0	6.10E-09	0.00E+00	6.09E-09	0.00E+00	
21	GRCOF2	19	0	-3.31E-09	0.00E+00	-3.30E-09	0.00E+00	
22	GRCOF2	20	0	2.16E-08	0.00E+00	2.16E-08	0.00E+00	

3.1.5 Repeat the previous step for all remaining GRACE L2 files.

3.1.6 Save the file with name "GRACE Raw Data.xls."

3.2. Remove the temporal mean of the data:

3.2.1. Open the file "GRACE Raw Data.xls."

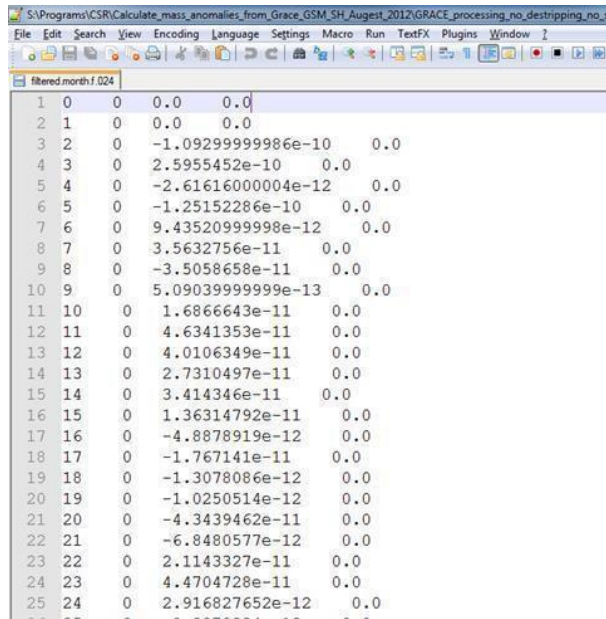
3.2.2. For all of the Clm values at all times, calculate the mean value "Clm_mean." Use the function "Average" in MS Excel.

	A	B	C	D	E	F	G	H	I
1	Coefficient	Degree	Order	Clm_Jan_2003	SIm_Jan_2003	Clm_Feb_2003	SIm_Feb_2003		
2	GRCOF2	0	0	1.00E+00	0.00E+00	1.00E+00	0.00E+00	=AVERAGE(D2:F2)	
3	GRCOF2	1	0	0.00E+00	0.00E+00	0.00E+00	0.00E+00		
4	GRCOF2	2	0	-4.84E-04	0.00E+00	-4.84E-04	0.00E+00		
5	GRCOF2	3	0	9.57E-07	0.00E+00	9.57E-07	0.00E+00		
6	GRCOF2	4	0	5.40E-07	0.00E+00	5.40E-07	0.00E+00		
7	GRCOF2	5	0	6.87E-08	0.00E+00	6.86E-08	0.00E+00		
8	GRCOF2	6	0	-1.50E-07	0.00E+00	-1.50E-07	0.00E+00		
9	GRCOF2	7	0	9.05E-08	0.00E+00	9.05E-08	0.00E+00		
10	GRCOF2	8	0	4.95E-08	0.00E+00	4.95E-08	0.00E+00		
11	GRCOF2	9	0	2.80E-08	0.00E+00	2.80E-08	0.00E+00		
12	GRCOF2	10	0	5.33E-08	0.00E+00	5.33E-08	0.00E+00		
13	GRCOF2	11	0	-5.08E-08	0.00E+00	-5.08E-08	0.00E+00		
14	GRCOF2	12	0	3.64E-08	0.00E+00	3.64E-08	0.00E+00		
15	GRCOF2	13	0	4.17E-08	0.00E+00	4.17E-08	0.00E+00		
16	GRCOF2	14	0	-2.27E-08	0.00E+00	-2.27E-08	0.00E+00		
17	GRCOF2	15	0	2.19E-09	0.00E+00	2.20E-09	0.00E+00		
18	GRCOF2	16	0	-4.71E-09	0.00E+00	-4.71E-09	0.00E+00		

3.2.3. Repeat the previous step for all of the SIm values to calculate "SIm_mean."

3.2.4 Subtract the "CIm_mean" and "SIm_mean" values form each monthly Clm and SIm value, respectively.

3.2.5. Save the new monthly values in SEPARATE ".txt" file for each month.



For each month: 1st column = l 2nd column = m 3rd column = Clm-
CIm_mean

4th column = SIm- SIm_mean

While saving the files use a unify name style. i.e, GRACE_001,
GRACE_002, ..., GRACE_010,
..., GRACE_100 , .. etc.

3.2.6. In some cases, you might need to format your monthly files generated from step(3.2.5). Use the code "File_Formating.f" to format your input files in such a way.

3.3. Calculate TWS Mass Anomalies:

3.3.1. Now you are ready to calculate GRACE mass anomalies. Use the code "Calculating_TWS_mass.exe" to calculate the mass anomalies.

The outputs of this code are files with longitude, latitude, and TWS (in cm; equivalent water thickness). The inputs for GRACE mass calculation code include:

- a- GRACE spherical Harmonics files. Outputs are from step 3.2.6. Those files should be in the specific format and certain file name style.
- b- File with the list of the input files listed in (a). Usually called "Month_to_process.txt." This file has to be in the specific format. The first row in this file should contain the number of months to be processed (e.g., 138 files). The second row all the way till the final row should contain the number of each file to be processed.
- c- Love number file.

2.1.1. Run "Calculating_TWS_mass.exe" code using different smoothing radii (e.g., 0 km, 250 km, 500 km, 750 km, and 1000 km).

2.2. Visualize the GRACE Mass Anomalies:

In this step, we will use ArcMap software to create maps from the outputs files of the previous step. For each of the generated files in step (3.3.2) you need to create an image/map out of them as the following:

2.2.1. Open each file using MS Excel. Use "Space Delimited" option.

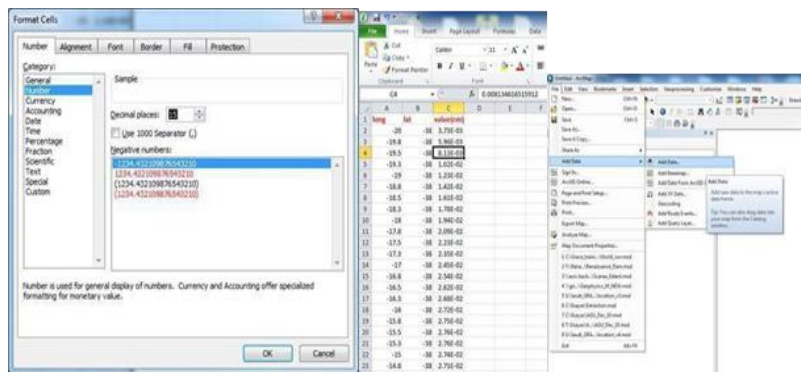
2.2.2. Insert "Long," "Lat," and "TWS (cm)" in the first row.

2.2.3. Select all rows/column, click “Format Cell” then select number and increase the “decimal places” to “15”. Save as MS Excel file.

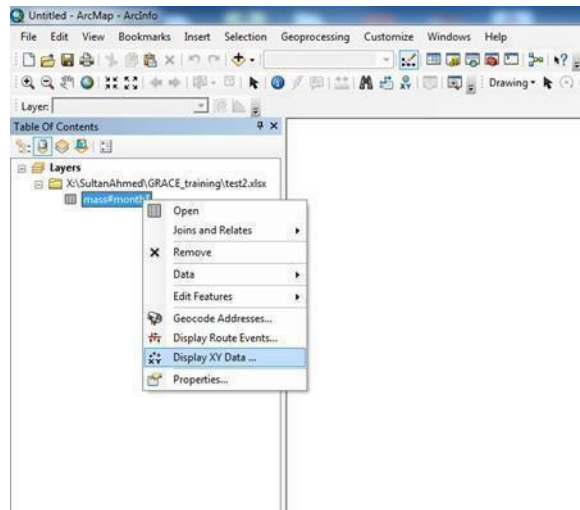
2.2.4. Save this file as "CSV Comma delimited." Use the same file name.

2.2.5. Open ArcMap program.

3.4.6 Add your “.CSV” file. Go to file-□ Add data □ Select your “.CSV” file



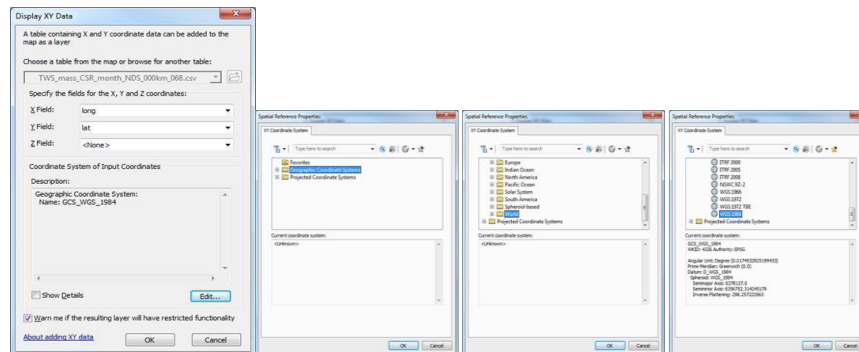
3.4.7. Right Click on the file you just added to ArcMap → Click “Display XY Data.”



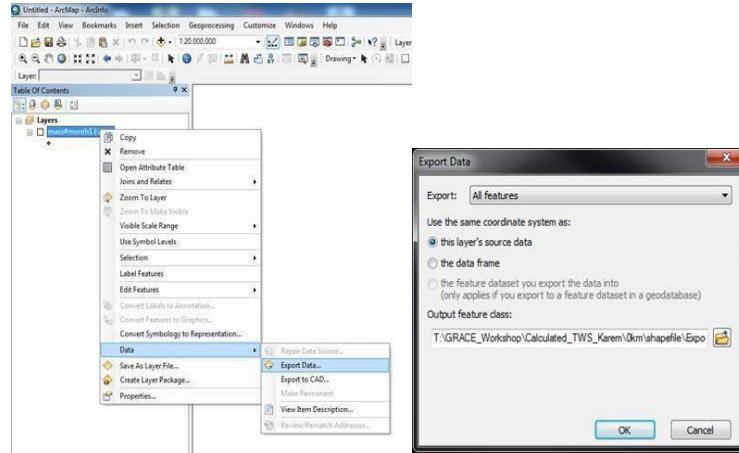
3.4.8. Select your

“X Field” → Long “Y Field” → Lat

“Coordinate System” → Edit → Geographic Coordinate System → World → WGS 1984 → OK

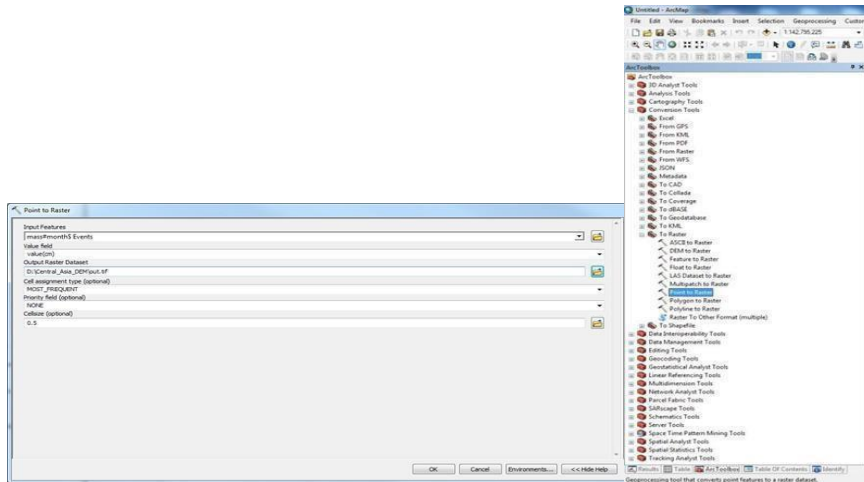


3.4.9. Export your shapefile. Right click on this file → Data → Export Data → Set the location.



3.4.10. Convert the Shapefile to Raster Image. Go to Arc Toolbox → Conversions Tools → To Raster → Point to Raster.

Select your file, field "TWS(cm)," output file name and location, add ".tif" to the file name, and Cell size: "0.5"



3.4.11. Add “Political Boundaries” Shapefile to your ArcMap.

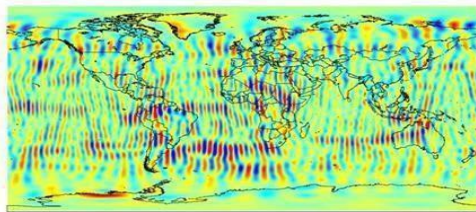
3.4.12. Zoom to full extent of the map and then “Print Screen.”

3.4.13. Save the print screen images in one MS word file.

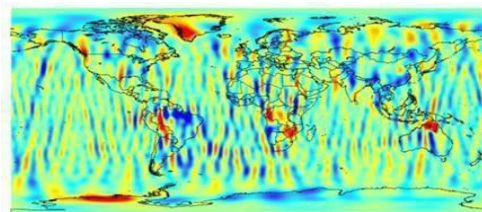
3.5. Interpretation of GRACE TWS Results:

3.5.1. Compare between the GRACE mass anomalies “images” at different Gaussian radii. Comment on the anomalies amplitude, shape, size, and distribution.

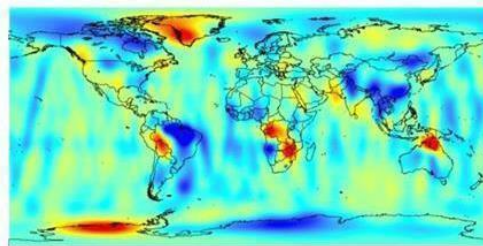
0 km



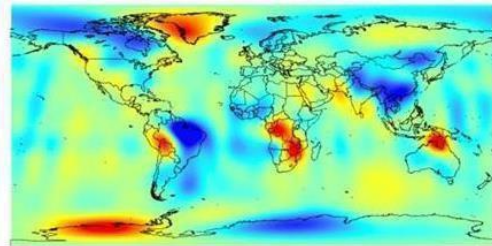
250km



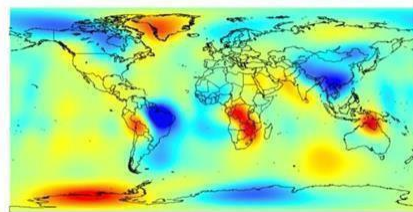
500km



750km



1000km



Saq aquifer simulation in SWAT model

Data collection, handling

1- Watershed delineator

➤ Topographic map

Watershed name	Area	Basin length	Maximum elevation	Soil (%)				
				(km ²)	(m)	(m a.m. s.l.)	Alluvium	Basement
Wadi_Al_Baten	27496.02	481966.10	1081.00	79.36	0.00	19.72	0.92	0.00
Wadi_Al_Rumah	215520.70	748900.20	2071.00	28.49	49.03	7.82	14.41	0.26
Al_Jowf_Wadi_Sarhan	113722.90	527028.10	1536.00	35.18	3.27	17.44	44.11	0.00
Tabuk_Wadi_Sarhan	20340.77	280104.70	2125.00	23.63	11.97	0.00	64.40	0.00

- DEM: 90 meter of the Shuttle Radar Topography

Mission (SRTM) was used to delineate most of the watersheds (4 watersheds) and their channel networks along the northwest to the southeast of the Saq aquifer. The DEM was utilized as an underlying parameter for creating slope and drainage based on the flow point (for the most part known as outlet focuses). The other sub-basin parameters, for example, slope angle, slope length of the territory and stream system qualities, channel slope, channel length and channel width were gotten

from DEM handling in the SWAT model.

- Stream delineation information for each watershed as the following
- Outlet definition : The outlet of Wadi_Al_Baten and Wadi_Al_Rumah are in the Gulf of Arab and for Al_Jowf_Wadi_Sarhan and Tabuk_Wadi_Sarhan outlets are in the Gulf of Aqaba.
- Calculation of sub-basin parameters

1- HRU analysis

- In SWAT, a basin is delineated into sub-basins, which are then further subdivided into Hydrological Respond Units (HRUs). The HRUs consist of homogeneous land use and soil type. The primary input, (DEM) digital elevation model, (LULC) land-use/land- cover, soil data and hydrogeological data such daily rainfall (mm), temperature (°C), solar (MJ/m²), Relative Humidity (fraction), and Wind (m/s).
- All that variables have been used for the initial SWAT model set-up SRTM elevation data presented in GRID can be downloaded for the whole world (<http://dwtkns.com/srtm/>). The SRTM data were provided into a WGS_1984_UTM_Zone_37N projection

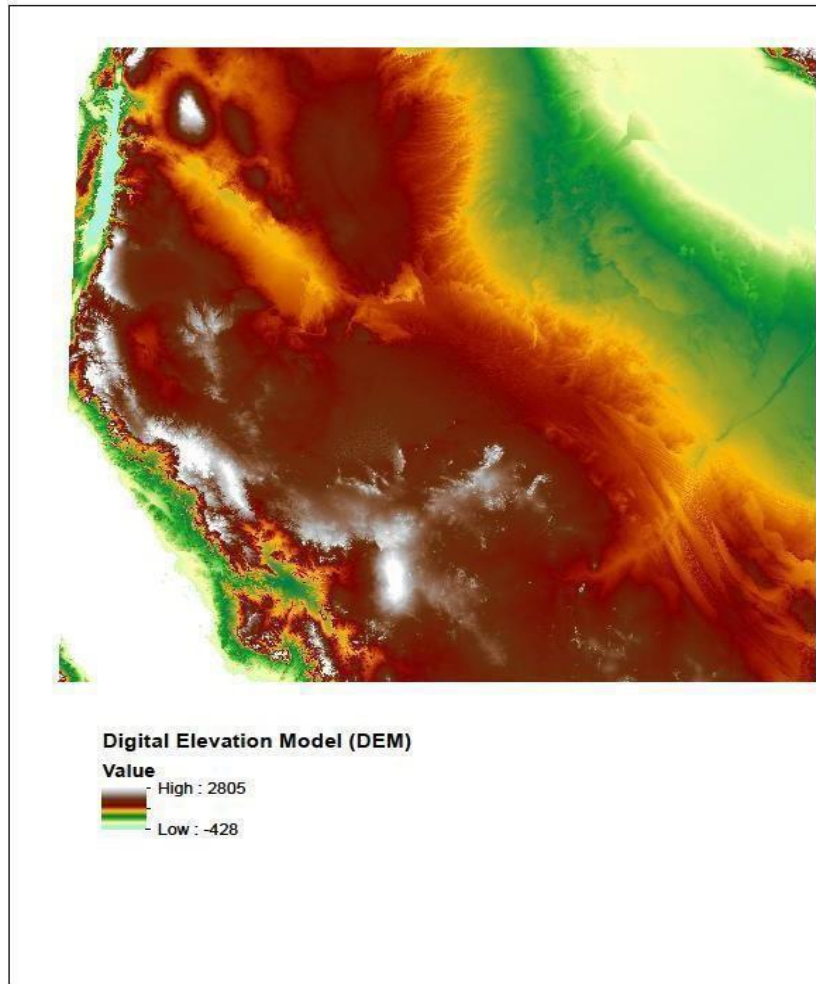
system and intended for scientific use with a Geographic Information System (GIS) or other special application software.

- The land-use map of the Saq Aquifer area was generated based on Global Land Cover 30 meter from (<http://www.globeland30.org/GLC30Download/index.aspx>)
- King Saudi Arabia hydrological map was applied for soil information and divided the soil data to FIVE types Gravel, Basement, limestone, Sandston, and Shale.
- The SWAT model requires every day hydro meteorological information for simulation of the model. The climate generator variables utilized as a part of this study for driving the hydrological balance are precipitation, wind, relative humidity, and solar for the period 1998-2014. These data were obtained from Global weather data for SWAT (<http://globalweather.tamu.edu/>). Also, we validated climate data from global weather site by compared with the field data that is available in our studying period by testing 15 gauges vs. 15 station from global weather sit which is they have same location and coordinate number, and the results was 85-95 percent similar.

2- Run the Model




- We have used the ArcSWAT 2012.10.18 version of SWAT model interface with ArcGIS 10.4 of ESRI product for processing the analysis. The main steps in the model setup involved data preparation, sub-basin discretization, HRU definition and overlay, parameterization, sensitivity analysis and calibration.
- After that, we have set-up the SWAT model to simulate the various hydrological components. The simulation part of the Saq aquifer was completed using the ArcSWAT interface of SWAT model.
- The model was calibrated by using parameters used in SWAT model (modified from Milewski et al. 2009). The manual calibration tool was used in the swat model to replace the parameters value using Milewski paper.

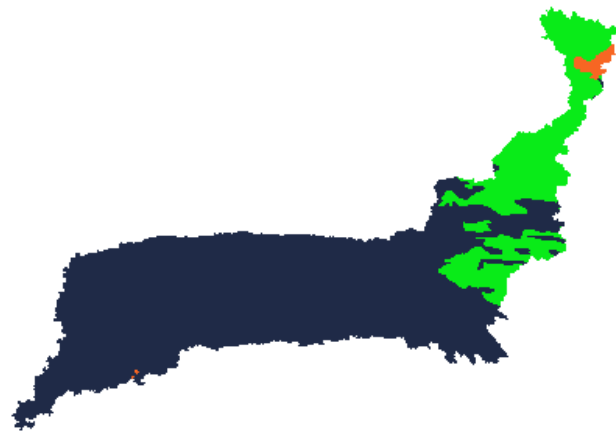
1-Wadi_Al_Baten

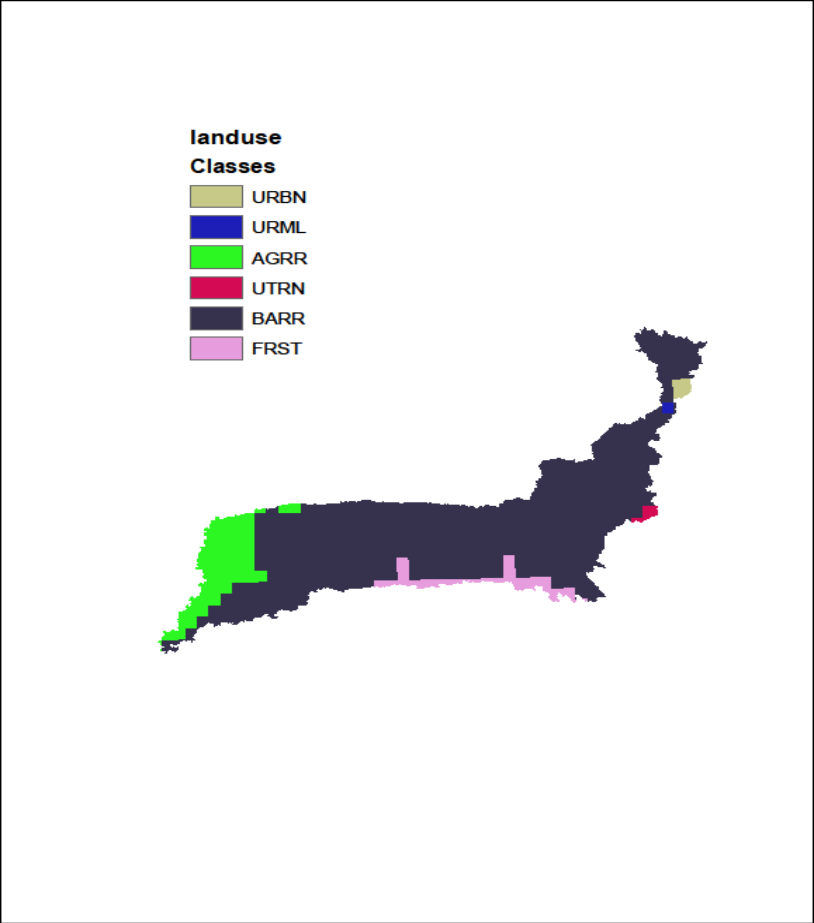


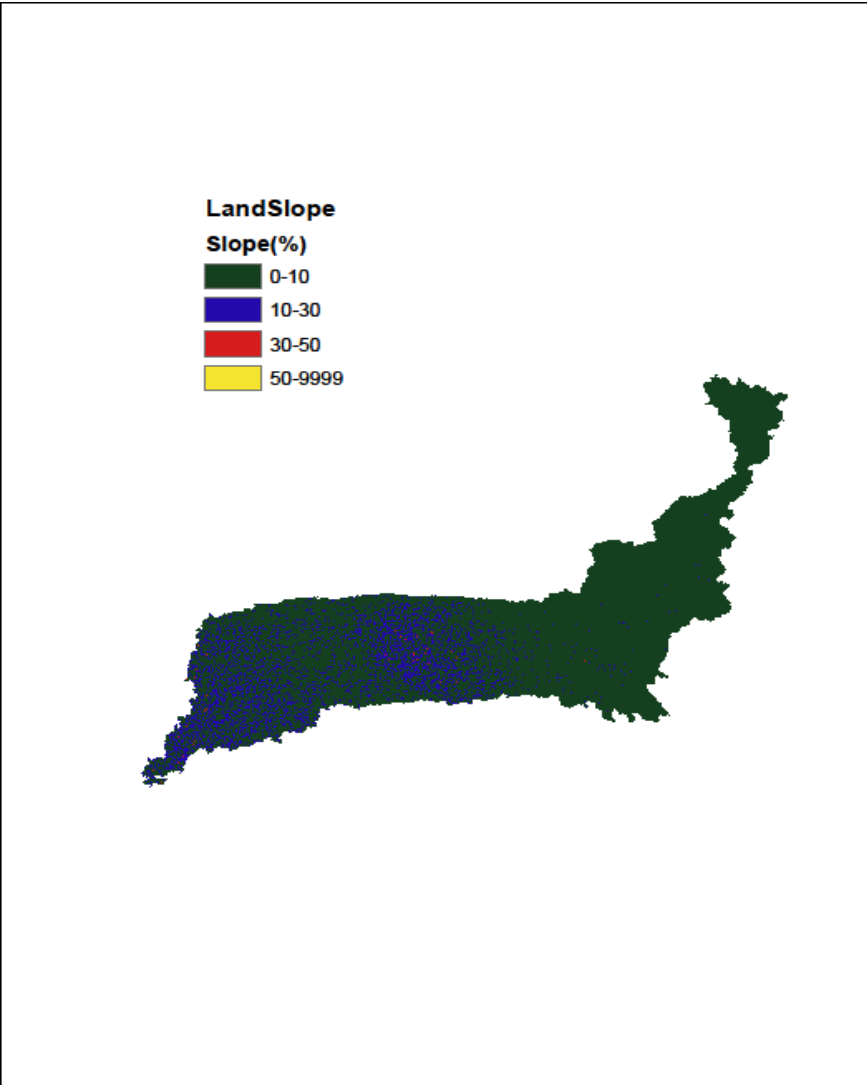
Soilmap

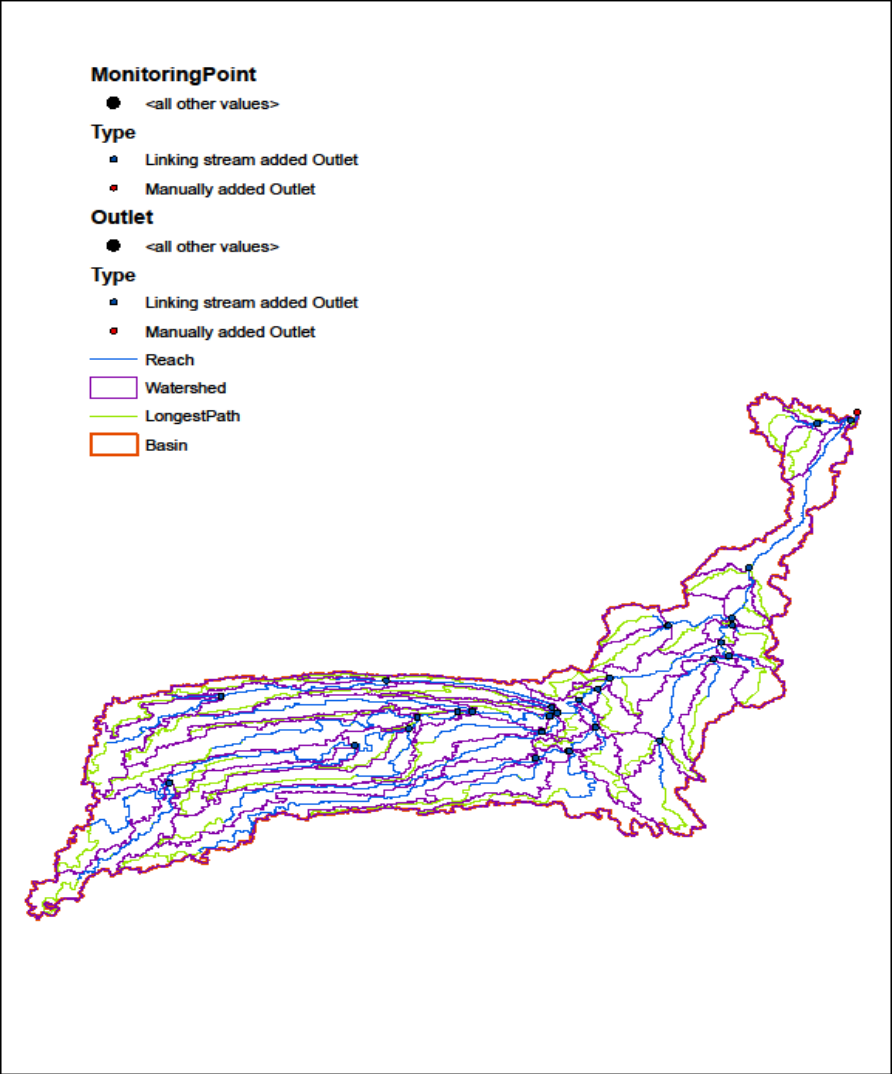
Classes

-  Alluvium (Sandy Loam)
-  Limestone
-  Sandstone

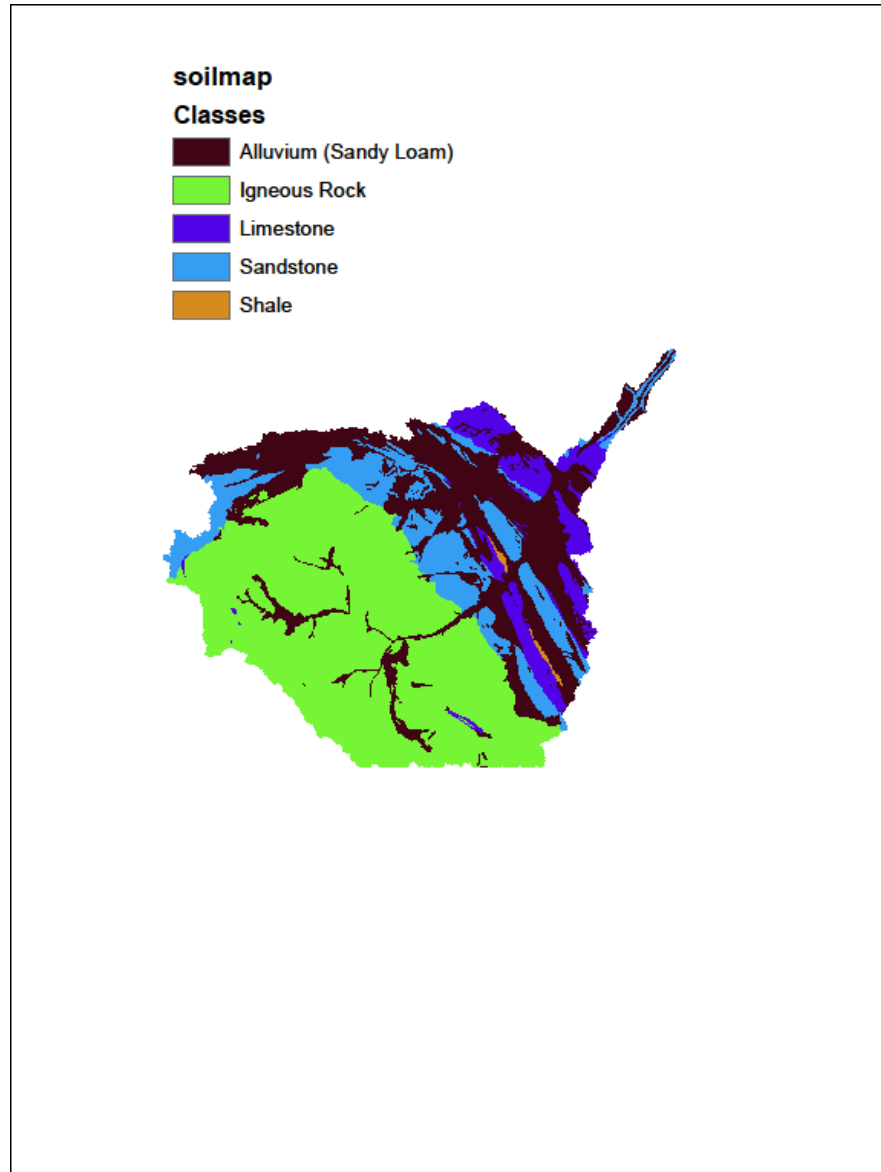


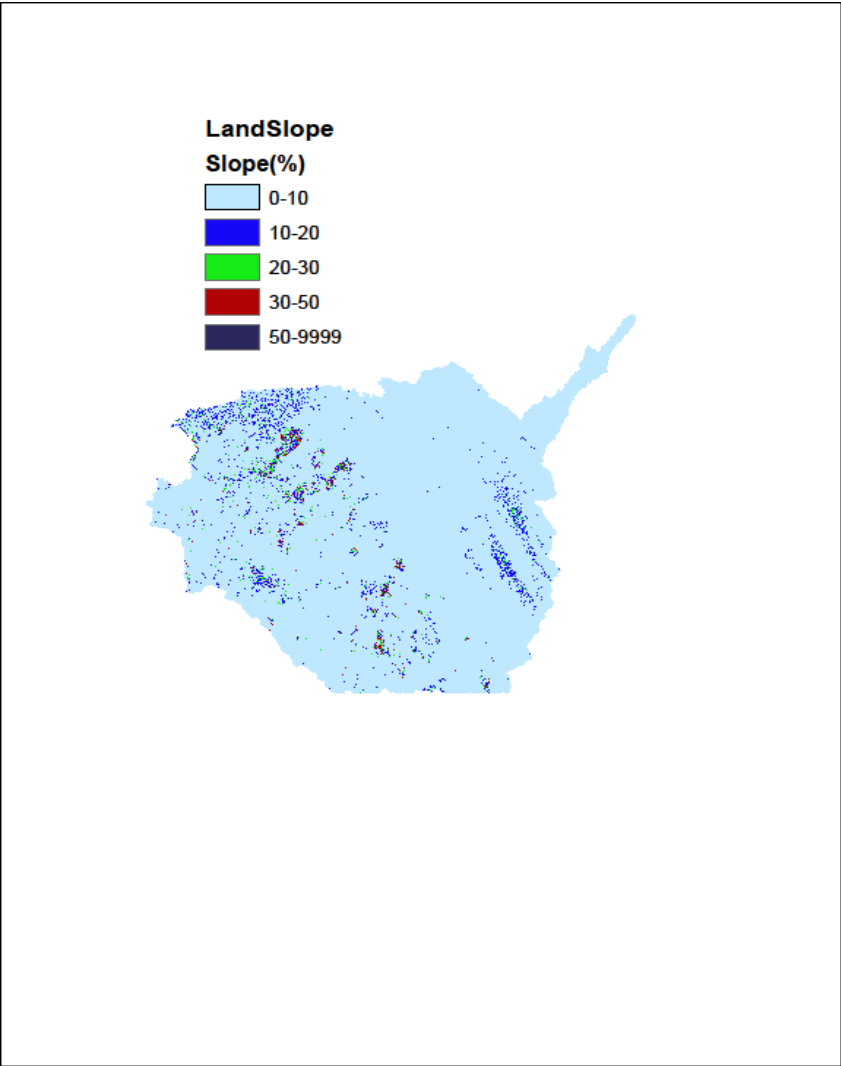


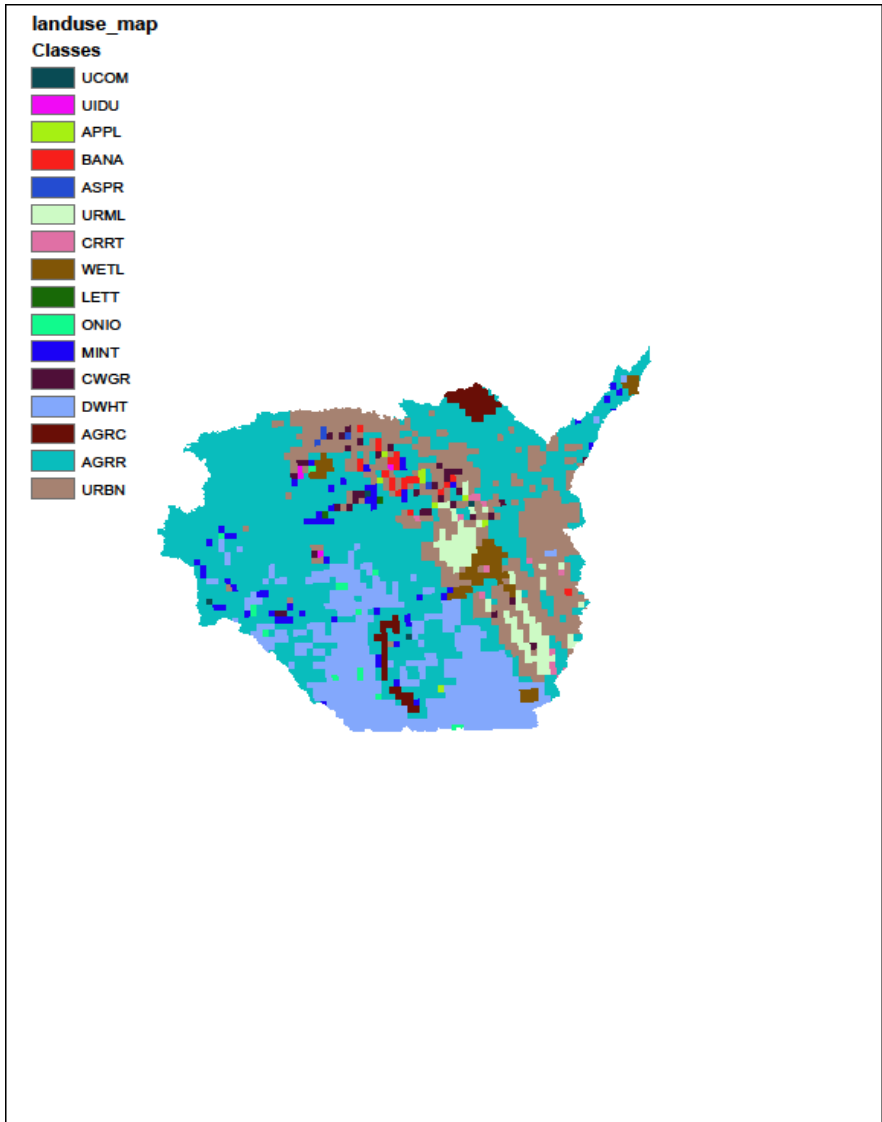


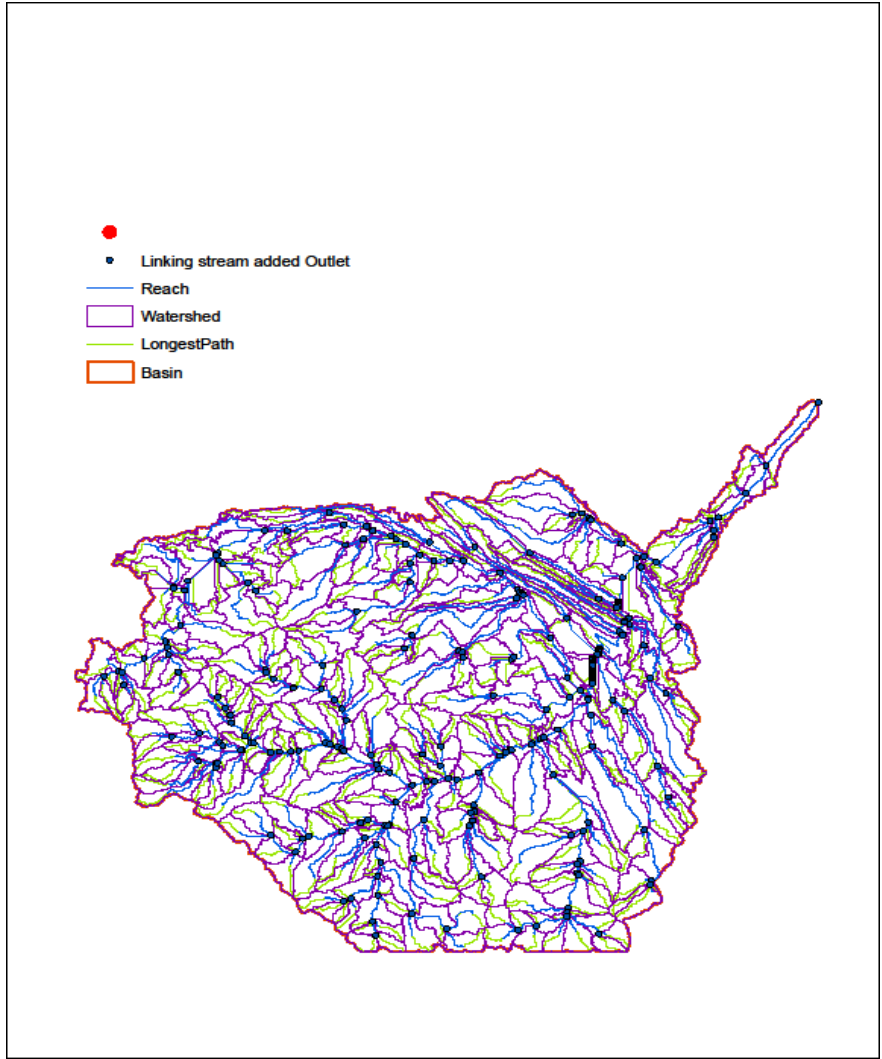


2- Wadi_Al_Rumah

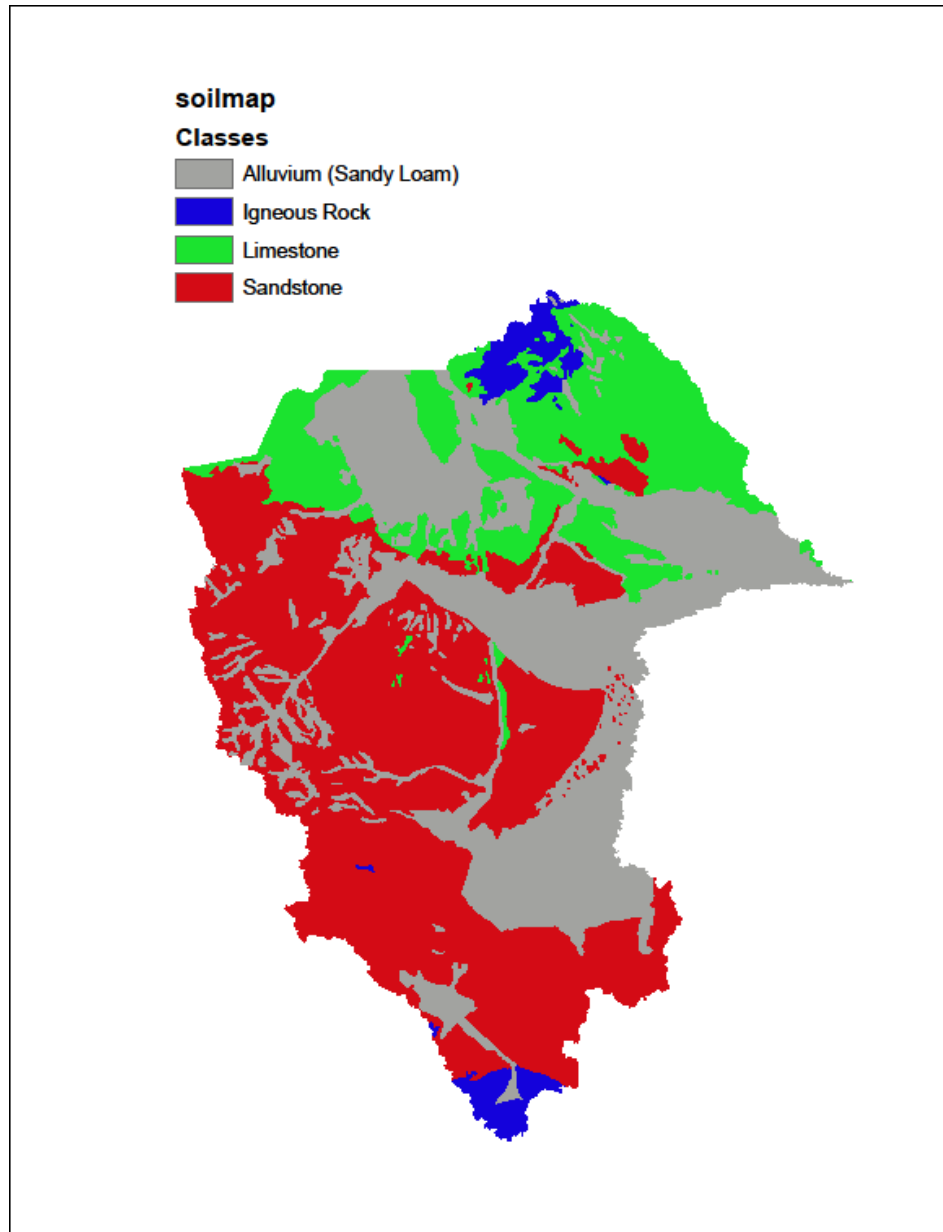


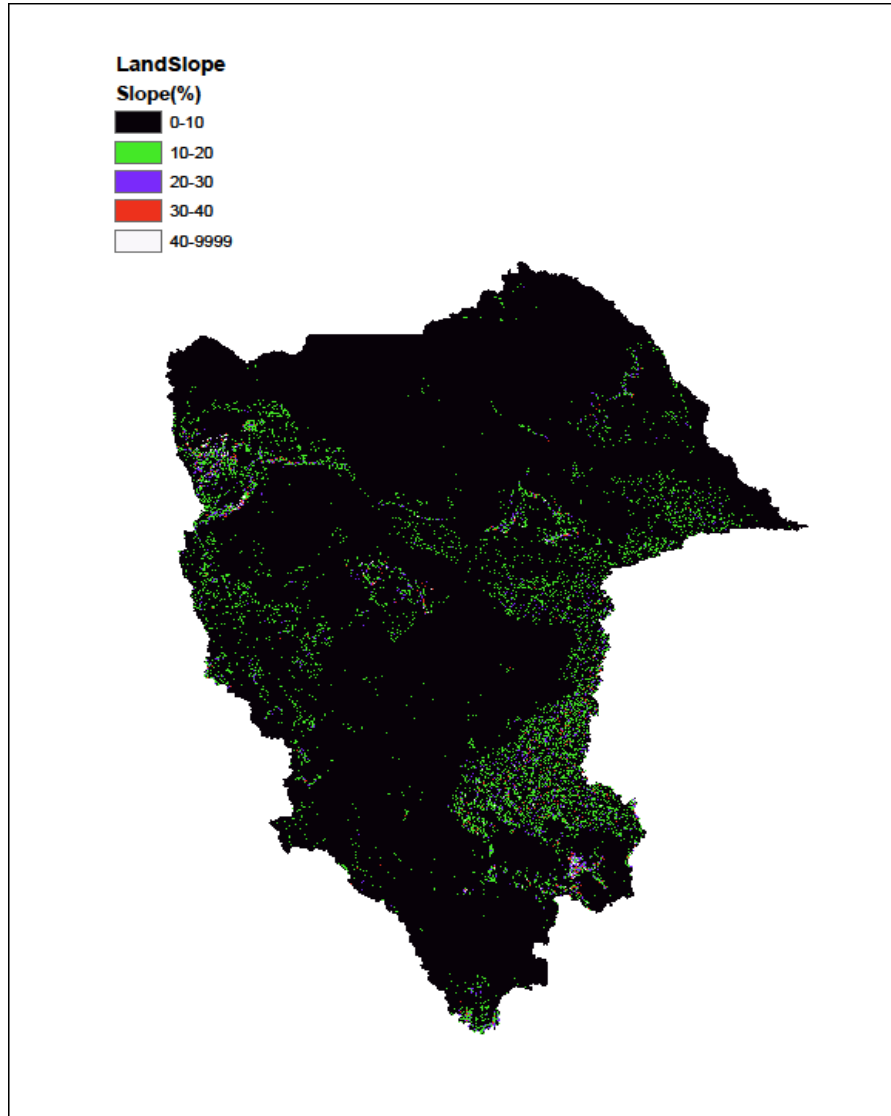


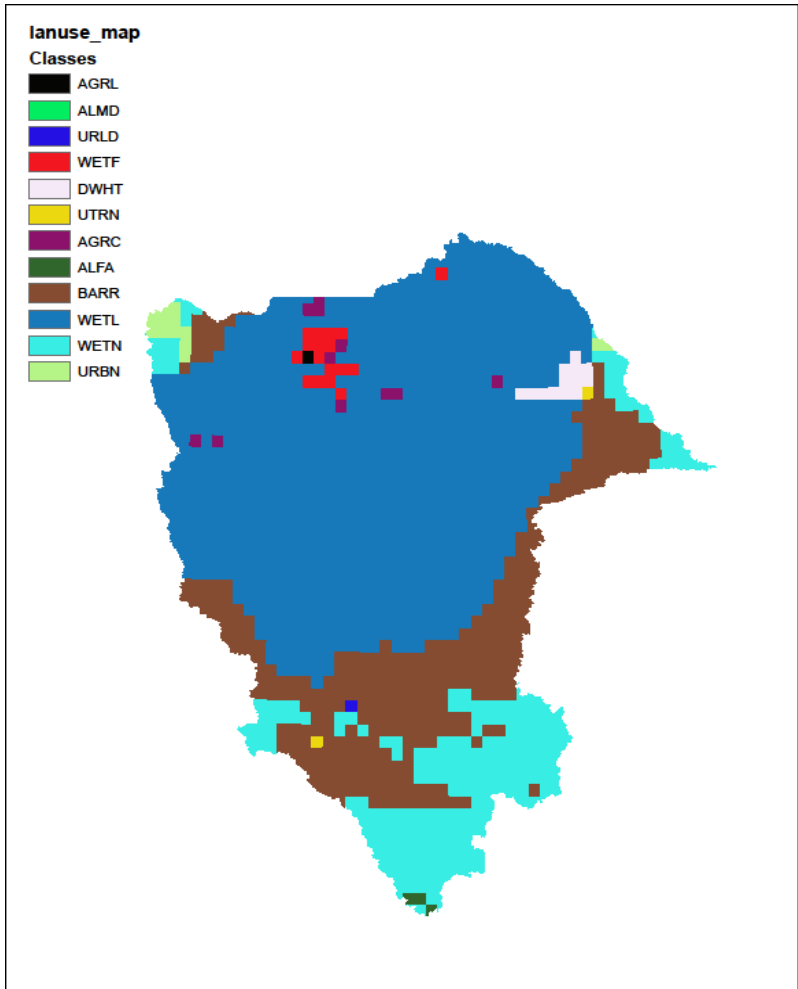


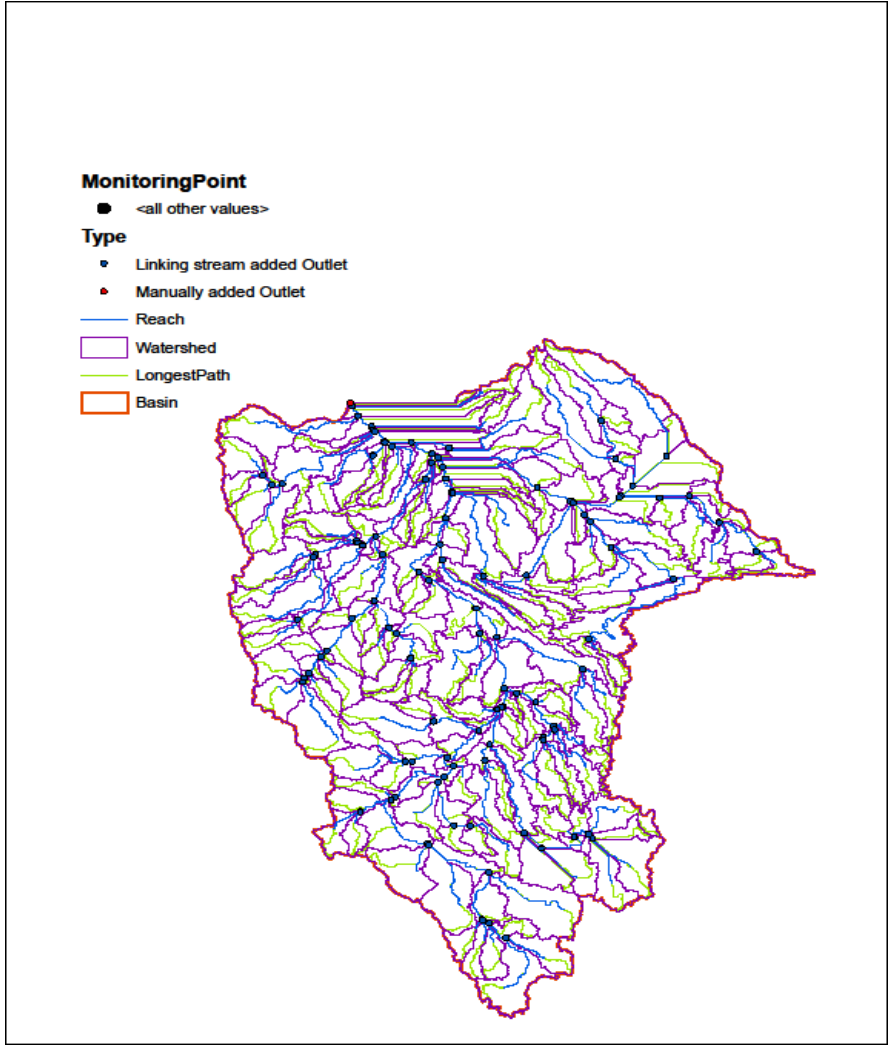


3- Al_Jowf_Wadi_Sarhan









4- Tabuk_Wadi_Sarhan

